Regulation and effector functions of IFNgamma-induced immunity to intracellular pathogens

Dissertation Advisor: Dr. Nir Hacohen Karolina Maciag

Regulation and effector functions of IFNγ-induced immunity to intracellular pathogens

Abstract

Macrophages are professional phagocytes that efficiently clear microbes, dying cells, and debris. Nonetheless, some pathogenic bacteria and parasites can subvert the macrophage phagosome into a vacuolar replicative niche. Exogenous macrophage activation by the cytokine interferon gamma (IFNγ) tips the equilibrium toward pathogen restriction, host survival, and subsequent adaptive immune responses. The relevance of IFNγ-induced immunity to human health has been demonstrated in patients with genetic defects in IFNγ signaling, who are profoundly susceptible to vacuolar pathogens such as *Mycobacterium tuberculosis*. Still, much remains to be discovered about IFNγ effector functions, and about their co-regulation by signaling downstream of the many innate immune sensors in macrophages.

First, we asked whether IFNγ-induced vesicle trafficking mechanisms affect the maturation of phagosomes containing the bacterium *Legionella pneumophila*, the causative agent of Legionnaire's disease. We used functional genetic screening to discover candidate genes involved. From 380 genes in a curated vesicle trafficking-related set, 15 were selected as candidate IFNγ pathway members by RNAi screening in cell line and primary mouse macrophages. Functional validation of top candidates was inconclusive, but revealed potential roles for membrane tetraspanins and the AP3 complex in IFNγ-induced microbial restriction.

Our second goal was to determine whether innate immune sensing affects IFNγ-induced bacterial restriction. Using macrophages from mice deficient in key elements of innate immune sensing pathways, we discovered that the antiviral transcription factor IRF3, which functions downstream of many nucleic acid sensing pathways, suppresses IFNγ-induced restriction of *L.*

pneumophila and the protozoan parasite *Trypanosoma cruzi*. While activated IRF3 localizes to the nuclei in resting macrophages infected with *L. pneumophila*, it is mostly excluded from nuclei in macrophages activated with IFNγ prior to infection. This suggests a cascade of suppression in which IFNγ responses inhibit IRF3 activation, but residual IRF3 activity antagonizes IFNγ effectors. IRF3-mediated inhibition of IFNγ-inducible nitric oxide synthase was partially, but incompletely responsible for the phenotype observed; further candidate effectors were identified by gene expression profiling. We speculate that antagonism between IFNγ and IRF3-mediated mechanisms may facilitate a balance of vacuolar pathogen immunity with viral defense, or with protection of tissue damage by nitric oxide and other IFNγ-dependent responses.

TABLE OF CONTENTS

Page

ACKNOWLEDGEMENTS AND GRATITUDE

First and foremost, I am profoundly grateful to my thesis advisor, Nir Hacohen, for allowing me the resources, freedom, and flexibility to pursue fascinating questions in host-pathogen biology. His enthusiastic and generous support is a true gift. He encouraged his lab members to ask bold questions, and he connected us to the resources that could make it possible to achieve our goals. In addition, the joy that he derives from the scientific process is an inspiration and a model for us all.

I would also like to thank all of the past and current members of the Hacohen Lab for instruction, guidance, and camaraderie. They were an enormous help to me upon my arrival in the lab as a new graduate student with a computational background, lacking many critical bench skills. I am grateful for their patience and help regarding protocols, reagents, experimental strategy, and many intangible details related to planning and executing a project. Even though our niche interests within the field of innate immunity often diverged, my labmates' support was a lifeline for me throughout these years. Thank you, especially, to Raktima Raychowdhury and Weibo Li for advice and assistance with Western blots and genotyping, and to Karen Smith for returning summer after summer to contribute her enthusiasm, dedication, and ever-increasing skill. Finally, tremendous thanks to the Committee on Comparative Medicine at MGH, especially Osvaldo Barros, for their detailed and compassionate stewardship of our laboratory mice.

Beyond the Hacohen Lab, I am grateful to then-postdoctoral fellow Jörn Coers, who taught me how to work with *L. pneumophila* and designed the RNAi screen. I am especially indebted to our collaborators Ricardo Gazzinelli and Rafael Barbosa for teaching me parasite infection skills and working with me through many cycles of experiments in order to test our hypothesis in the *T. cruzi* parasite infection model. Sincere thanks as well to Barbara Burleigh and Prasad Padmanabhan for sharing their lab space and hosting me in their lab during this time.

I am indebted to Schragi Schwartz and Max Mumbach in Aviv Regev's lab, who helped design the RNAseq analysis and patiently guided me through the sample preparation and analysis process. Many other members of the Regev Lab and the Lander Lab, our sixth-floor neighbors, were helpful as well, especially Alex Shishkin, Alex Shalek, Chris Ford, and Atray Dixit.

None of this work would have been possible without the help of the Hung Lab, which was truly a second home for me beyond the Hacohen Lab at the Broad Institute. Many thanks to Deb Hung, Sarah Stanley, Amy Barczak, Roi Avraham, Samantha Luo, and John Aquadro for sharing their lab space, equipment, and expertise, as well as their knowledge and passion for the study of intracellular bacterial infections.

Platform technologies are well-integrated into the infrastructure of the Broad Institute, which often makes it easy to take these stellar resources for granted. Still, I cannot thank the following people enough for their help, insights, and assistance: the CellProfiler team, especially Mark-Anthony Bray; Chemical Biology, particularly Leigh Carmody, Lynn Verplank, and Thomas Hasaka; and the RNAi platform, especially Serena Silver, David Root, Alan Derr, Glenn Cowley, Thomas Nieland, Sridevi Ponduru, and Shuba Gopal.

Conversations with the wider host-pathogen immunity community in Boston and beyond have been a highlight of the years spent in graduate school. Among many others, I am grateful to Ralph Isberg and Andrew Ensminger at Tufts, Lynda Stuart and Anna Sokolovska at MGH, Salil Garg and Victor Chu at Dana-Farber, Craig Roy and Vladimir Ivanov at Yale, and Stewart Vance at Berkeley for advice on *L. pneumophila* and associated techniques.

I have been immensely fortunate to have had the privilege of working with several wonderful mentors in the past. I am grateful for everything that they have taught me, and for the example they set of a life in science well lived. Without them, the idea of pursuing a doctoral project would have remained but a dream. I cannot thank these mentors enough: Steve Altschuler, Lani Wu, Tom Maniatis, Linda Wolff, Alejandro Schaffer, Duccio Cavalieri, and Biswajit Biswas.

Thank you to my DAC members: Jon Kagan, Arlene Sharpe, and Michael Brenner - for providing critical guidance and lending their substantial insights. I am also grateful to the programs that I have called home during my graduate years, with thanks especially to David Cohen, Rick Mitchell, and Patty Cunningham at HST, to Loren Walensky, Amy Cohen, and Linda Burnley at our close-knit MD/PhD Program, to Sue Perkins and Mike Carroll at the Immunology program, and to Anne Goldfeld and Michael Starnbach for hosting me as a rotation student. I am grateful for the members of defense committee: Kate Fitzgerald, Javier Irazoqui, and Jay Vyas, as well as Jon Kagan, for volunteering their time and expertise to serve on my dissertation defense committee.

To my students in the undergraduate immunology and HST microbiology courses, thank you for the keen interest, probing questions, and enthusiasm that you brought to our interactions. You challenged me to be a better teacher and communicator throughout my graduate school career and beyond. I am also grateful to Shiv Pillai, Harvey Simon, and Clyde Crumpacker, the inspiring educators for whom I served as a teaching assistant. To my colleagues at UAEM, thank you for sharing giving me a chance to work together with you toward global equity in biomedical research.

I am thankful to Matt for his steadfast love, support, and patience, as well as timely observations which have made me a better person and a better scientist. My small and close-knit, yet far-flung family has been a phenomenal inspiration and support throughout my life, especially Mom, Dad, and my brother Robert: you have made everything possible for me. I have been lucky to have wonderful friends with whom to share the joys, sorrows, and adventures with as well, and I am truly grateful to have them in my life.

LIST OF FIGURES

Chapter 1

Chapter 2

Chapter 3

LIST OF TABLES

LIST OF ABBREVIATIONS

+	having the indicated characteristic (read as “positive”)
-/-	genetically deficient (read as “knock-out”)
AIM2	absent in melanoma-2
AP3	adaptor protein 3
ARF	ADP-ribosylation factor
ARL	ADP-ribosylation factor-like
ASC	apoptosis-associated speck-like protein containing a CARD
B6	C57BL/6J
BMM	bone marrow-derived macrophage
CARD	caspase activation and recruitment domain
CEDNIK	cerebral dysgenesis, neuropathy, ichthyosis and keratoderma
cGAS	cyclic GMP-AMP synthase
cGMP	cyclic guanosine monophosphate
DAI	DNA-dependent activator of IRFs
DAPI	4',6-diamidino-2-phenylindole
DC	dendritic cell
DDX	DEAD (Asp-Glu-Ala-Asp) box
DHX	DEAH (Asp-Glu-Ala-His) box helicase
Dot/Icm	defect in organelle trafficking/intracellular multiplication
dsDNA	double-stranded DNA
dsRNA	double-stranded RNA
ER	endoplasmic reticulum
FBS	fetal bovine serum
GAF	gamma-activated factor
GAS	IFNγ activation site
GBP	guanylate binding protein
GFP	green fluorescent protein
GTPase	guanosine triphosphate hydrolase
HSP	heat shock protein
HPI	hours post infection
IFN	interferon
IFNAR	type I interferon receptor
IFNGR	type II interferon receptor
IgG	immunoglobulin G
IκB	inhibitor of NFκB
IKK	IκB kinase
IL	interleukin
iNOS	inducible nitric oxide synthase
IRG	immunity-related GTPase
ISGF3	interferon-stimulated gene factor 3

ISRE	interferon-sensitive response element
JAK	Janus kinase
LAMP	lysosomal-associated membrane protein
LCV	*Legionella*-containing vacuole
LRRFIP-1	leucine-rich repeat in flightless-I interacting protein 1
LPS	lipopolysaccharide
MAP	mitogen-activated protein
MAVS	mitochondrial antiviral-signaling protein
MBL	mannose-binding lectin
MCSF	macrophage colony-stimulating factor
MDA5	melanoma differentiation-associated gene 5
MDM	monocyte-derived macrophage
MEF	mouse embryonic fibroblast
MOI	multiplicity of infection
mRNA	messenger RNA
MYD88	myeloid differentiation primary response gene 88
NADPH	nicotinamide adenine dinucleotide phosphate
NAIP	NLR family, apoptosis inhibitory protein
NFκB	nuclear factor κ-light-chain-enhancer of activated B cells
NK	natural killer
NKT	natural killer T
NLR	NOD-like receptor
NLRC	NLR with N-terminal caspase activating and recruitment domain
NO	nitric oxide
NOD	nucleotide-binding oligomerization domain
NRAMP-1	natural resistance-associated macrophage protein 1
PAMP	pathogen-associated molecular pattern
PI3K	phosphatidylinositol 3 kinase
PRR	pattern recognition receptor
qPCR	quantitative polymerase chain reaction
RFP	red fluorescent protein
RIG-I	retinoic acid-inducible gene I
RIP1	receptor-interacting protein 1
RNAi	RNA interference
RNI	reactive nitrogen intermediates
ROS	reactive oxygen species
RZ score	robust Z-score
shRNA	short hairpin RNA
siRNA	short interfering RNA
SNAP	soluble N-ethylmaleimide-sensitive factor attachment protein
SNARE	SNAP receptor
SNX	sorting nexin

SOCS	suppressor of cytokine signaling
STAT	signal transducer and activator of transcription
STING	stimulator of type I IFN gene
STX	syntaxin
TBK	tank-binding kinase
Th1	T helper type one
TIR	toll-interleukin 1 receptor
TLR	toll-like receptor
TNF	tumor necrosis factor
Treg	regulatory T cell
TRIF	TIR-domain-containing adaptor inducing IFNβ
TSPAN	tetraspanin
VAMP	vesicle associated membrane protein
VTI1B	vesicle transport through interaction with t-SNAREs 1B
WT	wild-type

INTRODUCTORY NOTE

This thesis is focused on two independent studies on the restriction of *L. pneumophila* in interferon gamma (IFNγ)-activated murine macrophages. The first study investigated the role of vesicle trafficking genes in the IFNγ-induced restriction of this bacterium, while the second was directed toward understanding the effect of innate immune sensing on the IFNγ-activated state.

Chapter 1 provides an overview of macrophages, their interactions with vacuolar pathogens, and the effects of IFNγ on these interactions. The role of macrophages in phagocytic clearance of debris and non-subverting bacteria is discussed first, followed by an overview of vacuolar pathogens that subvert the macrophage phagosome. Next, IFNγ and its effectors in the activation of macrophage-intrinsic resistance to vacuolar pathogens is described. This is followed by an overview of the innate immune sensors that macrophages use to detect infection, as well as a discussion of the known and potential interactions between innate sensing and macrophage activation by IFNγ. Finally, the model macrophage pathogen *L. pneumophila* is introduced as a tool to investigate IFNγ effector mechanisms as well as to study potential interactions between innate immune sensor pathways and the IFNγ-activated state.

A genetic screening approach to investigating vesicle trafficking in IFNγ-induced restriction of *L. pneumophila* is discussed in **Chapter 2**. This includes a description of the pipeline used for the analysis of high-throughput screening data. The follow-up studies on individual hits using functional characterization assays are presented.

Chapter 3 describes experiments that investigate whether pathogen sensing affects IFNγ-induced microbial restriction in the context of *L. pneumophila* infection. Building upon the observation that IRF3 enhances bacterial growth in IFNγ-activated cells, potential ligands sensed upstream of IRF3 and effector mechanisms downstream of IRF3 are investigated. Relevance to parasitic infection with *Trypanosoma cruzi* are discussed as well.

Chapter 4 provides a perspective on the studies presented in Chapters 2 and 3. The hypotheses suggested in Chapter 3 are discussed in detail. Suggestions for further study are presented.

.

Chapter 1: Introduction

Macrophage-intrinsic defense against vacuolar pathogens
Subversion of macrophages by intracellular pathogens
IFNγ-mediated antimicrobial effectors
Macrophage pathogen sensing
Effects of pathogen sensing on IFNγ-mediated effectors
Legionella is a model pathogen to study IFNγ-mediated macrophage-intrinsic immunity
References

Macrophage-intrinsic defense against vacuolar pathogens

Macrophages are efficient "vacuum cleaners" found in nearly all tissues of the body. These professional phagocytes ingest and break down debris such as apoptotic cells and foreign matter. They also engulf, kill, and degrade potential pathogens such as bacteria, parasites, and fungi. Phagocytosis and phagosome maturation culminate in fusion with lysosomes and breakdown of cargo into units of constituent proteins, lipids, sugars, and nucleic acids, though orchestration of the process is highly variable depending on the nature of the cargo and the state of the macrophage. Macrophages play a wide range of roles beyond phagocytic clearance as well. In the context of tissue damage, these cells function in wound repair by secreting tissue repair factors, as well as by clearing damaged tissue. Macrophages figure prominently in the stroma of many tumors, where have been shown to either contribute to or suppress tumorigenesis and metastasis in a highly context-dependent manner [1]. Because macrophages can be skewed toward different functions in response to a range of stimuli, an understanding of how these cells are regulated and how their effector functions are deployed provides insight into a range of pathogenic processes that involve macrophages that are underactive, overactive, or misdirected.

The functions of macrophages in immune defense overlap with that of the other professional phagocytes, yet they are indispensable in a number of roles including pathogen control. Like neutrophils, macrophages ingest and kill microbes; like dendritic cells, they function as a bridge between innate and adaptive immunity by releasing signaling cytokines and chemokines and by presenting antigens to cells of the adaptive immune system. However, macrophage depletion in mice leads to increased susceptibility to some bacterial infections [2–5], revealing nonredundant roles in host immunity.

Phagosome maturation modulates membrane and luminal contents.

During phagocytosis, defined as the internalization of cargo over 0.5 microns in size (in contrast to endocytosis of smaller particles), plasma membrane-derived pseudopods engulf the target. After internalization, the membrane and luminal environment of the nascent phagosome undergo continuous remodeling through fusion of incoming vesicles and budding of outgoing vesicles (**Fig. 1-1**). In the early stages of maturation, the phagosome fuses with early endosomal compartments. Subsequent phases include fusion with late endosomes, multivesicular bodies, and lysosomes. Vesicles bearing newly synthesized proteins from the secretory pathway are targeted to the maturing phagosome as well [6]. Autophagy, the *de novo* formation of an enclosed compartment by seeding, elongation, and enclosure of a double membrane around cytosolic contents, destined for eventual fusion with lysosomes, can also play a role in phagosome maturation [7,8], in one of several ways: by engulfment of the entire phagosome by an autophagosome, by contributions of autophagic vesicles to the phagosome, or by participation of individual autophagy-related proteins in the process of phagosome maturation.

The luminal contents of donor vesicles contribute to microbial restriction. These include lipases, nucleases, glycosidases, cathepsins and other proteases, phosphatases, and antimicrobial peptides, including cationic defensins and cathelicidins, which form pores in bacterial membranes, as well as ubiquicidin, hepcidin, and ubiquitin-derived peptides [9–11].

The phagosome is further modulated by the acquisition of membrane-embedded enzymes including the NADPH phagocyte oxidase complex, comprised of cytosolic subunits (p21, p40, p47, and p67) that are activated upon binding the flavocytochrome b558 complex (p22, p91 also known as NOX2) at the phagosomal membrane [11,12]. This complex produces highly reactive superoxide and peroxide species (reactive oxygen species, or ROS) that damage microbes in the phagosome [13–15]. Ion channels from incoming vesicles function in bacterial restriction as well. Vacuolar ATPase acidifies the compartment, contributing to microbial degradation directly as well as indirectly, by

activating lysosomal hydrolases [12]. NRAMP1 channels deplete the phagosome of iron, zinc, and manganese, metals needed for microbial growth [16].

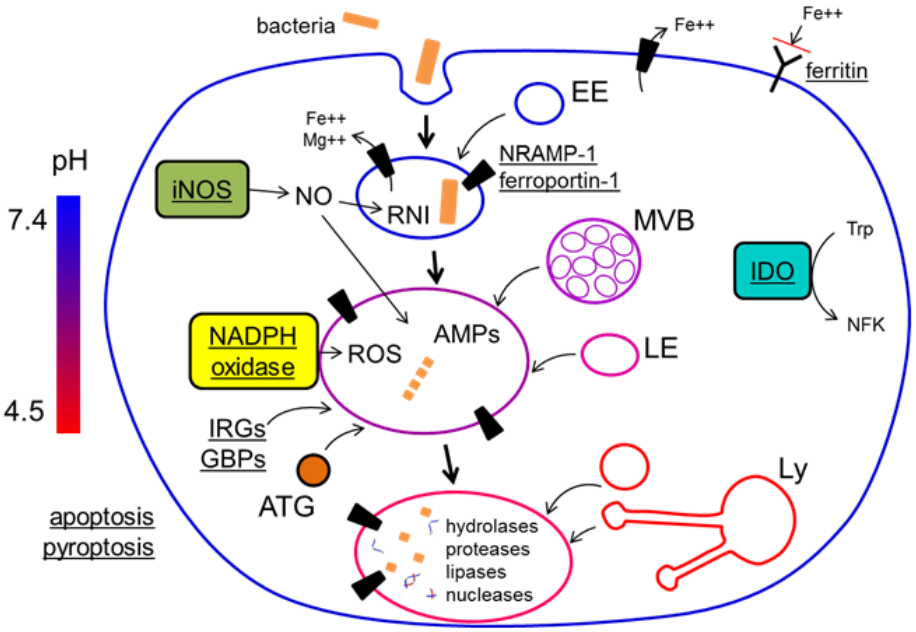

Figure 1-1. Mechanisms of vacuolar pathogen restriction in macrophages

Macrophages restrict and kill phagocytosed microbes by a number of effector mechanisms including phagosome acidification and maturation, autophagy, antimicrobial peptide delivery, nutrient restriction, damage by reactive oxygen species and nitrogen intermediates (ROS/RNI), and cell death. Mechanisms known to be dependent on or enhanced by macrophage activation by exogenous IFNγ.are underlined (Adapted from [11,17]).

Abbreviations used: EE, early endosome; MVB, multivesicular body; LE, late endosome; Ly, lysosome; iNOS, inducible nitric oxide synthase; NO, nitric oxide; RNI, reactive nitrogen intermediates; ROS, reactive oxygen species; AMPs, antimicrobial peptides; IDO, indoleamine 2,3-dioxygenase; IRG, immunity-related GTPase; ATG, autophagy related proteins

Phagosome maturation is highly regulated

Membrane-integral and associated proteins and lipids, especially of the Rab guanosine triphosphate hydrolase (GTPase) protein family, establish vacuolar identity and confer selectivity for

interactions with other cellular components [6]. The early phagosome is marked by Rab5 and its effectors vacuolar protein sorting 34 (VPS34), early endosome antigen 1 (EEA1), and syntaxin 13. Rab5 facilitates homotypic fusion with other Rab5-positive compartments (phagosomes and early endosomes), and with Rab4-positive recycling endosomes. Activity of the phosphatidylinositide (PI3) kinase VPS34 enriches the membrane in phosphatidylinositide(3) phosphate (PI3P), a lipid that recruits elements of the NADPH oxidase complex [18] and anchors EEA1 [19]. EEA1, in turn, serves as a docking and activating protein for syntaxin 13, a target- soluble N-ethylmaleimide-sensitive factor attachment protein receptor (t-SNARE) on early endosomes [10]. The class C VPS/ homotypic fusion and vacuole protein sorting (HOPS) complex mediates the conversion of Rab5 to Rab7, a hallmark of phagosome maturation [20]. In late phagosomes, cholesterol and PI(4,5)P2 membrane lipids predominate. Rab7 activates the Rab7-interacting lysosomal protein (RILP), which may induce fusion with lysosomes. The lysosomal-associated membrane proteins LAMP1 and LAMP2 are necessary for phagolysosomal fusion, though a precise mechanism is unknown [6].

Subversion of macrophages by intracellular pathogens

While macrophages ingest and then digest many microbes readily, certain pathogens subvert the inhospitable environment of the macrophage phagosome into a niche amenable for survival and replication. These vacuolar pathogens include the bacterial agents of Legionnaire's disease (*Legionella pneumophila*), salmonellosis (*Salmonella enterica*), melioidosis (*Burkholderia pseudomallei*), Q fever (*Coxiella burnetii*), pneumonic plague (*Yersinia pestis*), and tuberculosis (*Mycobacterium tuberculosis*), and the parasitic agents of Chagas disease (*Trypanosoma cruzi*), toxoplasmosis (*Toxoplasma gondii*), and leishmaniasis (*Leishmania spp.*), each of which deploys a range of effectors and virulence factors to evade and disable the antimicrobial mechanisms of the host macrophage. Some of the adaptive strategies used by intracellular pathogens include latency, acid resistance, and metal ion scavenging [11,12]. Any host antimicrobial mechanism could

potentially be targeted by intracellular pathogens directly as well. For example, ROS are converted to less toxic byproducts by bacterial catalase and superoxide dismutase [12]. Some bacteria arrest phagosome maturation by modifying phagosomal lipids [21] or proteins [22], and others remodel the phagosome into a compartment with an altogether different identity by secreting effector proteins and selectively recruiting vesicles or membrane fragments [22].

Activation by IFNγ can overcome macrophage subversion by intracellular pathogens

While resting macrophages are susceptible to subversion by phagosomal-resident microbes, macrophages activated by interferon gamma (IFNγ) produced by NK, NKT, Th1, and Treg cells gain the capacity to restrict many of these pathogens [23–25]. The central role of IFNγ in many bacterial and parasitic intracellular pathogens has been demonstrated in both humans and in model organisms [26]. In mice, IFNγ is required for resistance to several intracellular pathogens, including vacuolar *M. tuberculosis* [27], *L. pneumophila* [28], and *T. gondii* [29], as well as the bacteria *Listeria monocytogenes* [30], which are phagocytosed but escape to the cytosol. In humans, deficiency in IFNγ, its receptor, related downstream adaptors, or relevant signaling genes is strongly associated with susceptibility to mycobacterial diseases and other intracellular bacterial [31] and parasitic infections. In vitro, IFNγ activates both human and mouse macrophages to overcome bacterial evasion strategies and kill or restrict the growth of these intracellular pathogens [23,32,33].

IFNγ-mediated antimicrobial effectors

IFNγ stimulation activates several macrophage-intrinsic antimicrobial mechanisms that are not observed or that play a minimal role in resting cells. Among these mechanisms, outlined below, few mechanisms are induced exclusively by IFNγ; other cytokines, such as tumor necrosis factor α (TNFα), interleukin-12 (IL-12), interleukin-2 (IL-2), or lymphotoxin α (LTα), or microbial products such as lipopolysaccharide (LPS) can induce these effectors as well. However, activation by other

stimuli generally requires a combination of signals, or require concurrent IFNγ stimulation in order for significant activation to occur.

Inducible nitric oxide synthase restricts intracellular microbes

A chief IFNγ-mediated effector function in murine macrophages is the production of nitric oxide (NO) by inducible nitric oxide synthase (iNOS), also called NOS2. In mice, iNOS is a powerful antimicrobial effector required for restriction of intracellular bacteria including *M. tuberculosis, S. enterica, C. burnetti, L. monocytogenes* and of intracellular parasites including *T. cruzi, T. gondii, Leishmania* spp., certain *Plasmodia* species, and *Schistosoma mansonii*, as well as of certain viruses and fungi [34,35].

NO is produced in virtually all nucleated cells by the constitutive NO synthases NOS1 and NOS3, with roles ranging from the regulation of blood pressure to signaling in the central nervous system. However, its toxic microbicidal potential is revealed when NO builds up to critical concentrations. While the enzymatic activity of NOS1 and NOS3 is regulated by cellular calcium ion flux and is therefore short-lived, NOS2 is able to produce NO continuously. As a result, levels of NO produced by NOS2 in activated macrophages are orders of magnitude higher than in other cells. At high concentrations, NO reacts with elemental oxygen or thiols to form highly cytotoxic unstable intermediates in amounts that approach millimolar concentrations. Like ROS, these reactive nitrogen intermediates (RNI) can damage proteins, lipids, and nucleic acids. In addition, the reaction of NO with ROS produces dual ROS/RNI entities that are highly cytotoxic as well [36].

Beyond its roles in direct antimicrobial action, recent work has uncovered additional functions of NO in macrophages. A regulatory role for NO has been implicated in paracrine modulation of T cell function [37] as well in cell-intrinsic regulation of gene expression by modification of histone demethylases [38]. In addition, loss of iNOS has profound effects on the transcriptome of IFNγ-activated or *M. tuberculosis*-infected macrophages [39]. NO-dependent

apoptosis has been observed in macrophages infected with *M. tuberculosis* as well, resulting in enhanced pathogen clearance [40]. In addition, NO-dependent nitrosylation of cGMP leads to the production of a mediator, 9-nitro-cGMP, that induces autophagy and clearance of cytosolic bacteria in activated macrophages [41].

Notably, NO is a diffusible gas that can spread throughout as well as outside the host cell. The indiscriminate oxidizing and nitrosylating properties of RNI can lead to substantial bystander damage at the cell and tissue levels in the host [42]. In addition, the vasodilatory actions of NO can affect pathology in tissues when diffusion outside of macrophages is high, contributing to sepsis in extreme cases [43]. Therefore, like many immune effectors, iNOS can be a double-edged sword. In primary mouse macrophages, post-translational modification of iNOS led to association of ~50% of the enzyme with phagosomal membranes, thereby partially targeting the cytotoxic effects of RNI [44]. However, the effect is partial, and may be specific to certain macrophage types; in macrophage cell lines, phagosomal localization of iNOS was not observed [45].

The role of iNOS in human macrophages remains poorly defined, due to the inability to induce its expression in human monocytes and macrophages in vitro. However, NO levels in patient samples are consistent with robust iNOS activity. Furthermore, macrophages from blood or tissue samples from patients with chronic inflammatory or infectious diseases readily induce iNOS upon stimulation with IFNγ or combinations of other macrophage-activating stimuli. These studies have revealed that the regulation of NOS2 expression in humans is more complex than it is in the mouse. In the absence of a robust experimental system to assay the role and function of iNOS in human infection, this area remains poorly understood [34,46].

IFNγ-mediated mechanisms limit the availability of nutrients in the microbial vacuole

A different strategy to restrict intracellular pathogens involves limiting the supply of nutrients in the phagosome or microbial vacuole. The IFNγ-induced ion pump natural resistance-associated

macrophage protein 1 (NRAMP1) decreases intraphagosomal concentrations of Mg++ and Fe++ by localizing to phagosomal membranes and actively transporting these cations into the cytosol [11]. The Fe++ transporter ferroportin-1 is upregulated in response to IFNγ in some macrophage types and exports iron through both the phagosomal [47] and the plasma membrane [48]. Meanwhile, IFNγ signaling decreases macrophage iron uptake from the environment by downregulating the iron receptor ferritin [48].

Amino acid deprivation in the phagosome is accomplished by the cytosolic enzyme indoleamine 2,3-dioxygenase (IDO), which depletes cytosolic stores of tryptophan by conversion to the metabolite N-formylkynurenine [48]. Together, the nutrient-depleting mechanisms of IFNγ-activated macrophages have been demonstrated to play a nonredundant role in the restriction of bacterial (*Chlamydia* spp., *Francisella tularensis*) and parasitic (*Leishmania* spp., *T. gondii*) infections [48].

IRG proteins, induced by IFNγ in mice, influence phagosome maturation in mice and humans

Phagosomes in IFNγ-stimulated macrophages may be induced to mature due to p47 GTPases, also known as immunity-related GTPases (IRGs). In mice, there are 23 IRGs, many transcriptionally regulated by IFNγ. Upon infection, the IRGs relocalize from the ER or Golgi apparatus to phagosome membranes [49]. Different GTPases have been implicated in resistance to different pathogens in mouse models [50]. However in human cells, only three IRGs are conserved; two are pseudogenes, and the remaining gene, IRGM, is not transcriptionally responsive to IFNγ [51]. However, siRNA inhibition has confirmed the role of IRGM in IFNγ or rapamycin-induced autophagy as well as IFNγ-induced mycobacterial growth restriction in human cells [52]; furthermore, IRGM genetic variation has been linked to human susceptibility to MTb [53].

Four hypotheses for the role of IRGs in phagosome maturation have been proposed; they are not incompatible, and may be tailored to cellular conditions or specific pathogens [54]. First, the IRG proteins may drive phagosome maturation upon their recruitment to the pathogen-containing phagosome [55]. Second, they may induce vesiculation of the pathogen-bearing phagosome, effectively destroying its protective vacuolar niche and depositing it into the cytosol for subsequent autophagic degradation [56]. Third, the bacterial phagosome itself may be autophagocytosed, perhaps as a result of damage or modification by its resident bacterium [52]. Finally, IRG proteins may also help recruit Golgi-derived lipids to the phagosome [57]. More work is needed to elucidate and differentiate the IRG-dependent and independent mechanisms of IFNγ-activated phagosome maturation in macrophages.

Other effects of IFNγ on the phagosomal environment

There is limited evidence for the effects of IFNγ on the intraphagosomal environment. For example, the antimicrobial peptide hepcidin is upregulated in IFNγ-activated, *M. tuberculosis*-infected macrophages, localizes to the phagosome, and damages mycobacteria [10]

The regulatory effect of IFNγ on many of the proteins and lipids classically associated with phagosome maturation, however is still unknown. Notably, previous experiments with mouse macrophages have shown that contrary to expectation, IFNγ stimulation *decelerates* fusion events between phagosomes and lysosomes early after phagocytosis [17], although older experiments have shown the opposite result [58]. Instead, IFNγ appears to extend the time window in which phagosomes acquire lysosomal elements, from 0-2h after phagocytosis in resting macrophages to 0-10h in IFNγ-activated macrophages, perhaps to enhance antigen presentation. Therefore, IFNγ modulates the duration, selectivity, targeting of vesicle trafficking events [17].

IFNγ-induced cell death

"Sacrificial" cell death by infected macrophages represents another class of responses that can restrict intracellular pathogens. Recent work has shown that IFNγ-mediated induction of caspase-11 and the GBP proteins (GBP1-3, GBP5, GBP7) facilitates the rapid, pyroptotic death of BMMs infected with *L. pneumophila* [59]. Other modes of sacrificial cell death have been described in the control of vacuolar pathogens as well. At high moieties of infection (MOI), macrophages infected with *M. tuberculosis* undergo IFNg-mediated cell death that displays properties of both apoptosis and necrosis [60]; evidence suggests that *M. tuberculosis* actively subverts the antibacterial apoptotic response to instead stimulate necrotic death, which facilitates opportunistic spreading of the bacteria [61]. At lower MOIs, apoptosis followed by efferocytosis is an efficient restriction mechanism in macrophages infected with *M. tuberculosis* [62,63]. The contribution of IFNγ to efferocytotic restriction of *M. tuberculosis*, however, was not investigated.

IFNγ has been shown to enhance phagocytic clearance of apoptotic cells in macrophages derived from patients deficient in a key subunit of phagocyte oxidase subunit [64], but the relevance to infected macrophages in other genetic backgrounds remains to be determined. Likewise, the contribution of IFNγ to a variety of modes of inflammasome-mediated pyroptosis remains unknown. Current research is focused on determining the regulation of each mechanism, delineating the scope of pathogens to which each is applicable, and determining what other potential pathways of sacrificial death may play a role in infected cells [65].

Macrophage pathogen sensing

In addition to possessing receptors for cytokines like IFNγ, macrophages have an array of innate immune sensors that alert the cell to infection and facilitate the tailoring of immune responses (**Fig. 1-2**). These sensors are located both in the cytosol and on vacuolar or the cell plasma membrane, and transduce direct and indirect signals to immune effectors toward the goals of pathogen degradation or suicidal host cell death. Innate immune sensors are also called pattern recognition

receptors (PRRs) to reflect the fact that they detect classes of ligands that match a particular template (called a pathogen-associated molecular patterns, or PAMP), such as lipopolysaccharide (LPS) bacterial cell wall components or hypomethylated DNA, and to distinguish them from the exquisitely specific antigen receptors of the adaptive immune system. The chief families of PRRs, as classified by structure and function, are Toll-like receptors (TLRs), phagocytic receptors, cytosolic nucleic acid sensors, Nod-like receptors (NLRs), and inflammasomes [66].

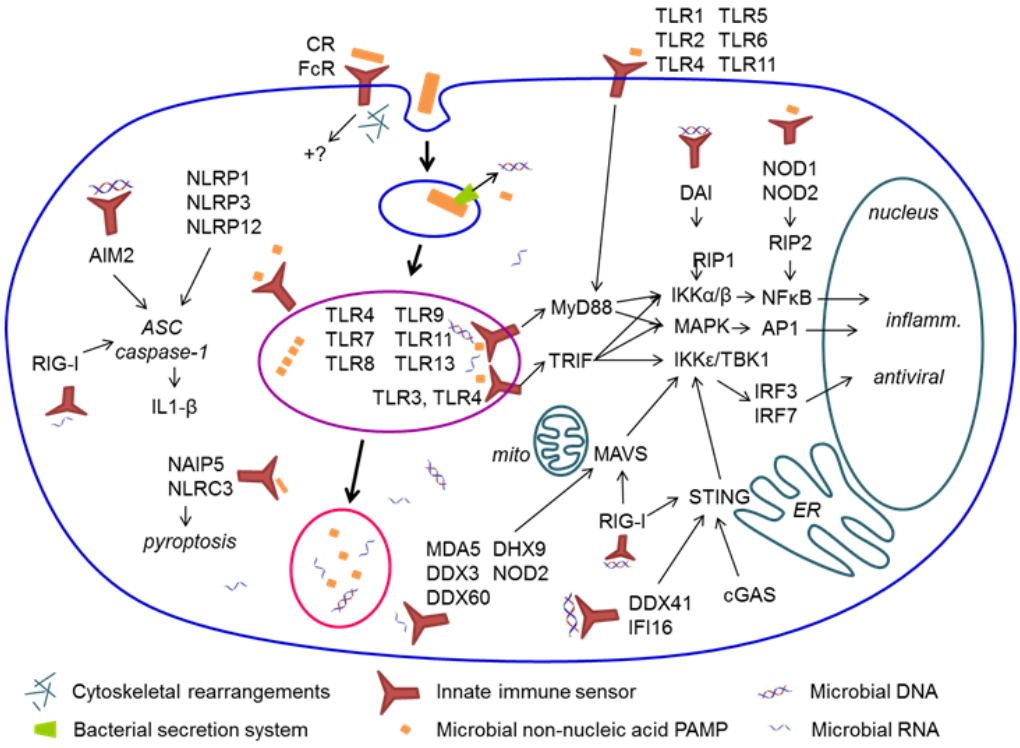

Fig. 1-2. Innate immune sensing of vacuolar pathogens

A partial collection of known sensors and pathways that respond to microbial ligands in the phagosome or translocated into the cytosol. TLRs drive inflammatory and antiviral gene expression programs through MYD88 and TRIF. NLRs and some nucleic acid sensors promote inflammatory IL-1β production and/or pyroptosis; NLRs may affect phagosome maturation. Cytosolic nucleic acid sensors drive inflammatory and antiviral gene expression, primarily through MAVS and STING. Phagocytic receptors induce cytoskeletal rearrangements, and may promote other responses as well. (Adapted from [66–68])

Recognition and signaling by TLRs

The Toll-like family of PRRs is a diverse and ancient array of sensors for a variety of microbial threats [69,70]. At the plasma membrane, bacterial components are sensed by TLRs 1 and 6 (lipoproteins), TLR2 (Gram-positive peptidoglycans, mycobacterial glycolipids, porins, atypical LPS), TLR4 (Gram-negative LPS), and TLRs 5 and 11 (flagellin) [66,71,72]. Also at the plasma membrane, parasites are sensed by TLR2 (mucins), viruses by TLR2 (hemagglutinin) and TLR4 (some viral fusion proteins), and fungi by TLR2, 4, and 6 (zymosan and mannans) [66,71]. TLR4 is internalized into endocytic and phagocytic vesicles and participates in sensing and signaling from these compartments as well as from the plasma membrane [72]. In addition, within endolysosomal or phagosomal compartments, unmethylated CpG DNA from all categories of microbes is sensed by TLR9 (though in humans, only in plasmacytoid dendritic cells and B cells), bacteria are sensed by mouse TLR13 (23S rRNA), parasites are sensed by TLR9 (hemozoin-coated DNA) and mouse TLRs 11 and 12 (profilin), and viruses are sensed by TLR3 (dsRNA) and mouse TLR7/human TLR8 (ssRNA) [66,71–73].

All of the TLRs except TLR3 transduce signals to the adaptor protein myeloid differentiation primary response gene 88 (MYD88) via the localizing adaptor MYD88 adapter-like/toll-interleukin 1 receptor domain containing adaptor protein1 (Mal/TIRAP). TLR3, as well as the bimodal TLR4, signal to the adaptor TIR-domain-containing adaptor inducing IFNβ (TRIF) via the localizing adaptor TRIF-related adaptor molecule (TRAM). MYD88 and TRIF activate transcription factors and kinases in a context-dependent manner, informed by further signals from TLR co-receptors [70,74].

In general, both MYD88 and TRIF activate the canonical IKK kinases IKKα/β to promote inflammatory gene expression driven by the transcription factor NFκB, due to the phosphorylation and subsequent degradation of its inhibitory subunit IκBα [67]. In addition, MYD88 activation engages MAP kinases, resulting in activation of inflammatory gene expression via the transcription

factor activator protein 1 (AP1) [67]. Meanwhile, TRIF activates the noncanonical IκB kinases IKKε and TBK1 to promote the expression of antiviral genes, including Type I interferons, due to the phosphorylation and subsequent nuclear translocation of the transcription factors IRF3 and IRF7 [67,70,73,75]. Studies in mice deficient in individual or combinations of TLRs and/or adapters have begun to decipher the role of each TLR for different pathogens, showing that TLR deficiency can profoundly affect resistance to bacteria [76,77], parasites [78], fungi [79], and viruses [80] both in vivo and in vitro.

Recognition and signaling by phagocytic receptors

Intracellular bacteria, parasites, and fungi enter macrophages through passive or induced phagocytosis. Both modes are facilitated by phagocytic receptors on the macrophage surface, including scavenger receptors, C-type lectins, the mannose receptor, and crystallizable fragment receptor (FcR) or complement receptors for antibody- or complement-opsonized microbes, respectively [66]. The signaling roles of phagocytic receptors upon infection are difficult to separate from their roles in phagocytosis; in some cases, however, structure can provide a clue to function. For instance, the fungal-binding lectin Dectin-1 contains immunoreceptor tyrosine-based activation motif-like sequences (ITAMs) that stimulate the expression of inflammatory cytokines [66].

Recognition and signaling by cytosolic RNA sensors

While cytosolic DNA and non-host RNA are a hallmark of viral infection, nucleic acids derived from vacuolar pathogens can translocate to the host cell cytosol as well due to phagosomal permeabilization or transport through bacterial specialized secretion systems. While most of the evidence demonstrating the relevance of nucleic acid sensors in innate immunity focuses on the response to viral pathogens or cytosolic bacteria such as *L. monocytogenes*, several have been shown to either play a role in the protection against bacterial and parasitic vacuolar pathogens.

The RNA sensor retinoic acid-inducible gene I (RIG-I) detects ssRNA lacking 5' triphosphate caps characteristic of host mRNA, while the RNA sensor melanoma differentiation-associated gene 5 (MDA5) detects long dsRNA forms present in some viral replication cycles [75]. Both contain a DExD/H box RNA helicase domain to bind the ligand and a caspase activation and recruitment domain (CARD) to interact with a common downstream adaptor, mitochondrial antiviral signaling protein (MAVS, also known as IPS-1, VISA, and Cardif). Activated MAVS forms multimeric aggregates of MAVS units and adaptor proteins that serve as a platform to activate the noncanonical IκB kinases, leading to the induction of antiviral genes as described above [73,75]. RIG-I is also capable of activating a different adaptor, stimulator of type I IFN gene (STING) which, similarly to TRIF, activates both the canonical and noncanonical IκB kinases to initiate inflammatory (NFκB-driven) and antiviral (IRF3/7-driven) programs of gene expression [67,75], and activates the transcription factor STAT6 as well [81]. Data have implicated RIG-I and MDA5 in sensing of RNA translocated to the host cytosol by the vacuolar bacteria *L. pneumophila* [82], while another study has demonstrated MAVS-dependent responses to *L. pneumophila* that are independent of RIG-I and MDA5 [83]. Curiously, RIG-I has also been linked to *L. pneumophila* sensing in a roundabout manner, by binding to RNA transcribed by host RNA polymerase III using translocated bacterial DNA as a template [84].

In addition to RIG-I and MDA5, several other RNA helicases have been linked to MAVS activation and the downstream activation of noncanonical IκB kinases and the antiviral transcription factors IRF3 and IRF7, including DDX3 (ssRNA), DHX9 (dsRNA), and DDX60 (both ssRNA and dsRNA) [67]. Another group of dsRNA helicases, comprised of DDX1, DDX21, and DHX36, interact with the adaptor protein TRIF previously described in the context TLR3/4 signaling, leading to the activation of both canonical (NFκB –activating) and noncanonical IκB kinases as described above [67,73,85]. In addition, upon binding dsRNA, the leucine-rich repeat in flightless-I interacting protein 1 (LRRFIP1) interacts with β-catenin, which translocates to the nucleus and acts as a

potentiator of IRF3-driven transcription [67,86]. IRF3 has been shown to facilitate Type I interferon gene expression in response to infection with the vacuolar parasite *T. cruzi* independently of MAVS, possibly through the RNA sensors described above or through sensing of DNA, described below [87].

While the signaling mechanisms downstream from RNA sensing described above depend on the activation of transcription factors, the MAVS and STING-activating dsRNA sensor RIG-I also triggers an entirely different, post-transcriptionally regulated cellular machinery: the inflammasome. Upon binding dsRNA, RIG-I is thought to facilitate the assembly of multimeric complexes of apoptosis-associated speck-like protein containing a CARD (ASC) and caspase-1, called ASC inflammasomes [67,88]. Inflammasome assembly results in activation of caspase-1, which cleaves cytosolic reserves of pro-IL-1β to active, proinflammatory IL-1β. The response to microbial RNA is therefore diverse, and follows several nonredundant pathways.

Recognition and signaling by cytosolic DNA sensors

Several redundant sensors recognize microbial or aberrantly localized host DNA in the cytosol. DDX60, DHX36, and LRRFIP are thought to recognize cytosolic DNA as well as RNA. In the case of DDX60, activation leads to formation of MAVS complexes and IRF3/7-driven expression of antiviral genes due to activation of noncanonical IκB kinases [67]. In the case of DHX36, DNA binding leads to interaction with STING, which activates both the canonical and noncanonical IκB kinases to initiate inflammatory (NFκB-driven) and antiviral (IRF3/7-driven) programs of gene expression [67,73,85]. Notably, data from *M. tuberculosis*-infected macrophages deficient in the cytosolic DNase Trex1 suggest a role for STING in detection of mycobacterial DNA secreted into the cytosol [89], though the identity of the DNA sensor is unknown. DNA-bound LRRFIP, meanwhile, activates β-catenin to enhance the transcriptional activity of IRF3 [67].

The dedicated DNA helicases IFI16 and DDX41 also interact with STING to initiate inflammatory (NFκB-driven) and antiviral (IRF3/7-driven) programs of gene expression [67,73,85]. In plasmacytoid dendritic cells, the DNA helicases DHX36 and DHX9 activate TRIF and MYD88, respectively, leading to the induction of gene expression programs driven by IRF3 and NFκB or by IRF7 [67].

The dedicated DNA sensor absent in melanoma-2 (AIM2) assembles caspase-1-activating inflammasome complexes with ASC to produce mature, inflammatory IL-1β [67,73,85]. AIM2 plays a major role in recognition of bacteria that escape the phagosome to reach the cytosol [90], but is also activated in infection by the non-pathogenic vacuolar *Mycobacterium bovis* [91]. Evidence from macrophages infected with pathogenic *M. tuberculosis* and *L. pneumophila* is consistent with a model in which bacterial effector proteins counter-evolved to thwart sensing mechanisms, such as AIM2, by minimizing the cytosolic release of nucleic acids [92,93].

The DNA-dependent activator of IRFs (DAI), also called Z-DNA–binding protein (ZBP), is hypothesized to activate the STING-dependent antiviral and inflammatory signaling pathways [67]. However, DAI is also thought to form interactions with three other branches of innate immune signaling [94]. First, DAI interacts with TBK1 directly to activate IRF3. Second, DAI activates the receptor-interacting protein 1 (RIP1), which signals to NFκB via the canonical IκB kinases. Finally, interactions of DAI with receptor-interacting protein 3 (RIP3) lead to caspase-independent necrosis [94].

Several DNA damage response elements have been implicated in cytosolic DNA sensing, in a cell type-dependent manner. In mouse dendritic cells, as well as some human cell types, evidence links the meiotic recombination 11 (MRE11), a key player in recognition and initiation of double-stranded breaks in nuclear DNA, to the activation of STING and IRF3 [85,95].

Finally, recent evidence is consistent with a major role for the cyclic GMP-AMP synthase

(cGAS) as a cytosolic DNA sensor [85]. Upon binding dsDNA, cGAS synthesizes the second messenger molecule cyclic GMP-AMP (cGAMP). This small molecule binds directly to STING to initiate IRF3 and NFkB-dependent transcription [85].

Recognition and signaling by sensors of bacterial cyclic dinucleotides

It has recently been appreciated that the DNA sensor DDX41 as well as the DNA sensing adaptor protein STING also function as sensors of cyclic dinucleotides. As mentioned above, STING binds to cGAMP produced by host cGAS upon sensing of cytosolic DNA. In contrast to sensing second messengers produced by the host, however, both STING and DDX41 are able to sense the bacterial cyclic dinucleotide c-di-GMP and initiate a signaling response [96,97]. Furthermore, DDX41 recognizes bacterial c-di-AMP, a second type of cyclic dinucleotide, as well [97]. In macrophage cell lines infected with modified strains of *L. pneumophila*, the induction of Type I interferon in response to infection directly correlated with the levels of c-diGMP or c-diAMP secreted by each strain [98]. The response was partially dependent on TBK1 and IRF3, as well as the Type I interferon receptor IFNAR and Type I/II interferon-activated signal transducer and activator of transcription 1 (STAT1) [98]. Candidate sensors of these bacterial ligands identified by mass spectrometry included the phagosomal protein coronin 1A, mRNA cap guanine-N7 methyltransferase, and cyclophilin H [98]. Consistent with other mechanisms of pathogen sensing, macrophages likely use redundant mechanisms to detect bacterial cyclic dinucleotides; however, STING is thought to be the major signaling adaptor for these diverse receptors [99,100]

Recognition and signaling by NODs and NLRs

Another important arm of the cytosolic surveillance machinery is made up of the nucleotide-binding and oligomerization domain (NOD) proteins and the NOD-like receptors (NLRs), which detect a variety of microbial ligands. There are 23 known NODs and NLRs in human cells, and 34 in

mouse cells [72], classified into five categories by their N-terminal effector domains: NLRA (acidic activation domain), NLRB (baculoviral inhibitory repeat, or BIR-like domain, also called NLR family, apoptosis inhibitory protein 5 [NAIP]), NLRC (caspase activating and recruitment domain, or CARD), NLRP (pyrin domain), and NLRX (no domain homology) [101]. Several NODs and NLRs that have been implicated in responses to vacuolar pathogens are mentioned below.

The NLRC receptors NOD1 and NOD2, known to be activated by bacterial peptidoglycan, facilitate an inflammatory NFκB-driven response to *S. typhimurium* in a manner dependent on bacterial secretion through the phagosomal membrane [102] and are critical to control of infection with *L. pneumophila* [103], *T. cruzi* (via NOD1) [104], and *T. gondii* (via NOD2) [105] *in vivo*. NOD1/2, as well as the orphan receptor NLRP4 (also known as NACHT-LRR-PYD-containing protein-4 or NALP4, and as pyrin-containing APAF-1-like protein 4 or PYPAF4), are also involved with the recruitment and modulation of autophagic machinery at newly formed bacterial phagosomes of the cytosolic bacteria *L. monocytogenes, Shigella flexneri*, and the extracellular bacteria *Staphylococcus aureus* [106,107], though it is not known whether they fulfill similar functions in the context of vacuolar pathogens.

NLRC4 (also known as interleukin-converting enzyme protease-activating factor, or IPAF) is a sensor for the flagellins and/or secretion system "needle" proteins of some vacuolar bacteria, including *Salmonella* spp. and *L. pneumophila*, in tandem with NAIP1 (human NLRB) or mouse NAIP5 [108–114]. In concert with cytokine signaling, NLRC4/NAIP5 trigger inflammasome assembly and rapid programmed death, termed pyroptosis, in the host macrophage following *L. pneumophila* infection, thus restricting intracellular bacterial restriction [115].

NLRP1, also called NACHT leucine-rich-repeat protein 1 (NALP1), and NLRP3 sense and trigger an inflammasome-mediated response to the vacuolar parasite *T. gondii* [116]. NLRP3 also facilitates an inflammatory, IL-1β response to a virulence factor secreted into the cytosol by *M. tuberculosis* [117]. NLRP3 was also found to be recruited to the maturing phagosomes of

phagocytosed Gram-positive bacteria and to facilitate phagosome acidification, though it is unknown whether the effect extends to vacuolar pathogens [118]. NLRP12 (also called Monarch-1) facilitate inflammasome-mediated IL-1β and IL-12 production in vacuolar *Y. pestis* [119]. However, NLR sensors that are inflammatory in certain contexts can play an inhibitory role as well, illustrated by modulation of the macrophage response to *M. tuberculosis* and *S. typhimurium* by NLRP12 [90,120].

Effects of pathogen sensing on IFNγ-mediated effectors

Studies have begun to reveal mechanisms by which cell-autonomous innate immune sensing affects IFNγ activation in macrophages. Several interactions are known to occur at the level of signaling and transcription [121–123]. Little remains known, however, about the effects of innate sensing on pathogen restriction in IFNγ-activated cells.

The IFNγ signaling cascade

IFNγ responses are facilitated by the transcriptional activity of homodimers of the transcription factor STAT1, also known as gamma-activated factor (GAF). Ligation of the IFNγ receptor (a heterodimer of subunits IFNGR1 and IFNGR2) on the cell surface leads to receptor crosslinking, creating cytosolic domains that recruit adaptor proteins [26]. The canonical sequence of macrophage activation by IFNγ involves the recruitment of Janus kinases 1 and 2 (JAK1-2), autophosphorylation of JAK2, and phosphorylation of JAK1 by JAK2 [26]. Jak1 then phosphorylates the IFNGR cytoplasmic tail to create a docking site to recruit monomers of inactive signal transducer and activator of transcription 1 (STAT1) [26]. Subsequently, JAK2 phosphorylates bound STAT1 on tyrosine residue 701 (Y701) [26]. This signaling is not strictly dependent on JAK1, due to partial redundancy within the JAK family [124]. Noncanonical JAK2-independent activation of STAT1pY701 homodimers in response to IFNγ signaling have been described as well, dependent on

the activity of phosphatidylinositol 3-kinase [125].

STAT1pY701 forms parallel homodimers upon dissociation from the IFNGR/JAK complex and translocates to the nucleus, where it drives gene expression from promoters containing IFNγ activation site (GAS) elements [26,126]. STAT1 homodimers occupy DNA for only a brief time, especially if they become acetylated at lysines 410 and 413, perhaps by the action of histone acetylase proteins [126]. As STAT1 homodimers dissociate from DNA, they take on an antiparallel configuration that expose them to nuclear phosphatases, and trigger export from the nucleus [126].

In addition, Jak1-dependent yet STAT1-independent effects of IFNγ signaling on gene expression have been described in $STAT1^{-/-}$ mice [127]. The effects of STAT1-independent IFNγ-mediated macrophage activation on vacuolar pathogens are not yet understood.

IFNγ signaling is amplified by the effects of transcription factors themselves induced by IFNγ. Three members of the IRF family of transcription factors, IRF1, IRF2, and IRF9, are IFNγ targets themselves. Most prominently, IRF1 seems to have a profound facilitating effect on GAS promoter-driven gene expression, and at high levels of IRF1, synergizes with IFNγ signals to drive apoptosis [26].

IFNγ signaling is inhibited by the suppressor of cytokine signaling (SOCS) protein SOCS1, which directly competes with IFNγ binding of the IFNGR. SOCS1 is induced by IFNγ signaling in a negative feedback loop, with duration and magnitude of expression tied tightly to the magnitude of IFNγ activation [123]. SOCS1 is essential to the prevention of unchecked IFNγ responses, which are so damaging that they lead to neonatal lethality in $SOCS1^{-/-}$ mice [126].

Effects of TLR signaling on IFNγ-activated macrophages

TLR activity potentiates the cellular response to IFNγ through multiple mechanisms [121]. First, MAP kinases activated in response to TLR signaling further phosphorylate STAT1 at serine

residue 727 (S727). The capacity of STAT1 dimers phosphorylated at both S727 and Y701 to drive gene expression at promoters bearing GAS elements is enhanced in comparison with dimers phosphorylated at Y701 only. Furthermore, expression of many IFNγ-activated transcripts is enhanced by coordinate binding and activity of the transcription factor NFkB, activated downstream of TLR signals; these genes include IRF1 and NOS2, described above, as well as the C-X-C motif chemokine 10 (CXCL10), also known as interferon gamma-induced protein 10 (IP-10), used by macrophages to attract and modulate other monocytic and lymphoid cells, and intercellular adhesion molecule 1 (ICAM-1), used by leukocytes in tissue transmigration [121]. The transcription-inducing activity of IRF1 has been described as a "second wave" of IFNγ-initiated signaling [26], and is an especially relevant potential substrate for modulation of the IFNγ-activated state.

In fluorometric studies of phagosome maturation using ligand-coated beads, IFNγ and TLR signaling produced different effects depending on whether the signals were applied together or separately. For instance, TLR and IFNγ signals alone each increased the duration of lysosome recruitment to phagosomes, but TLR and IFNγ signaling together also decreased its initial rate [17]. TLR signals may affect also IFNγ-induced autophagy to enhance phagosome maturation. TLR signaling from within the phagosome affects the recruitment of autophagic proteins to augment phagosome maturation [128].

Effects of Type I IFN on IFNγ-activated macrophages

Many TLR or nucleic acid-sensing elements in macrophages stimulate the production of Type I interferons, comprised of over a dozen subtypes of IFNα , a single IFNβ, and (in humans but not in mice) a single IFNω. The Type I and II interferons share a partially overlapping set of transcriptional targets [121,129]. One study has calculated a "beta-gamma mixture" for each target gene depending on its induction by IFNβ and/or IFNγ, concluding that the targets lie on a fairly continuous spectrum

between the two [129]. Therefore, signaling by Type I and II interferons can lead to augmentation or suppression of each in a context-dependent manner.

Antagonism between Type I and II responses has been described in human peripheral blood monocyte-derived macrophage (MDMs), particularly at low concentrations of Type I interferon [130]. However, another study in mouse embryonic fibroblasts (MEFs) found evidence that tonic IFNAR signaling primed cells for IFNγ signaling [131]. The effects of interferon cross-talk are likely to be exquisitely dependent on the context, level and duration of activation.

Type I IFN signaling antagonizes IFNγ signaling by downregulating of IFNγ receptor in mouse bone marrow-derived macrophages (BMMs) infected with cytosolic *L. monocytogenes* [132]. In human MDMs infected with *Mycobacterium leprae*, Type I IFNs suppress the IFNγ-activated expression of the antimicrobial peptides beta-defensin and cathelicidin [133].

Effects of nucleic acid sensing on IFNγ-activated macrophages

In mouse fibroblasts, the IFNγ-mediated restriction of the cytosolic bacterial pathogen *Shigella flexneri* is dependent on elements of the RNA sensing machinery, including RIG-I and MAVS [134]. In this study, RIG-I and MAVS expression levels were driven by IFNγ-activated IRF1. However, RIG-I and MAVS were both dispensable for efficient restriction of *S. flexneri* in response to IFNγ in BMMs [134].

Legionella **is a model pathogen to study IFNγ-mediated macrophage-intrinsic immunity**

Legionella pneumophila is a Gram-negative facultative intracellular bacterium that naturally parasitizes amoebae, but has adapted to live in mammalian macrophages as well. In humans, *L. pneumophila* is a significant agent of community-acquired pneumonia, which can take the form of mild Pontiac Fever or severe, life-threatening Legionnaire's disease. *L. pneumophila* grow in

permissive mouse and human macrophages *in vitro*, but its growth is restricted in cells activated by IFNγ [28,135]; furthermore, IFNγ signaling is required for control of *L. pneumophila in vivo* [136,137].

Membrane trafficking events in L.pneumophila-infected macrophages

L. pneumophila remodels the phagosome within minutes of phagocytosis, failing to acquire markers of late endosomes but instead decorating the *Legionella*-containing vacuole (LCV) with ER-derived membrane recruited from vesicular traffic from endoplasmic reticulum (ER) exit sites [138,139] and the trans-Golgi lipid PI(4)P [140]. The LCV associates with autophagy markers ATG7 and ATG8 [141], but avoids colocalization with lysosomal markers. Within the LCV, *L. pneumophila* multiply approximately every 2 hours, leading to expansion of the LCV and eventual lysis of the host cell after about 14-24h, releasing progeny bacteria to infect other host cells.

Formation of the protected LCV and bacterial survival are dependent on the bacterial Dot/Icm Type IV secretion system, which delivers over 100 virulence factors so far identified to the host cell cytosol; only several have been characterized so far. While none of the Dot/Icm substrates are essential for the bacterium, bacteria deficient in Dot/Icm itself cannot form an ER-decorated LCV, cannot replicate in cells, and are shunted into the phagosome maturation pathway [142].

IFNγ-activated cell-line or primary macrophages infected with wildtype *L. pneumophila* are similar to resting macrophages infected with Dot/Icm-deficient bacteria, based on their kinetics of acquisition of lysosomal markers, nearly identical growth restriction, and lack of ER-derived membrane on the LCV, observed at 4 hours after phagocytosis [143]. Whether *L. pneumophila* in IFNγ-stimulated macrophages fail to form an ER-decorated LCV at earlier time points is not clear. In addition, GBP proteins contribute to caspase-1-independent pyroptotic cell death that is required for restricts *L. pneumophila* in IFNγ-activated macrophages [59].

Innate immune sensing of L. pneumophila

A number of studies have investigated the role of specific innate immune signaling pathways in *L. pneumophila* restriction *in vivo*, or in the production of inflammatory signals such as Type I interferons or IL-12 in infected cells. Bacterial clearance in mice requires signaling through MYD88 [144,145], which is at least partially explained by the requirement for MYD88 for the IL-12 mediated induction of IFNγ production by NK cells [146]. TLR sensing of *L. pneumophila* is based on largely redundant signaling from TLRs2, 5, and 9 [144,145,147–150], but not TLR4 [145,149,151], due to a modified LPS structure that isinstead sensed by TLR2 [152,153].

In addition to signaling through MYD88, other sensing mechanisms responsible that facilitate the NFκB, IRF3, or IRF7-dependent induction of inflammatory responses to *L. pneumophila* infection include NOD1/2 [103,154], STING [83,155], MAVS [84], and RIP2 [156], though the requirements for each are not absolute. Notably, the studies cited above have not yielded completely consistent results, possibly because of differences in experimental technique or substrains of *L. pneumophila* used. Sensing of cytosolic ligands is dependent on the bacterial secretion system Dot/Icm [156]. The response to Dot/Icm translocated *L. pneumophila* DNA relies on IRF3 but is independent of NFκB [157]. Furthermore, AIM2 is capable of triggering a response to *L. pneumophila* DNA as well, but its action is curtailed by secreted bacterial effectors [93].

Outlook

Following the discovery of the interferons in the 1950s, the prediction of a macrophage activating factor (MAF) lymphokine that restricts intracellular pathogens in the late 1960s, and the characterization of MAF in the 1970s and early 1980s, MAF and IFNγ were recognized as one and the same in 1983 [158]. In the years since, much has been learned about the effects of IFNγ signaling on macrophages and its relevance to infectious disease by vacuolar pathogens *in vitro*, *in vivo*, and in

human disease.

Despite the breadth of knowledge about the regulation and transcriptional activation of IFNγ, immunologists are still unraveling the mechanisms by which IFNγ-activated macrophages are better able to kill or restrict intracellular pathogens. One challenge to understanding the system has been the redundancy and complexity of the pathways involved in microbial restriction. For example, BMMs derived from mice quadruply deficient in the IFNγ effectors NOS2, NOX2, IRGM1 and IRGM3 are still capable of restricting *L. pneumophila* in response to IFNγ [59]. Second, pathogens employ unique strategies for immune evasion, which mask target host mechanisms from investigation and make it challenging to generalize findings across infection models. *M. tuberculosis,* for instance, expresses two redundant protective reductase genes that provide resistance killing by ROI/RNI [159]. Third, some immune effectors are not well conserved between mice and humans. The IRG gene family, for instance, a class of 23 mostly IFNγ-regulated murine genes that significantly affect macrophage vesicle trafficking events at bacterial or parasitic phagosomes, is represented by only one functional, non-IFNγ-responsive gene in human cells [51].

Furthermore, despite our burgeoning knowledge of bacterial ligands and the pathways induced when they are sensed, relatively little is known about whether and how these innate sensing pathways affect the restriction of vacuolar pathogens in macrophages activated by IFNγ. A reasonable *a priori* assumption is that innate sensors tailor the powerful IFNγ-mediated host response based on the nature of the pathogen. However, immune signaling generally involves a number of inhibitory feedback loops that make combinatorial signal integration difficult to predict. The characterization of the IFNγ-activated state, its effectors, and its intersection with innate immune sensing remains a rich area of investigation.

The work described in this dissertation undertook two aims. First, we attempted to discover members of the vesicle trafficking machinery that facilitate bacterial restriction in IFNγ activated

macrophages, using a functional genetic screening approach. Second, we asked whether innate immune sensing during infection affected IFNγ-dependent mechanisms of microbial restriction in macrophage. We conclude with a roadmap for further investigation.

REFERENCES

1. Murray PJ, Wynn TA (2011) Protective and pathogenic functions of macrophage subsets. Nat Rev Immunol 11: 723–737. doi:10.1038/nri3073.

2. Cote CK, Van Rooijen N, Welkos SL (2006) Roles of macrophages and neutrophils in the early host response to Bacillus anthracis spores in a mouse model of infection. Infect Immun 74: 469–480. doi:10.1128/IAI.74.1.469-480.2006.

3. Bär W (1988) Role of murine macrophages and complement in experimental Campylobacter infection. J Med Microbiol 26: 55–59.

4. Qiu H, KuoLee R, Harris G, Van Rooijen N, Patel GB, et al. (2012) Role of macrophages in early host resistance to respiratory Acinetobacter baumannii infection. PloS One 7: e40019. doi:10.1371/journal.pone.0040019.

5. Goldmann O, Rohde M, Chhatwal GS, Medina E (2004) Role of macrophages in host resistance to group A streptococci. Infect Immun 72: 2956–2963.

6. Kinchen J, Ravichandran K (2008) Phagosome maturation: going through the acid test. Nat Rev Mol Cell Biol 9: 781–795. doi:10.1038/nrm2515.

7. Shui W, Sheu L, Liu J, Smart B, Petzold C, et al. (2008) Membrane proteomics of phagosomes suggests a connection to autophagy. Proc Natl Acad Sci U S A 105: 16952–16957. doi:10.1073/pnas.0809218105.

8. Kumar Y, Valdivia R (2009) Leading a sheltered life: intracellular pathogens and maintenance of vacuolar compartments. Cell Host Microbe 5: 593–601. doi:10.1016/j.chom.2009.05.014.

9. Alonso S, Pethe K, Russell DG, Purdy GE (2007) Lysosomal killing of Mycobacterium mediated by ubiquitin-derived peptides is enhanced by autophagy. Proc Natl Acad Sci U S A 104: 6031–6036. doi:10.1073/pnas.0700036104.

10. Sow FB, Florence WC, Satoskar AR, Schlesinger LS, Zwilling BS, et al. (2007) Expression and localization of hepcidin in macrophages: a role in host defense against tuberculosis. J Leukoc Biol 82: 934–945. doi:10.1189/jlb.0407216.

11. Flannagan RS, Cosío G, Grinstein S (2009) Antimicrobial mechanisms of phagocytes and bacterial evasion strategies. Nat Rev Microbiol 7: 355–366. doi:10.1038/nrmicro2128.

12. Flannagan RS, Jaumouillé V, Grinstein S (2011) The cell biology of phagocytosis. Annu Rev Pathol 7: 61–98. doi:10.1146/annurev-pathol-011811-132445.

13. Adams L, Dinauer M, Morgenstern D, Krahenbuhl J (1996) Comparison of the roles of reactive oxygen and nitrogen intermediates in the host response to Mycobacterium tuberculosis using transgenic mice. Tuber Lung Dis Off J Int Union Tuberc Lung Dis 78: 237–246.

14. Sbarra AJ, Jacobs AA, Strauss RR, Paul BB, Mitchell GW (1971) The biochemical and antimicrobial activities of phagocytizing cells. Am J Clin Nutr 24: 272–281.

15. Segal AW, Peters TJ (1976) Characterisation of the enzyme defect in chronic granulomatous disease. Lancet 1: 1363–1365.

16. Forbes JR, Gros P (2003) Iron, manganese, and cobalt transport by Nramp1 (Slc11a1) and Nramp2 (Slc11a2) expressed at the plasma membrane. Blood 102: 1884–1892. doi:10.1182/blood-2003-02-0425.

17. Yates RM, Hermetter A, Taylor GA, Russell DG (2007) Macrophage activation downregulates the degradative capacity of the phagosome. Traffic Cph Den 8: 241–250. doi:10.1111/j.1600-0854.2006.00528.x.

18. Nunes P, Demaurex N, Dinauer MC (2013) Regulation of the NADPH oxidase and associated ion fluxes during phagocytosis. Traffic Cph Den 14: 1118–1131. doi:10.1111/tra.12115.

19. Vieira OV, Botelho RJ, Rameh L, Brachmann SM, Matsuo T, et al. (2001) Distinct roles of class I and class III phosphatidylinositol 3-kinases in phagosome formation and maturation. J Cell Biol 155: 19–25. doi:10.1083/jcb.200107069.

20. Rink J, Ghigo E, Kalaidzidis Y, Zerial M (2005) Rab conversion as a mechanism of progression from early to late endosomes. Cell 122: 735–749. doi:10.1016/j.cell.2005.06.043.

21. Vergne I, Chua J, Lee H-HH, Lucas M, Belisle J, et al. (2005) Mechanism of phagolysosome biogenesis block by viable Mycobacterium tuberculosis. Proc Natl Acad Sci U S A 102: 4033–4038. doi:10.1073/pnas.0409716102.

22. Brumell JH, Scidmore MA (2007) Manipulation of Rab GTPase Function by Intracellular Bacterial Pathogens. Microbiol Mol Biol Rev 71: 636–652. doi:10.1128/MMBR.00023-07.

23. Nathan C, Murray H, Wiebe M, Rubin B (1983) Identification of interferon-gamma as the lymphokine that activates human macrophage oxidative metabolism and antimicrobial activity. J Exp Med 158: 670–689.

24. Shirahata T, Shimizu K (1982) Growth inhibition of Toxoplasma gondii in cell cultures treated with murine type II interferon. Nihon Juigaku Zasshi Jpn J Vet Sci 44: 865–871.

25. Murray HW, Rubin BY, Rothermel CD (1983) Killing of intracellular Leishmania donovani by lymphokine-stimulated human mononuclear phagocytes. Evidence that interferon-gamma is the activating lymphokine. J Clin Invest 72: 1506–1510. doi:10.1172/JCI111107.

26. Schroder K, Hertzog PJ, Ravasi T, Hume DA (2004) Interferon-gamma: an overview of signals, mechanisms and functions. J Leukoc Biol 75: 163–189. doi:10.1189/jlb.0603252.

27. Flynn J, Chan J, Triebold K, Dalton D, Stewart T, et al. (1993) An essential role for interferon gamma in resistance to Mycobacterium tuberculosis infection. J Exp Med 178: 2249–2254.

28. Klein T, Yamamoto Y, Brown H, Friedman H (1991) Interferon-gamma induced resistance to Legionella pneumophila in susceptible A/J mouse macrophages. J Leukoc Biol 49: 98–9103.

29. Suzuki Y, Orellana M, Schreiber R, Remington J (1988) Interferon-gamma: the major mediator of resistance against Toxoplasma gondii. Science 240: 516–518.

30. Buchmeier N, Schreiber R (1985) Requirement of endogenous interferon-gamma production for resolution of Listeria monocytogenes infection. Proc Natl Acad Sci U S A 82: 7404–7408.

31. Zhang S-YY, Stéphanie B-D, Chapgier A, Yang K, Bustamante J, et al. (2008) Inborn errors of interferon (IFN)-mediated immunity in humans: insights into the respective roles of IFN-alpha/beta, IFN-gamma, and IFN-lambda in host defense. Immunol Rev 226: 29–40. doi:10.1111/j.1600-065X.2008.00698.x.

32. Crawford RM, Leiby DA, Green SJ, Nacy CA, Fortier AH, et al. (1994) Macrophage activation: a riddle of immunological resistance. Immunol Ser 60: 29–46.

33. Schaible U, S S-K, Schlesinger P, Russell D (1998) Cytokine activation leads to acidification and increases maturation of Mycobacterium avium-containing phagosomes in murine macrophages. J Immunol Baltim Md 1950 160: 1290–1296.

34. MacMicking J, Xie QW, Nathan C (1997) Nitric oxide and macrophage function. Annu Rev Immunol 15: 323–350. doi:10.1146/annurev.immunol.15.1.323.

35. Chakravortty D, Hensel M (2003) Inducible nitric oxide synthase and control of intracellular bacterial pathogens. Microbes Infect Inst Pasteur 5: 621–627.

36. Nathan C, Shiloh M (2000) Reactive oxygen and nitrogen intermediates in the relationship between mammalian hosts and microbial pathogens. Proc Natl Acad Sci U S A 97: 8841–8848.

37. Bingisser RM, Tilbrook PA, Holt PG, Kees UR (1998) Macrophage-derived nitric oxide regulates T cell activation via reversible disruption of the Jak3/STAT5 signaling pathway. J Immunol Baltim Md 1950 160: 5729–5734.

38. Hickok JR, Vasudevan D, Antholine WE, Thomas DD (2013) Nitric oxide modifies global histone methylation by inhibiting Jumonji C domain-containing demethylases. J Biol Chem 288: 16004–16015. doi:10.1074/jbc.M112.432294.

39. Ehrt S, Schnappinger D, Bekiranov S, Drenkow J, Shi S, et al. (2001) Reprogramming of the macrophage transcriptome in response to interferon-gamma and Mycobacterium tuberculosis: signaling roles of nitric oxide synthase-2 and phagocyte oxidase. J Exp Med 194: 1123–1140. doi:10.1084/jem.194.8.1123.

40. Herbst S, Schaible U, Schneider B (2011) Interferon gamma activated macrophages kill mycobacteria by nitric oxide induced apoptosis. PloS One 6. Available: http://dx.doi.org/10.1371/journal.pone.0019105.

41. Ito C, Saito Y, Nozawa T, Fujii S, Sawa T, et al. (2013) Endogenous Nitrated Nucleotide Is a Key Mediator of Autophagy and Innate Defense against Bacteria. Mol Cell 52: 794–804. doi:10.1016/j.molcel.2013.10.024.

42. Perrone LA, Belser JA, Wadford DA, Katz JM, Tumpey TM (2013) Inducible Nitric Oxide Contributes to Viral Pathogenesis Following Highly Pathogenic Influenza Virus Infection in Mice. J Infect Dis 207: 1576–1584. doi:10.1093/infdis/jit062.

43. Fortin CF, McDonald PP, Fülöp T, Lesur O (2010) Sepsis, leukocytes, and nitric oxide (NO): an intricate affair. Shock Augusta Ga 33: 344–352. doi:10.1097/SHK.0b013e3181c0f068.

44. Vodovotz Y, Russell D, Xie Q, Bogdan C, Nathan C (1995) Vesicle membrane association of nitric oxide synthase in primary mouse macrophages. J Immunol Baltim Md 1950 154: 2914–2925.

45. Webb J, Harvey M, Holden D, Evans T (2001) Macrophage nitric oxide synthase associates with cortical actin but is not recruited to phagosomes. Infect Immun 69: 6391–6400. doi:10.1128/IAI.69.10.6391-6400.2001.

46. Fang FC, Vazquez-Torres A (2002) Nitric oxide production by human macrophages: there's NO doubt about it. Am J Physiol Lung Cell Mol Physiol 282: L941–943. doi:10.1152/ajplung.00017.2002.

47. Van Zandt KE, Sow FB, Florence WC, Zwilling BS, Satoskar AR, et al. (2008) The iron export protein ferroportin 1 is differentially expressed in mouse macrophage populations and is present in the mycobacterial-containing phagosome. J Leukoc Biol 84: 689–700. doi:10.1189/jlb.1107781.

48. MacMicking JD (2012) Interferon-inducible effector mechanisms in cell-autonomous immunity. Nat Rev Immunol 12: 367–382. doi:10.1038/nri3210.

49. Tiwari S, Choi H-P, Matsuzawa T, Pypaert M, MacMicking J (2009) Targeting of the GTPase Irgm1 to the phagosomal membrane via PtdIns(3,4)P(2) and PtdIns(3,4,5)P(3) promotes immunity to mycobacteria. Nat Immunol 10: 907–917. doi:10.1038/ni.1759.

50. Henry SC, Daniell XG, Burroughs AR, Indaram M, Howell DN, et al. (2009) Balance of Irgm protein activities determines IFN-gamma-induced host defense. J Leukoc Biol 85: 877–885. doi:10.1189/jlb.1008599.

51. Bekpen C, Hunn JP, Rohde C, Parvanova I, Guethlein L, et al. (2004) The interferon-inducible p47 (IRG) GTPases in vertebrates: loss of the cell autonomous resistance mechanism in the human lineage. Genome Biol 6. Available: http://dx.doi.org/10.1186/gb-2005-6-11-r92.

52. Singh SB, Davis AS, Taylor GA, Deretic V (2006) Human IRGM induces autophagy to eliminate intracellular mycobacteria. Science 313: 1438–1441. doi:10.1126/science.1129577.

53. Intemann CD, Thye T, Niemann S, Browne ENL, Amanua Chinbuah M, et al. (2009) Autophagy gene variant IRGM -261T contributes to protection from tuberculosis caused by Mycobacterium tuberculosis but not by M. africanum strains. PLoS Pathog 5: e1000577. doi:10.1371/journal.ppat.1000577.

54. Taylor GA, Feng CG, Sher A (2007) Control of IFN-gamma-mediated host resistance to intracellular pathogens by immunity-related GTPases (p47 GTPases). Microbes Infect Inst Pasteur 9: 1644–1651. doi:10.1016/j.micinf.2007.09.004.

55. MacMicking J, Taylor G, McKinney J (2003) Immune control of tuberculosis by IFN-gamma-inducible LRG-47. Science 302: 654–659. doi:10.1126/science.1088063.

56. Ling YM (2006) Vacuolar and plasma membrane stripping and autophagic elimination of Toxoplasma gondii in primed effector macrophages. J Exp Med 203: 2063–2071. doi:10.1084/jem.20061318.

57. Nelson DE, Virok DP, Wood H, Roshick C, Johnson RM, et al. (2005) Chlamydial IFN-gamma immune evasion is linked to host infection tropism. Proc Natl Acad Sci U S A 102: 10658–10663. doi:10.1073/pnas.0504198102.

58. Kielian M, Cohn Z (1981) Modulation of phagosome-lysosome fusion in mouse macrophages. J Exp Med 153: 1015–1020.

59. Pilla DM, Hagar JA, Haldar AK, Mason AK, Degrandi D, et al. (2014) Guanylate binding proteins promote caspase-11-dependent pyroptosis in response to cytoplasmic LPS. Proc Natl Acad Sci U S A 111: 6046–6051. doi:10.1073/pnas.1321700111.

60. Lee J, Kornfeld H (2010) Interferon-γ Regulates the Death of M. tuberculosis-Infected Macrophages. J Cell Death 3: 1–11.

61. Wong K-W, Jacobs WR (2013) Mycobacterium tuberculosis exploits human interferon to stimulate macrophage extracellular trap formation and necrosis. J Infect Dis 208: 109–119. doi:10.1093/infdis/jit097.

62. Behar S, Martin C, Booty M, Nishimura T, Zhao X, et al. (2011) Apoptosis is an innate defense function of macrophages against Mycobacterium tuberculosis. Mucosal Immunol 4: 279–287. doi:10.1038/mi.2011.3.

63. Martin CJ, Booty MG, Rosebrock TR, Nunes-Alves C, Desjardins DM, et al. (2012) Efferocytosis is an innate antibacterial mechanism. Cell Host Microbe 12: 289–300. doi:10.1016/j.chom.2012.06.010.

64. Fernandez-Boyanapalli R, McPhillips KA, Frasch SC, Janssen WJ, Dinauer MC, et al. (2010) Impaired phagocytosis of apoptotic cells by macrophages in chronic granulomatous disease is reversed by IFN-γ in a nitric oxide-dependent manner. J Immunol Baltim Md 1950 185: 4030–4041. doi:10.4049/jimmunol.1001778.

65. Ashida H, Mimuro H, Ogawa M, Kobayashi T, Sanada T, et al. (2011) Host-pathogen interactions: Cell death and infection: A double-edged sword for host and pathogen survival. J Cell Biol 195: 931–942. doi:10.1083/jcb.201108081.

66. Plüddemann A, Mukhopadhyay S, Gordon S (2011) Innate immunity to intracellular pathogens: macrophage receptors and responses to microbial entry. Immunol Rev 240: 11–24. doi:10.1111/j.1600-065X.2010.00989.x.

67. Desmet CJ, Ishii KJ (2012) Nucleic acid sensing at the interface between innate and adaptive immunity in vaccination. Nat Rev Immunol 12: 479–491. doi:10.1038/nri3247.

68. Kawai T, Akira S (2011) Toll-like receptors and their crosstalk with other innate receptors in infection and immunity. Immunity 34: 637–650. doi:10.1016/j.immuni.2011.05.006.

69. Kopp E, Medzhitov R (2003) Recognition of microbial infection by Toll-like receptors. Curr Opin Immunol 15: 396–401. doi:10.1016/S0952-7915(03)00080-3.

70. Kawai T, Akira S (2010) The role of pattern-recognition receptors in innate immunity: update on Toll-like receptors. Nat Immunol 11: 373–384. doi:10.1038/ni.1863.

71. Uematsu S, Akira S (2008) Toll-Like receptors (TLRs) and their ligands. Handb Exp Pharmacol: 1–20. doi:10.1007/978-3-540-72167-3_1.

72. Broz P, Monack DM (2013) Newly described pattern recognition receptors team up against intracellular pathogens. Nat Rev Immunol 13: 551–565. doi:10.1038/nri3479.

73. Atianand MK, Fitzgerald KA (2013) Molecular basis of DNA recognition in the immune system. J Immunol Baltim Md 1950 190: 1911–1918. doi:10.4049/jimmunol.1203162.

74. Underhill DM (2003) Toll-like receptors: networking for success. Eur J Immunol 33: 1767–1775. doi:10.1002/eji.200324037.

75. Loo Y-M, Gale M (2011) Immune signaling by RIG-I-like receptors. Immunity 34: 680–692. doi:10.1016/j.immuni.2011.05.003.

76. Albiger B, Dahlberg S, Henriques-Normark B, Normark S (2007) Role of the innate immune system in host defence against bacterial infections: focus on the Toll-like receptors. J Intern Med 261: 511–528. doi:10.1111/j.1365-2796.2007.01821.x.

77. Gerold G, Zychlinsky A, de Diego JL (2007) What is the role of Toll-like receptors in bacterial infections? Semin Immunol 19: 41–47. doi:10.1016/j.smim.2006.12.003.

78. Gazzinelli RT, Denkers EY (2006) Protozoan encounters with Toll-like receptor signalling pathways: implications for host parasitism. Nat Rev Immunol 6: 895–906. doi:10.1038/nri1978.

79. Bourgeois C, Kuchler K (2012) Fungal pathogens-a sweet and sour treat for toll-like receptors. Front Cell Infect Microbiol 2: 142. doi:10.3389/fcimb.2012.00142.

80. Arpaia N, Barton GM (2011) Toll-like receptors: key players in antiviral immunity. Curr Opin Virol 1: 447–454. doi:10.1016/j.coviro.2011.10.006.

81. Holm CK, Paludan SR, Fitzgerald KA (2013) DNA recognition in immunity and disease. Curr Opin Immunol 25: 13–18. doi:10.1016/j.coi.2012.12.006.

82. Monroe KM, M M, Sarah, Vance RE (2009) Identification of host cytosolic sensors and bacterial factors regulating the type I interferon response to Legionella pneumophila. PLoS Pathog 5. Available: http://dx.doi.org/10.1371/journal.ppat.1000665.

83. Opitz B, Vinzing M, van Laak V, Schmeck B, Heine G, et al. (2006) Legionella pneumophila induces IFNbeta in lung epithelial cells via IPS-1 and IRF3, which also control bacterial replication. J Biol Chem 281: 36173–36179. doi:10.1074/jbc.M604638200.

84. Chiu Y-H, Macmillan J, Chen Z (2009) RNA polymerase III detects cytosolic DNA and induces type I interferons through the RIG-I pathway. Cell 138: 576–591. doi:10.1016/j.cell.2009.06.015.

85. Unterholzner L (2013) The interferon response to intracellular DNA: why so many receptors? Immunobiology 218: 1312–1321. doi:10.1016/j.imbio.2013.07.007.

86. Hillesheim A, Nordhoff C, Boergeling Y, Ludwig S, Wixler V (2014) β-catenin promotes the type I IFN synthesis and the IFN-dependent signaling response but is suppressed by influenza A virus-induced RIG-I/NF-κB signaling. Cell Commun Signal CCS 12: 29. doi:10.1186/1478-811X-12-29.

87. Chessler A-DC, Ferreira L, Chang T-H, Fitzgerald K, Burleigh B (2008) A novel IFN regulatory factor 3-dependent pathway activated by trypanosomes triggers IFN-beta in macrophages and fibroblasts. J Immunol Baltim Md 1950 181: 7917–7924.

88. Poeck H, Bscheider M, Gross O, Finger K, Roth S, et al. (2010) Recognition of RNA virus by RIG-I results in activation of CARD9 and inflammasome signaling for interleukin 1 beta production. Nat Immunol 11: 63–69. doi:10.1038/ni.1824.

89. Manzanillo P, Shiloh M, Portnoy D, Cox J (2012) Mycobacterium tuberculosis activates the DNA-dependent cytosolic surveillance pathway within macrophages. Cell Host Microbe 11: 469–480. doi:10.1016/j.chom.2012.03.007.

90. Vladimer GI, Marty-Roix R, Ghosh S, Weng D, Lien E (2013) Inflammasomes and host defenses against bacterial infections. Curr Opin Microbiol 16: 23–31. doi:10.1016/j.mib.2012.11.008.

91. Yang Y, Zhou X, Kouadir M, Shi F, Ding T, et al. (2013) the AIM2 inflammasome is involved in macrophage activation during infection with virulent Mycobacterium bovis strain. J Infect Dis 208: 1849–1858. doi:10.1093/infdis/jit347.

92. Saiga H, Kitada S, Shimada Y, Kamiyama N, Okuyama M, et al. (2012) Critical role of AIM2 in Mycobacterium tuberculosis infection. Int Immunol 24: 637–644. doi:10.1093/intimm/dxs062.

93. Ge J, Gong Y-NN, Xu Y, Shao F (2012) Preventing bacterial DNA release and absent in melanoma 2 inflammasome activation by a Legionella effector functioning in membrane trafficking. Proc Natl Acad Sci U S A 109: 6193–6198. doi:10.1073/pnas.1117490109.

94. Welz P-S, Pasparakis M (2012) A Way to DAI. Cell Host Microbe 11: 223–225. doi:10.1016/j.chom.2012.02.003.

95. Kondo T, Kobayashi J, Saitoh T, Maruyama K, Ishii KJ, et al. (2013) DNA damage sensor MRE11 recognizes cytosolic double-stranded DNA and induces type I interferon by regulating STING trafficking. Proc Natl Acad Sci U S A 110: 2969–2974. doi:10.1073/pnas.1222694110.

96. McWhirter SM, Barbalat R, Monroe KM, Fontana MF, Hyodo M, et al. (2009) A host type I interferon response is induced by cytosolic sensing of the bacterial second messenger cyclic-di-GMP. J Exp Med 206: 1899–1911. doi:10.1084/jem.20082874.

97. Corrigan RM, Gründling A (2013) Cyclic di-AMP: another second messenger enters the fray. Nat Rev Microbiol 11: 513–524. doi:10.1038/nrmicro3069.

98. Abdul-Sater AA, Grajkowski A, Erdjument-Bromage H, Plumlee C, Levi A, et al. (2012) The overlapping host responses to bacterial cyclic dinucleotides. Microbes Infect Inst Pasteur 14: 188–197. doi:10.1016/j.micinf.2011.09.002.

99. Diner E, Burdette D, Wilson S, Monroe K, Kellenberger C, et al. (2013) The Innate Immune DNA Sensor cGAS Produces a Noncanonical Cyclic Dinucleotide that Activates Human STING. Cell Rep 3: 1355–1361. doi:10.1016/j.celrep.2013.05.009.

100. Schaap P (2013) Cyclic di-nucleotide signaling enters the eukaryote domain. IUBMB Life 65: 897–903. doi:10.1002/iub.1212.

101. Ting JP-Y, Lovering RC, Alnemri ES, Bertin J, Boss JM, et al. (2008) The NLR Gene Family: A Standard Nomenclature. Immunity 28: 285–287. doi:10.1016/j.immuni.2008.02.005.

102. Keestra AM, Winter MG, Klein-Douwel D, Xavier MN, Winter SE, et al. (2011) A Salmonella virulence factor activates the NOD1/NOD2 signaling pathway. mBio 2. doi:10.1128/mBio.00266-11.

103. Berrington W, Iyer R, Wells R, Smith K, Skerrett S, et al. (2010) NOD1 and NOD2 regulation of pulmonary innate immunity to Legionella pneumophila. Eur J Immunol 40: 3519–3527. doi:10.1002/eji.201040518.

104. Silva GK, Gutierrez FRS, Guedes PMM, Horta CV, Cunha LD, et al. (2010) Cutting edge: nucleotide-binding oligomerization domain 1-dependent responses account for murine resistance against Trypanosoma cruzi infection. J Immunol Baltim Md 1950 184: 1148–1152. doi:10.4049/jimmunol.0902254.

105. Clay GM, Sutterwala FS, Wilson ME (2014) NLR proteins and parasitic disease. Immunol Res. doi:10.1007/s12026-014-8544-x.

106. Jounai N, Kobiyama K, Shiina M, Ogata K, Ishii KJ, et al. (2011) NLRP4 Negatively Regulates Autophagic Processes through an Association with Beclin1. J Immunol 186: 1646–1655. doi:10.4049/jimmunol.1001654.

107. Travassos LH, Carneiro LAM, Ramjeet M, Hussey S, Kim Y-G, et al. (2010) Nod1 and Nod2 direct autophagy by recruiting ATG16L1 to the plasma membrane at the site of bacterial entry. Nat Immunol 11: 55–62. doi:10.1038/ni.1823.

108. Wright E, Goodart S, Growney J, Hadinoto V, Endrizzi M, et al. (2003) Naip5 affects host susceptibility to the intracellular pathogen Legionella pneumophila. Curr Biol CB 13: 27–36.

109. Fortier A, de Chastellier C, Balor S, Gros P (2007) Birc1e/Naip5 rapidly antagonizes modulation of phagosome maturation by Legionella pneumophila. Cell Microbiol 9: 910–923. doi:10.1111/j.1462-5822.2006.00839.x.

110. Ren T, Zamboni DS, Roy CR, Dietrich WF, Vance RE (2006) Flagellin-deficient Legionella mutants evade caspase-1- and Naip5-mediated macrophage immunity. PLoS Pathog 2. Available: http://dx.doi.org/10.1371/journal.ppat.0020018.

111. Lightfield KL, Persson J, Trinidad NJ, Brubaker SW, Kofoed EM, et al. (2011) Differential requirements for NAIP5 in activation of the NLRC4 inflammasome. Infect Immun 79: 1606–1614. doi:10.1128/iai.01187-10.

112. Zhao Y, Yang J, Shi J, Gong Y-N, Lu Q, et al. (2011) The NLRC4 inflammasome receptors for bacterial flagellin and type III secretion apparatus. Nature 477: 596–600. doi:10.1038/nature10510.

113. Yang J, Zhao Y, Shi J, Shao F (2013) Human NAIP and mouse NAIP1 recognize bacterial type III secretion needle protein for inflammasome activation. Proc Natl Acad Sci U S A 110: 14408–14413. doi:10.1073/pnas.1306376110.

114. Rayamajhi M, Zak DE, Chavarria-Smith J, Vance RE, Miao EA (2013) Cutting edge: Mouse NAIP1 detects the type III secretion system needle protein. J Immunol Baltim Md 1950 191: 3986–3989. doi:10.4049/jimmunol.1301549.

115. Coers J, Vance RE, Fontana MF, Dietrich WF (2007) Restriction of Legionella pneumophila growth in macrophages requires the concerted action of cytokine and Naip5/Ipaf signalling pathways. Cell Microbiol 9: 2344–2357. doi:10.1111/j.1462-5822.2007.00963.x.

116. Ewald SE, Chavarria-Smith J, Boothroyd JC (2014) NLRP1 is an inflammasome sensor for Toxoplasma gondii. Infect Immun 82: 460–468. doi:10.1128/IAI.01170-13.

117. Mishra BB, Moura-Alves P, Sonawane A, Hacohen N, Griffiths G, et al. (2010) Mycobacterium tuberculosis protein ESAT-6 is a potent activator of the NLRP3/ASC inflammasome: Inflammasome activation during M. tuberculosis infection. Cell Microbiol 12: 1046–1063. doi:10.1111/j.1462-5822.2010.01450.x.

118. Sokolovska A, Becker CE, Ip W, Rathinam VA, Brudner M, et al. (2013) Activation of caspase-1 by the NLRP3 inflammasome regulates the NADPH oxidase NOX2 to control phagosome function. Act Caspase-1 NLRP3 Inflammasome Regul NADPH Oxidase NOX2 Control Phagosome Funct 14: 543–553. doi:10.1038/ni.2595.

119. Vladimer GI, Weng D, Paquette SWM, Vanaja SK, Rathinam VAK, et al. (2012) The NLRP12 inflammasome recognizes Yersinia pestis. Immunity 37: 96–107. doi:10.1016/j.immuni.2012.07.006.

120. Zaki MH, Man SM, Vogel P, Lamkanfi M, Kanneganti T-D (2014) Salmonella exploits NLRP12-dependent innate immune signaling to suppress host defenses during infection. Proc Natl Acad Sci U S A 111: 385–390. doi:10.1073/pnas.1317643111.

121. Schroder K, Sweet M, Hume D (2006) Signal integration between IFNgamma and TLR signalling pathways in macrophages. Immunobiology 211: 511–524. doi:10.1016/j.imbio.2006.05.007.

122. Gough D, Levy D, Johnstone R, Clarke C (2008) IFNgamma signaling-does it mean JAK-STAT? Cytokine Growth Factor Rev 19: 383–394. doi:10.1016/j.cytogfr.2008.08.004.

123. Hu X, Chakravarty SD, Ivashkiv LB (2008) Regulation of interferon and Toll-like receptor signaling during macrophage activation by opposing feedforward and feedback inhibition mechanisms. Immunol Rev 226: 41–56. doi:10.1111/j.1600-065X.2008.00707.x.

124. Kotenko SV, Izotova LS, Pollack BP, Muthukumaran G, Paukku K, et al. (1996) Other kinases can substitute for Jak2 in signal transduction by interferon-gamma. J Biol Chem 271: 17174–17182.

125. Hardy P-O, Diallo TO, Matte C, Descoteaux A (2009) Roles of phosphatidylinositol 3-kinase and p38 mitogen-activated protein kinase in the regulation of protein kinase C-alpha activation in interferon-gamma-stimulated macrophages. Immunology 128: e652–660. doi:10.1111/j.1365-2567.2009.03055.x.

126. Hu X, Ivashkiv LB (2009) Cross-regulation of signaling pathways by interferon-gamma: implications for immune responses and autoimmune diseases. Immunity 31: 539–550. doi:10.1016/j.immuni.2009.09.002.

127. Gil MP, Bohn E, O'Guin AK, Ramana CV, Levine B, et al. (2001) Biologic consequences of Stat1-independent IFN signaling. Proc Natl Acad Sci U S A 98: 6680–6685. doi:10.1073/pnas.111163898.

128. Sanjuan MA, Dillon CP, Tait SWG, Moshiach S, Dorsey F, et al. (2007) Toll-like receptor signalling in macrophages links the autophagy pathway to phagocytosis. Nature 450: 1253–1257. doi:10.1038/nature06421.

129. Ng S-LL, Friedman BA, Schmid S, Gertz J, Myers RM, et al. (2011) IκB kinase epsilon (IKK(epsilon)) regulates the balance between type I and type II interferon responses. Proc Natl Acad Sci U S A 108: 21170–21175. doi:10.1073/pnas.1119137109.

130. Yoshida R, Murray H, Nathan C (1988) Agonist and antagonist effects of interferon alpha and beta on activation of human macrophages. Two classes of interferon gamma receptors and blockade of the high-affinity sites by interferon alpha or beta. J Exp Med 167: 1171–1185. doi:10.1084/jem.167.3.1171.

131. Takaoka A, Mitani Y, Suemori H, Sato M, Yokochi T, et al. (2000) Cross talk between interferon-gamma and -alpha/beta signaling components in caveolar membrane domains. Science 288: 2357–2360.

132. Rayamajhi M, Humann J, Penheiter K, Andreasen K, Lenz L (2010) Induction of IFN-alphabeta enables Listeria monocytogenes to suppress macrophage activation by IFN-gamma. J Exp Med 207: 327–337. doi:10.1084/jem.20091746.

133. Teles RM, Graeber TG, Krutzik SR, Montoya D, Schenk M, et al. (2013) Type I interferon suppresses type II interferon-triggered human anti-mycobacterial responses. Science 339: 1448–1453. doi:10.1126/science.1233665.

134. Jehl S, Nogueira C, Zhang X, Starnbach M (2012) IFNγ inhibits the cytosolic replication of Shigella flexneri via the cytoplasmic RNA sensor RIG-I. PLoS Pathog 8. Available: http://dx.doi.org/10.1371/journal.ppat.1002809.

135. Bhardwaj N, Nash T, Horwitz M (1986) Interferon-gamma-activated human monocytes inhibit the intracellular multiplication of Legionella pneumophila. J Immunol Baltim Md 1950 137: 2662–2669.

136. Heath L, Chrisp C, Huffnagle G, LeGendre M, Osawa Y, et al. (1996) Effector mechanisms responsible for gamma interferon-mediated host resistance to Legionella pneumophila lung infection: the role of endogenous nitric oxide differs in susceptible and resistant murine hosts. Infect Immun 64: 5151–5160.

137. Shinozawa Y, Matsumoto T, Uchida K, Tsujimoto S, Iwakura Y, et al. (2002) Role of interferon-gamma in inflammatory responses in murine respiratory infection with Legionella pneumophila. J Med Microbiol 51: 225–230.

138. Horwitz M (1983) Formation of a novel phagosome by the Legionnaires' disease bacterium (Legionella pneumophila) in human monocytes. J Exp Med 158: 1319–1331.

139. Kagan JC, Roy CR (2002) Legionella phagosomes intercept vesicular traffic from endoplasmic reticulum exit sites. Nat Cell Biol 4: 945–954. doi:10.1038/ncb883.

140. Brombacher E, Urwyler S, Ragaz C, Weber SS, Kami K, et al. (2009) Rab1 guanine nucleotide exchange factor SidM is a major phosphatidylinositol 4-phosphate-binding effector protein of Legionella pneumophila. J Biol Chem 284: 4846–4856. doi:10.1074/jbc.M807505200.

141. Amer A, Swanson M (2005) Autophagy is an immediate macrophage response to Legionella pneumophila. Cell Microbiol 7: 765–778. doi:10.1111/j.1462-5822.2005.00509.x.

142. Roy C, Berger K, Isberg R (1998) Legionella pneumophila DotA protein is required for early phagosome trafficking decisions that occur within minutes of bacterial uptake. Mol Microbiol 28: 663–674. doi:10.1046/j.1365-2958.1998.00841.x.

143. Santic M, Molmeret M, Abu Kwaik Y (2005) Maturation of the Legionella pneumophila-containing phagosome into a phagolysosome within gamma interferon-activated macrophages. Infect Immun 73: 3166–3171. doi:10.1128/IAI.73.5.3166-3171.2005.

144. Hawn TR, Smith KD, Aderem A, Skerrett SJ (2006) Myeloid differentiation primary response gene (88)- and toll-like receptor 2-deficient mice are susceptible to infection with aerosolized Legionella pneumophila. J Infect Dis 193: 1693–1702. doi:10.1086/504525.

145. Archer K, Roy C (2006) MyD88-dependent responses involving toll-like receptor 2 are important for protection and clearance of Legionella pneumophila in a mouse model of Legionnaires' disease. Infect Immun 74: 3325–3333. doi:10.1128/IAI.02049-05.

146. Spörri R, Joller N, Albers U, Hilbi H, Oxenius A (2006) MyD88-dependent IFN-gamma production by NK cells is key for control of Legionella pneumophila infection. J Immunol Baltim Md 1950 176: 6162–6171.

147. Archer KA, Alexopoulou L, Flavell RA, Roy CR (2008) Multiple MyD88-dependent responses contribute to pulmonary clearance of Legionella pneumophila. Cell Microbiol 11: 21–36. doi:10.1111/j.1462-5822.2008.01234.x.

148. Bhan U, Trujillo G, Kenneth L-K, Newstead MW, Zeng X, et al. (2008) Toll-like receptor 9 regulates the lung macrophage phenotype and host immunity in murine pneumonia caused by Legionella pneumophila. Infect Immun 76: 2895–2904. doi:10.1128/IAI.01489-07.

149. Akamine M, Higa F, Arakaki N, Kawakami K, Takeda K, et al. (2005) Differential roles of Toll-like receptors 2 and 4 in in vitro responses of macrophages to Legionella pneumophila. Infect Immun 73: 352–361. doi:10.1128/IAI.73.1.352-361.2005.

150. Fuse ET, Tateda K, Kikuchi Y, Matsumoto T, Gondaira F, et al. (2007) Role of Toll-like receptor 2 in recognition of Legionella pneumophila in a murine pneumonia model. J Med Microbiol 56: 305–312. doi:10.1099/jmm.0.46913-0.

151. Lettinga KD, Florquin S, Speelman P, van Ketel R, van der Poll T, et al. (2002) Toll-like receptor 4 is not involved in host defense against pulmonary Legionella pneumophila infection in a mouse model. J Infect Dis 186: 570–573. doi:10.1086/341780.

152. Girard R, Pedron T, Uematsu S, Balloy V, Chignard M, et al. (2003) Lipopolysaccharides from Legionella and Rhizobium stimulate mouse bone marrow granulocytes via Toll-like receptor 2. J Cell Sci 116: 293–302.

153. Braedel-Ruoff S, Faigle M, Hilf N, Neumeister B, Schild H (2005) Legionella pneumophila mediated activation of dendritic cells involves CD14 and TLR2. J Endotoxin Res 11: 89–96. doi:10.1179/096805105X35189.

154. Frutuoso M, Hori J, Pereira M, Junior D, Sônego F, et al. (2010) The pattern recognition receptors Nod1 and Nod2 account for neutrophil recruitment to the lungs of mice infected with Legionella pneumophila. Microbes Infect Inst Pasteur 12: 819–827. doi:10.1016/j.micinf.2010.05.006.

155. Lippmann J, Rothenburg S, Deigendesch N, Eitel J, Meixenberger K, et al. (2008) IFNbeta responses induced by intracellular bacteria or cytosolic DNA in different human cells do not require ZBP1 (DLM-1/DAI). Cell Microbiol 10: 2579–2588. doi:10.1111/j.1462-5822.2008.01232.x.

156. Shin S, Case CL, Archer KA, Nogueira CV, Kobayashi KS, et al. (2008) Type IV secretion-dependent activation of host MAP kinases induces an increased proinflammatory cytokine response to Legionella pneumophila. PLoS Pathog 4. Available: http://dx.doi.org/10.1371/journal.ppat.1000220.

157. Stetson DB, Medzhitov R (2005) Recognition of cytosolic DNA activates an IRF3-dependent innate immune response. Immunity 24: 93–9103. doi:10.1016/j.immuni.2005.12.003.

158. Billiau A, Matthys P (2009) Interferon-gamma: a historical perspective. Cytokine Growth Factor Rev 20: 97–113. doi:10.1016/j.cytogfr.2009.02.004.

159. Lee WL, Gold B, Darby C, Brot N, Jiang X, et al. (2009) Mycobacterium tuberculosis expresses methionine sulphoxide reductases A and B that protect from killing by nitrite and hypochlorite. Mol Microbiol 71: 583–593. doi:10.1111/j.1365-2958.2008.06548.x.

Chapter 2: A screen-based approach to identify vesicle trafficking mechanisms that mediate IFNγ-induced restriction of intracellular bacteria

ABSTRACT

Vacuolar pathogens such as *Legionella pneumophila* are able to subvert the macrophage phagosome into a replicative niche. Macrophages activated by interferon gamma (IFNγ), however, are capable to overcome this subversion, leading to phagosome maturation, bacterial restriction, and macrophage survival. Our goal is to uncover IFNγ-dependent vesicle trafficking mechanisms that govern the spatial distribution and targeting of antimicrobial effectors to *L. pneumophila* vacuoles in macrophages, a process which remains poorly understood. We adopted a functional genetic screening approach to address this topic. Using shRNA in a murine macrophage cell line, we systematically perturbed each of 380 genes in a curated set of vesicle trafficking-related genes in mouse macrophages, then assessed the growth of *L. pneumophila* in resting and in IFNγ-stimulated cells. Candidate genes were selected from the screen using a robust computational method that accounts for the effects of each shRNA on host cell survival and proliferation, without relying on *a priori* assumptions about the relationship between host cell number and bacterial growth. The screen enabled the discovery of candidate *L pneumophila* host factors as well as of factors that mediate IFNγ-induced bacterial restriction. Eleven of 73 candidate host factors and 26 of 84 candidate IFNγ pathway members were validated in a secondary screen in primary murine macrophages. Functional assays of candidate proteins in wildtype macrophages, as well as bacterial restriction assays in macrophages deficient in candidate genes, further refined the list of candidate IFNγ pathway genes. While our results are inconclusive, the screen identified the tetraspanin TSPAN6 and the AP3 complex as possible elements in vesicle trafficking processes that restrict *L. pneumophila* in IFNγ-activated macrophages. Furthermore, our studies demonstrated that VTI1B and ARL8B, two key members of trafficking between endosomal and lysosomal compartments, are not required for IFNγ-mediated bacterial restriction.

INTRODUCTION

Interferon gamma (IFNγ) can activate macrophages to kill or restrict the growth of intracellular bacterial pathogens, including some that arrest phagosome maturation and replicate in resting macrophages. Although some events and entities in vesicle transport are known to affect phagosome maturation, some significant gaps in knowledge remain. First, there is a dearth of experimental evidence linking specific vesicle trafficking events to targeting of the bacterial phagosome for fusion with lysosomes, autophagy-related proteins, or other proteins or compartments involved in phagosome maturation. Second, the mechanisms by which IFNγ activation orchestrates vesicle trafficking events at the phagosome are poorly understood. Existing data indicate that IFNγ activation actually *decreases* lysosomal targeting to the phagosome with the first two hours after phagocytosis, and only cause an augmentative effect two hours after phagocytosis onwards [1]. However, experiments with intracellular bacteria such as *Legionella pneumophila* indicate that IFNγ stimulation actually results in dramatic phagosome maturation within one hour of phagocytosis [2]. The mechanism by which IFNγ overcomes phagosome maturation arrest by *L. pneumophila* within the first hours after phagocytosis is not known.

The IFNγ-dependent vesicle trafficking mechanisms that have been described so far include the targeting of GBP and IRG proteins to phagosomal compartments and several effector actions of GBPs, especially at vacuoles containing the parasitic pathogen *Toxoplasma gondii* [3,4]. For instance, IRGM1 trafficks to mycobacterial phagosomes in IFNγ –activated cells and inhibits phagosome maturation vacuoles in fibroblasts arrest [5]. IRGM5, IRGA6, and IRGB10 are involved in restriction of *Chlamydia spp*. [6,7] due in part to restriction of host lipids from the pathogen vacuole [8]. *T. gondii* vacuoles were shown to be disrupted in a process dependent on IRG proteins in IFNγ –activated fibroblasts and macrophages, exposing the parasite to the cytosol and enhancing clearance [9,10]. Meanwhile, the GBP proteins, including mouse GBP1-11, have been implicated in the IFNγ-dependent recruitment of autophagic machinery and phagocyte oxidase to mycobacterial

phagosomes [11], and in the recruitment of IRGA6 to *T. gondii* vacuoles [12]. However, the mouse IRG gene family is reduced to a single, non- IFNγ –activated gene in human cells [13], while the human GBP system lacks four of the mouse GBP genes, and both families are thought to be attenuated in humans due to decreased evolutionary pressure from *T. gondii* [14]. Meanwhile, the canonical elements of phagosome maturation, such as the maturity-defining Rab proteins Rab5 and Rab7, have not yet been found to have a specific role in the context of IFNγ –dependent pathogen restriction.

RNAi screening has been used successfully in the past to investigate both host-pathogen interactions and vesicle trafficking processes in a high-throughput fashion. Recently, a genome-wide shRNA screen in human macrophage-like THP-1 cells identified and validated six effectors of IFNγ-mediated immunity to the vacuolar pathogen *Francisella tularensis*, including two mitochondrial membrane trafficking mediators in the translocase of the outer membrane (TOM) complex [15]. Targeted screening of 36 genes encoding Nod-like receptor (NLR)-related proteins in THP-1 cells infected with *M. tuberculosis* identified a critical role for three genes in mounting an inflammatory response to the mycobacterial virulence factor ESAT6 [16]. Genome-wide dsRNA screening in *Drosophila* macrophage-like S2 hemocytes identified regulators of endogenous resistance to vacuolar *Chlamydia muridarum*, while shRNA validation supported the role of two of these factors in a human cell line [17]. In mosquito macrophage-like hemocytes, targeted dsRNA screening identified innate immune factors involved in the response to purified peptidoglycan ligands and to phagocytosed *E. coli* [18]. A study of primary human monocyte-derived macrophages (MDMs) infected with *Mycobacterium bovis* strain Bacille Calmette-Guerin combined chemical and genetic screening to locate the significant effector function of three drug candidates within the host cellular pathways of endocytosis and autophagy [19], demonstrating the potential of screening approaches in illuminating our understanding of drug targets. Multiple screens have probed the innate immune response to viruses or to purified innate immune ligands, leading among others to the discovery of

novel splicing factors for the Toll-like receptor adaptor MYD88 [20] and novel elements of the cytosolic DNA sensing machinery [21].

A number of RNAi screens have identified host factors for intracellular pathogens. Genome-wide screening in human THP1 macrophage-like cells identified autophagy-related proteins as host factors for *M. tuberculosis* [22]. Genome-wide siRNA screening in human epithelial cell lines discovered new host factors for the vacuolar pathogen *Salmonella typhimurium* [23] and recovered several known host factors for the intracellular parasite *Trypanosoma cruzi* [24]. Targeted siRNA screening identified candidate host factors for *Chlamydia trachomatis* in a human epithelial cell line [25]. Genome-wide dsRNA screening in *Drosophila* S2 hemocytes identified host factors of the vacuolar *Mycobacterium fortuitum* [26], *S. typhimurium* [27], *F. tularensis* [28], and *Chlamydia caviae* [29], while targeted screening yielded candidate host factors for the vacuolar pathogens *L. pneumophila* [30], *Brucella abortus* [31], and *Pseudomonas aeruginosa* [32]. Two and three of the candidate host factors of *C. caviae* and *F. tularensis*, respectively, were additionally validated in a human cell line by siRNA [11,12].

Vesicle trafficking mechanisms have also been successfully investigated using RNAi screening as well. Three of eight genes identified as mediators of bacterial phagocytosis in a large-scale random dsRNA screen in *Drosophila* S2 cells were validated by siRNA in mouse macrophage-like RAW264.7 cells [33]. Targeted screening in the J774A.1 mouse macrophage-like cell line discovered a common role for the small GTP-binding protein in both complement and FcR-mediated phagocytosis [34]. A targeted dsRNA screen in *C. elegans* elucidated mechanisms of phagosome maturation after engulfment of apoptotic cells [35].

The existing RNAi screen of IFNγ-induced restriction factors or *F. tularensis* identified three hits related to vesicle trafficking, including two autophagy-related proteins as well as pleckstrin 2, an actin-organizing protein that drives membrane ruffling. The study was performed as a genome-wide pooled screen, in which shRNA constructs are recovered from cells following transduction and

phenotype assay, identified by sequencing, and classified based on phenotype. After sequencing of cells from this screen, 3386 shRNA constructs were recovered from a total of 50 thousand tested, indicating that many false negatives remain to be discovered [15]. In particular, we were interested whether any other vesicle trafficking mediators, aside from autophagy-related proteins, could be involved in targeting the early bacterial phagosome.

A set of 380 mouse genes, curated by a consortium of laboratories including ours, relevant to vesicle transport in diverse biological contexts has been made available as a screening resource through the RNAi Consortium [36–38]. We therefore used this set in an arrayed screen of IFNγ-induced macrophage-intrinsic immunity to *L. pneumophila*. Phagosome composition is a fundamental fate determinant for this bacterial pathogen [39], but it is readily sensitive to IFNγ-mediated restriction. A better understanding of the re-routing of vesicles in IFNγ-activated macrophages would illuminate our understanding of the determinants of bacterial restriction *vs* host subversion, and inform the development of therapeutic regimens that combine antibiotics with immune activators to address drug-resistant vacuolar pathogens.

RESULTS

Primary RNAi screen in the RAWγNO macrophage-like cell line

Quantitation of L. pneumophila in mouse macrophages

In order to efficiently quantitate the restriction of *L. pneumophila* in macrophages, we used strain LP02 delFlaA *lux*, a bioluminescent, flagellin-deficient thymidine auxotroph compatible with both low- and high-throughput assays. The parent strain, the thymidine auxotroph LP02, is avirulent *in vivo* [40]. Furthermore, it lacks flagellin, a deficiency which has no effect on replication in "permissive," Naip5-mutant A/J strain mouse macrophages, but prevents NAIP5/NLRC3-dependent

inflammasome activation and pyroptotic host cell death in macrophages derived from mice bearing functional NAIP5 alleles, including in C57BL/6J (B6) BMMs [41]. Finally, this strain expresses the *lux* operon of *Photorhabdus luminescens*, in which the enzyme, substrate, and cofactors are transcribed under the constitutively active *ahpC* promoter. These bacteria generate a signal which is proportional to colony-forming unit (CFU) counts and enables the use of a non-endpoint assay in which individual wells can be read at repeated timepoints using a luminescence meter [42].

IFNγ-induced activity of nitric oxide synthase 2 (NOS2) is partially responsible for restriction of *L. pneumophila* in RAW264.7 murine macrophage-like cells [43]. Due to its magnitude, the NOS2-mediated response in these cells could obliterate potentially more subtle phenotypic effects induced by our genetic perturbations. In order to mask the significant effect of NOS2 and focus on pathways of interest, we used the RAW264.7 cell line derivative RAWγNO, which is deficient in NOS2 induction [44].

Stimulation of RAWγNO macrophages with IFNγ for 24h before infection with LP02 delFlaA *lux* restricts bacterial growth over the next 48h in a dose-dependent manner (**Fig 2-1a**). Over one hundred-fold reduction in signal was observed in bacteria grown in cells treated with 100U/ml IFNγ compared to mock-treated cells, a robust difference that verifies the suitability of RAWγNO host cells and the LP02 delFlaA *lux* strain of *L. pneumophila* as a model system to investigate intracellular bacterial restriction in response to IFNγ .

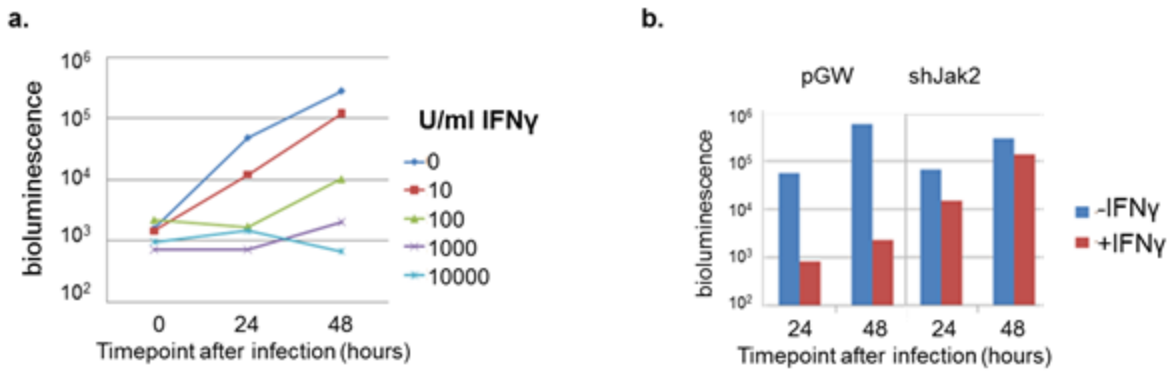

Figure 2-1. Proof of concept for primary screen

a. RAWγNO cells restrict *L. pneumophila* in an IFNγ–dependent manner. RAWγNO cells were seeded in 96-well plates,pre-stimulated with IFNγ for 24h, and infected with bioluminescent *L. pneumophila*. Bioluminescence was measured using a plate reader.

b. shRNA-based depletion of JAK2 attenuates IFNγ–dependent bacterial restriction in RAWγNO cells. RAWγNO cells were seeded in 96-well plates, infected with lentivirus encoding shRNA targeting JAK2 transcript or with control pGW lentivirus, selected with puromycin for 2 days, pre-stimulated with IFNγ for 24h, and infected with bioluminescent *L. pneumophila*. Bioluminescence was measured using a plate reader.

Lentiviral knockdown of vesicle trafficking genes

A proof-of-concept experiment of the primary screen showed that shRNA-based knockdown of JAK2, a key signaling adaptor of the IFNγ pathway, could attenuate the IFNγ-dependent bacterial restriction phenotype in RAWγNO cells (**Fig 2-1b**).

Arrayed screening was performed using the mouse vesicle trafficking set and control shRNAs, both from the RNAi Consortium [36]. Each gene is targeted by multiple shRNA sequences (on average, 5 shRNAs/gene), and each shRNA sequence is delivered in a single lentiviral construct [37,38]. RAWγNO cells were infected with lentivirus in 96-well plates, using two replicate wells per construct. Two shRNA constructs targeting the positive control JAK2 were included as positive controls in the screen. Negative control genes were targeted by multiple shRNA constructs (green

fluorescent protein [GFP], 24 constructs; red fluorescent protein [RFP], 10 constructs; β-galactosidase [lacZ], 13 constructs; luciferase, 23 constructs). 1985 shRNA constructs were used in total.

RNAi can affect cellular survival and proliferation through both on-target and off-target effects. Changes in cell number affect observed bacterial growth, as host macrophages are the substrate for bacterial expansion. In order to allow normalization based on the number of host cells for each plate in which bacterial luminescence was measured, we quantified cell numbers in a replicate plate using the fluorometric Alamar Blue assay.

Cells were seeded in 96-well plates, infected with lentivirus, and selected with puromycin. For the bioluminescence assay, RAWγNO cells were in solid-bottom white 96-well plates (**Fig. 2-2a**). Cells were infected with bioluminescent *L. pneumophila* and washed with PBS 2h after infection. Bioluminescence (bacterial growth) was measured at two timepoints using a plate reader. For the Alamar Blue assay, cells were in clear-bottom black 96-well plates cells. Cells were incubated with the Alamar Blue reagent and fluorescence (host cell number) was measured once using a plate reader.

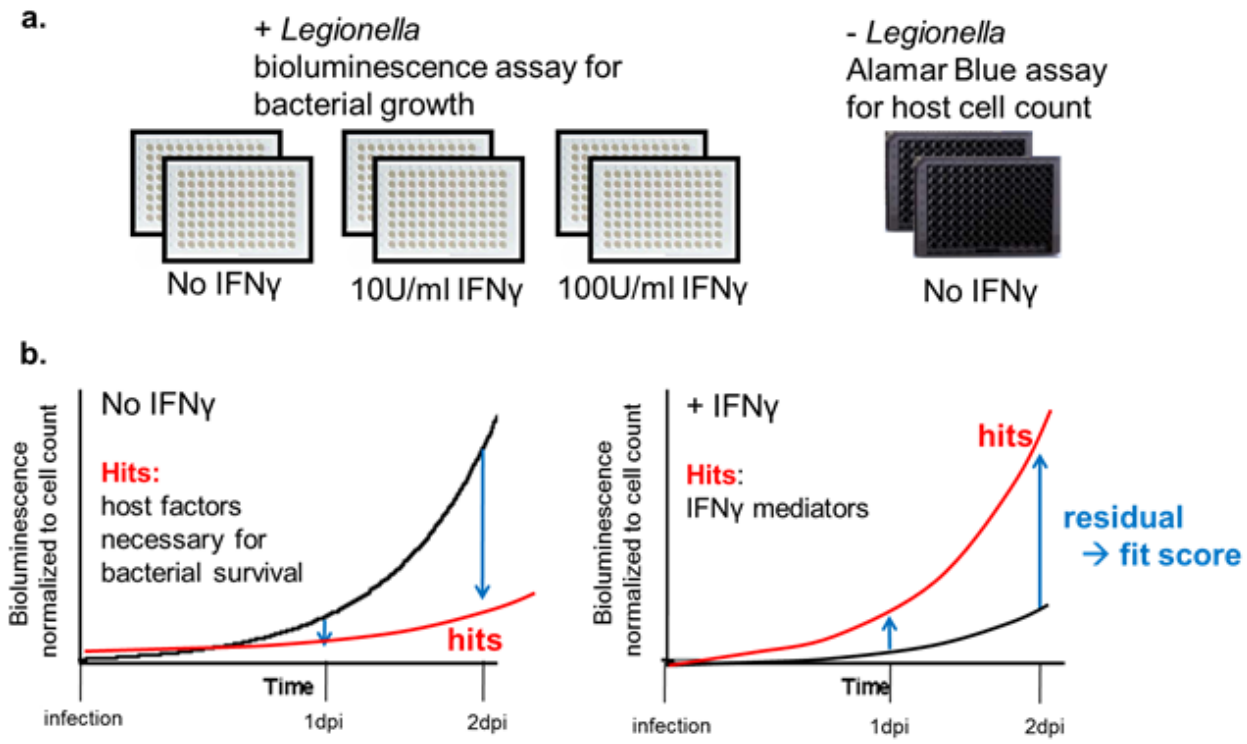

Figure 2-2. Primary screen schematic

RAWγNO cells were seeded in duplicate 96-well plates, infected with lentivirus, selected with puromycin, and used in bioluminescence and Alamar Blue assays.

a. In the bioluminescence assay, shRNA-transduced cells in white, solid-bottom 96-well plates were stimulated with the indicated concentrations of IFNγ for 24h, then infected with bioluminescent *L. pneumophila*. Bioluminescence was measured at 1 and 2 days post-infection using a plate reader. In the Alamar Blue assay, shRNA-transduced cells in black, clear-bottom plates were incubated with the Alamar Blue reagent for 8h, and fluorescence was measured using a plate reader.

b. After normalization to cell number, bioluminescence measured at each timepoint was used to identify hits in the screen. In cells that were not treated with IFNγ, shRNA constructs that corresponded to low relative bacterial growth were classified as candidate host factors. In cells that were treated with IFNγ at both concentrations, shRNA constructs that corresponded to high relative bacterial growth were classified as candidate IFNγ mediators. The residual of the observed *vs* expected (based on the majority of shRNAs) normalized bioluminescence was used to calculate a fit score for each experimental shRNA at each condition and timepoint.

Primary screen data analysis pipeline

We developed an analysis pipeline to pick hits from the screen in an unbiased manner; this method can be generalized to any screen where selecting hits based on one variable (*eg*, bacterial growth) needs to be normalized to another variable (*eg*, cell number).

Data were pre-processed prior to analysis. Bacterial growth (bioluminescence) data from each timepoint and cell count (Alamar Blue fluorescence) data were independently quality-controlled, log-transformed and plate-normalized. shRNA constructs with highly variable replicate data were identified using a custom MATLAB script and excluded. Next, data were log-transformed in order to approximate a normal distribution. The data were then plate-normalized to adjust for systematic error, replacing each raw datapoint with a robust z-score (RZ score) using the bioinformatics application RNAeyes [45]. Replicate data for each shRNA construct were then combined using the geometric mean (average of log-transformed values) using RNAeyes.

Next, we selected shRNA constructs that have a significant effect on bacterial growth (bioluminescence) independent of their effect on cell growth (Alamar Blue fluorescence) (**Fig. 2-2b**). Bioluminescence RZ scores were therefore normalized to Alamar Blue fluorescence RZ scores for each batch, timepoint, and condition, using a custom script written in MATLAB. In short, a best-fit curve (**Fig. 2-3a**) was calculated to correlate the two types of data, using a robust moving average that is unaffected by outlier data, extrapolates at the edges where data are sparse, produces a smooth curve, and is unbiased by assumption of any particular mathematical model of correlation between bacterial signal and cell count. The deviation of each datapoint from the fit-curve represents the effect of the corresponding shRNA construct on bacterial growth, independent of cell count. This deviation was quantified as a fit-score using the residual of each data point from the fit-curve divided by the standard deviation of all residuals from the curve (**Fig. 2-2b**).

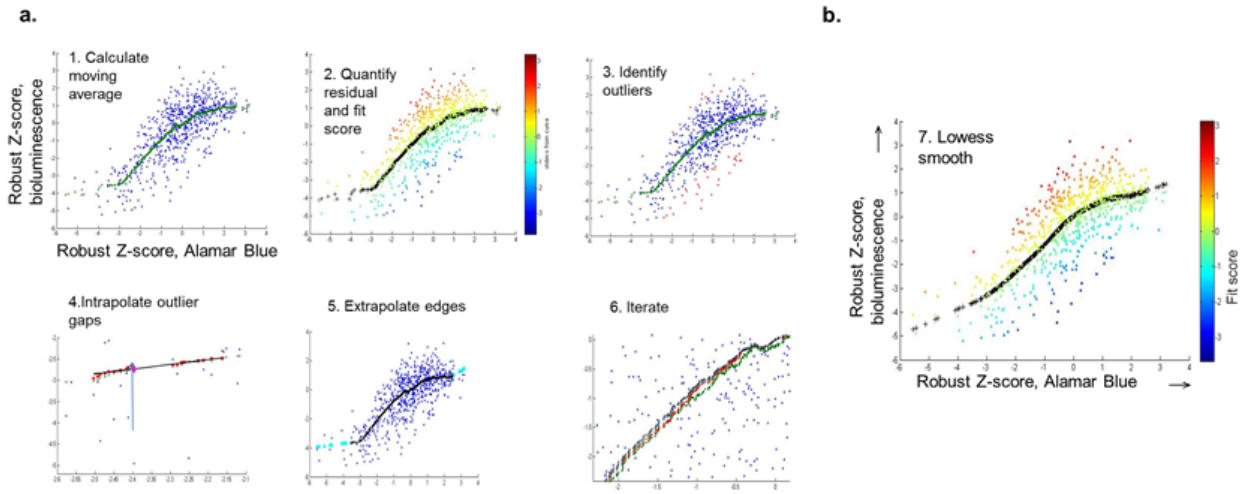

Figure 2-3. Primary screen data analysis pipeline

a. Best fit curves were calculated for each batch of screening data based on robust z-scores of bioluminescence and cell number. Outliers were identified and removed, gaps introduced by outlier removal were intrapolated, edge values were extrapolated, and the process was iterated until convergence. Details are described in the Methods section.

b. The converged best fit curve was smoothed using the Lowess method, and the fit-score of each shRNA construct was calculated as a normalized residual of its datapoint from the best fit curve.

Data regarding knockdown efficiency of shRNA constructs in Hepa cells were available from the RNAi Consortium for 51% (1953) of the experimental set. Of these, 63% (600) were classified as "good" quality data. We eliminated from further analysis those shRNA constructs for which "good" quality knockdown data in Hepa cells was available and indicated poor knockdown efficiency, defined as over 69% transcript remaining.

Selection of candidate IFNγ pathway mediators from the primary screen

Candidate regulators or effectors of the IFNγ pathway were selected by identifying shRNA that increases bacterial signal relative to host cell counts in the presence of IFNγ at the 2dpi timepoint. In order to make the selection of hits more robust, we considered independent data

obtained using different IFNγ treatment conditions. The main criterion for selection was the fit score calculated from cells treated with a high concentration of IFNγ (100U/ml), with a strict (high) threshold (fit score >1.5) applied to identify the best hits. The intermediate criterion for selection was the fit score calculated from cells treated with a low concentration of IFNγ (10U/ml), with a lower threshold (fit score >1.2) applied (**Fig. 2-3a**). The two fit scores generally correlated with each other, but the secondary criterion eliminated several shRNA constructs which produced inconsistent results.

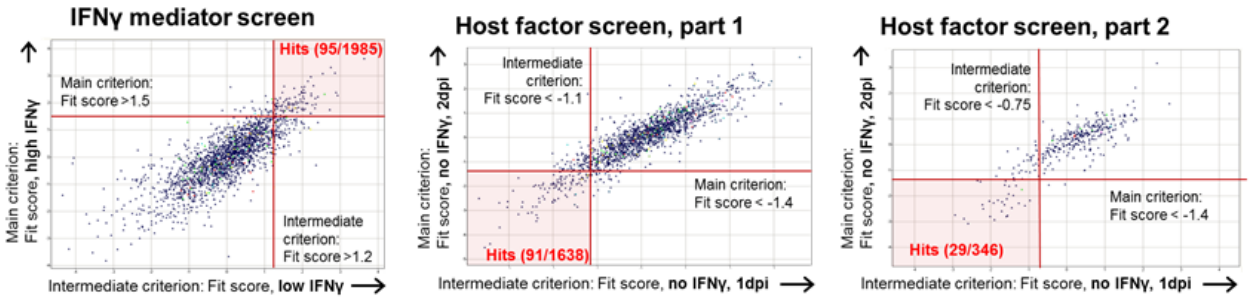

Figure 2-4. Primary screen hit selection criteria

Candidate IFNγ mediators were selected on the basis of fit scores at both low and high concentrations of IFNγ, both measured at the 2dpi timepoint. Candidate *L. pneumophila* host factors were selected on the basis of fit scores from the 1dpi and 2dpi timepoints only in cells not treated with IFNγ.

95 shRNA constructs satisfied both criteria and were classified as hits in the IFNγ pathway screen (**Fig. 2-4, left**), corresponding to 84 genes. These candidates included the positive control JAK2 (main criterion fit score, 1.85), though surprisingly, 39 shRNA constructs yielded stronger phenotypes. Another hit known to fall into the IFNγ pathway is PIK3R4 (main criterion fit score, 2.1), a peptide in the regulatory subunit of phosphatidylinositol 3 kinase (PI3K). PI3K plays an important role in phagosome maturation because its product, phosphatidylinositol(3)phosphate, tethers the Rab5 effector early endosome antigen 1 (EEA1) at the early endosomal membrane [46]. PIK3 has also been implicated in the JAK2-independent arm of the IFNγ response, and its inhibition

leads to decreased transcriptional changes in response to IFNγ [47]. In addition, both subunits of the key phagosome/endosome maturation protein RAB5 were classified as hits, and the Rab5b subunit was represented by two different shRNA constructs (main criterion fit scores: Rab5a, 1.75; Rab5b, 1.86 and 1.95).

Several known phagosome maturation-related genes are notably absent among the genes classified as hits. False negatives may be due to incomplete knockdown. For instance, all five shRNA constructs for EEA1 yielded >94% transcript remaining according to knockdown validation data in Hepa cells from by the RNAi Consortium. Also, compensatory pathways often make it difficult or impossible to yield a significant phenotype through the depletion of a single gene transcript. Finally, some relevant genes, most prominently members of the interferon-induced GTPase (IRG) and autophagy-related (ATG) gene families, were simply not present in the vesicle trafficking set. However, the primary screen confirmed that it is possible to discover genes relevant to IFNγ-mediated bacterial killing in mouse cells through arrayed genetic perturbation, and yielded an initial list of candidate genes for continued testing.

Selection of candidate L. pneumophila host factors from the primary screen

We were able to identify candidate *L. pneumophila* host factors by selecting shRNA constructs that decrease bacterial bioluminescence in the absence of IFNγ (**Fig. 2-4, right**). In this arm of the screen, we also selected hits based on two criteria. The main criterion was the fit score calculated from observations at the 2dpi timepoint; a strict (low) threshold (fit score < -1.4) was applied to identify the best hits. The intermediate criterion was the fit score calculated from observations at the 1dpi timepoint; a higher threshold (fit score < -1.1) was applied. For the intermediate criterion in the first batch of the screen, a relaxed threshold was applied (fit score <0.75) due to the high data variability at this timepoint. 120 shRNA constructs satisfied both criteria and

were classified as candidate host factors. After removing shRNAs with inconsistent data over replicates, 87 candidates remained, representing 73 genes.

Three genes were classified as both candidate IFNγ pathway members and as candidate host factors, representing either false positives or proteins that have dual modes of action dependent on the IFNγ-induced activation status of the cell. For example, Dynamin 2 (DNM2), one of the dual hits, has been found to be required for phagocytosis of antibody or complement-opsonized particles, but not apoptotic cells, by mouse macrophages [48]. DNM2 is therefore a host factor since it is involved in bacterial internalization. After phagocytosis of apoptotic cells, however, DNM2 is necessary for phagosome maturation, possibly playing a role in recruitment of Rab5 via VPS34 in early phagosomes [35]. DNM2 therefore acts as a restriction factor as well as a host factor for bacterial growth.

Some of the candidate host factors identified have a known role in intracellular survival and growth of *L. pneumophila*. The small GTPases ADP-ribosylation factor 1 (ARF1) and secretion associated, Ras related GTPase 1 (SAR1) are important *L. pneumophila* host factors, as shown by experiments in which overexpression of dominant negative form of either was associated with failure to recruit ER-derived membrane fragments to form a replicative *Legionella*-containing vacuole (LCV) [49,50]. ARF1 and SAR1 regulate the coat protein I (COPI) and coat protein II (COPII)-coated vesicles, respectively, that are involved in ER-Golgi transport [51]. Multiple shRNA constructs led to the classification of SAR1 as a hit in the host factor screen, targeting SAR1A (main criterion fit score, -2.3), and SAR1B (-3.2 and -1.8). Likewise, the ARF1-related ARF1 (main criterion fit score, -1.7) and ARF-related protein 1 (ARFRP1) (-4.4), as well as the ARF-family member ARF3 (-2.8) and ARF4 (-3.1) were classified as candidate host factors as well. SEC22B (main criterion fit score: -2.1), another gene classified as a candidate host factor, is a component of the vesicle-associated soluble N-ethylmaleimide-sensitive factor attachment protein receptor (v-SNARE) on ER-derived vesicles [52], associates with LCVs in an ARF1 and SAR1-dependent

manner, we can discover bacterial host factors and is functionally important for *L. pneumophila* replication in macrophages [53]. Therefore, the host factor arm of the screen in RAWγNO cells reconstituted known host factors as well as identifying new candidates.

Confirmation of hits in a secondary screen using primary mouse macrophages

shRNA constructs that were classified as hits in either the IFNγ or host factor screen were validated in C57BL/6J (B6) mouse bone-marrow derived macrophages (BMMs), in order to exclude candidate genes that may only be relevant in the context of a cell line.

First, we re-tested the ability of *L. pneumophila* strain LP02 delFlaA *lux* to grow in BMMs, the ability of IFNγ-stimulated BMMs to restrict intracellular *L. pneumophila*, and the potential of shJak2 lentiviral transduction to overcome IFNγ-based growth restriction. We found that stimulation of a concentration of IFNγ (10U/ml) lower than that used in the primary screen (100U/ml) provided the greatest differentiation between cells transduced with shJak2 and those transduced with the shGFP control (**Fig. 2-5**). There are three possible explanations for the discrepancy in stimulation conditions between RAWγNOcells and BMMs. First, the knockdown of JAK2 transcript may be less complete in BMMs than in RAWγNOcells, so that less IFNγ signaling is required to obtain a threshold level of activity. Second, BMMs may be more sensitive to IFNγ signaling via residual JAK2 protein remaining after incomplete shRNA-mediated knockdown. Third, the JAK2-independent IFNγ signaling pathway may be more active in BMMs than in RAWγNOcells.

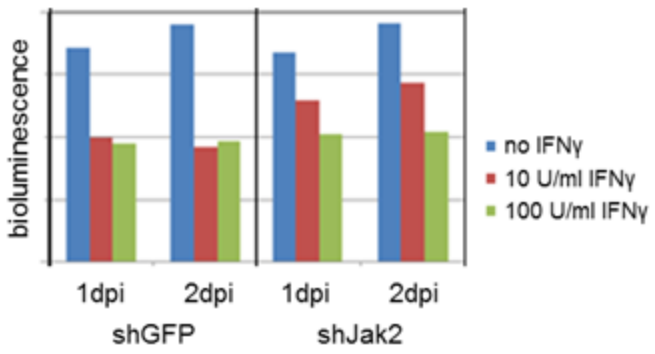

Fig. 2-5. Proof of concept for secondary screen

WT BMMs cells restrict *L. pneumophila* in an IFNγ–dependent manner, and shRNA-based depletion of JAK2 attenuates IFNγ–dependent bacterial restriction in RAWγNO cells.

We tested 275 shRNA constructs in total, targeting 84 IFNγ pathway candidates and 73 *L. pneumophila* host factor candidates from the primary screen, as well as the negative control genes (GFP, RFP, lacZ, luciferase), and the positive control Jak2. In order to account for potentially differing effects of shRNA on cell survival or proliferation under different conditions of stimulation, the Alamar Blue assay was performed for both resting and IFNγ-stimulated cells.

In resting BMMs (**Fig. 2-6a**), shRNA-mediated depletion of many host-factor candidate gene transcripts (blue) decreases bacterial growth relative to controls (black). Interestingly, in most cases, depletion of most host factors does not decrease bacterial growth relative to controls in IFNγ-activated cells (**Fig. 2-6b**), perhaps because the strong effect of IFNγ-mediated restriction obscures restriction due to depletion of host factors. Because the number of shRNA constructs tested in the secondary screen was limited, we classified candidate host factors as validated by hand, based on data in resting cells (**Fig. 2-6a**).

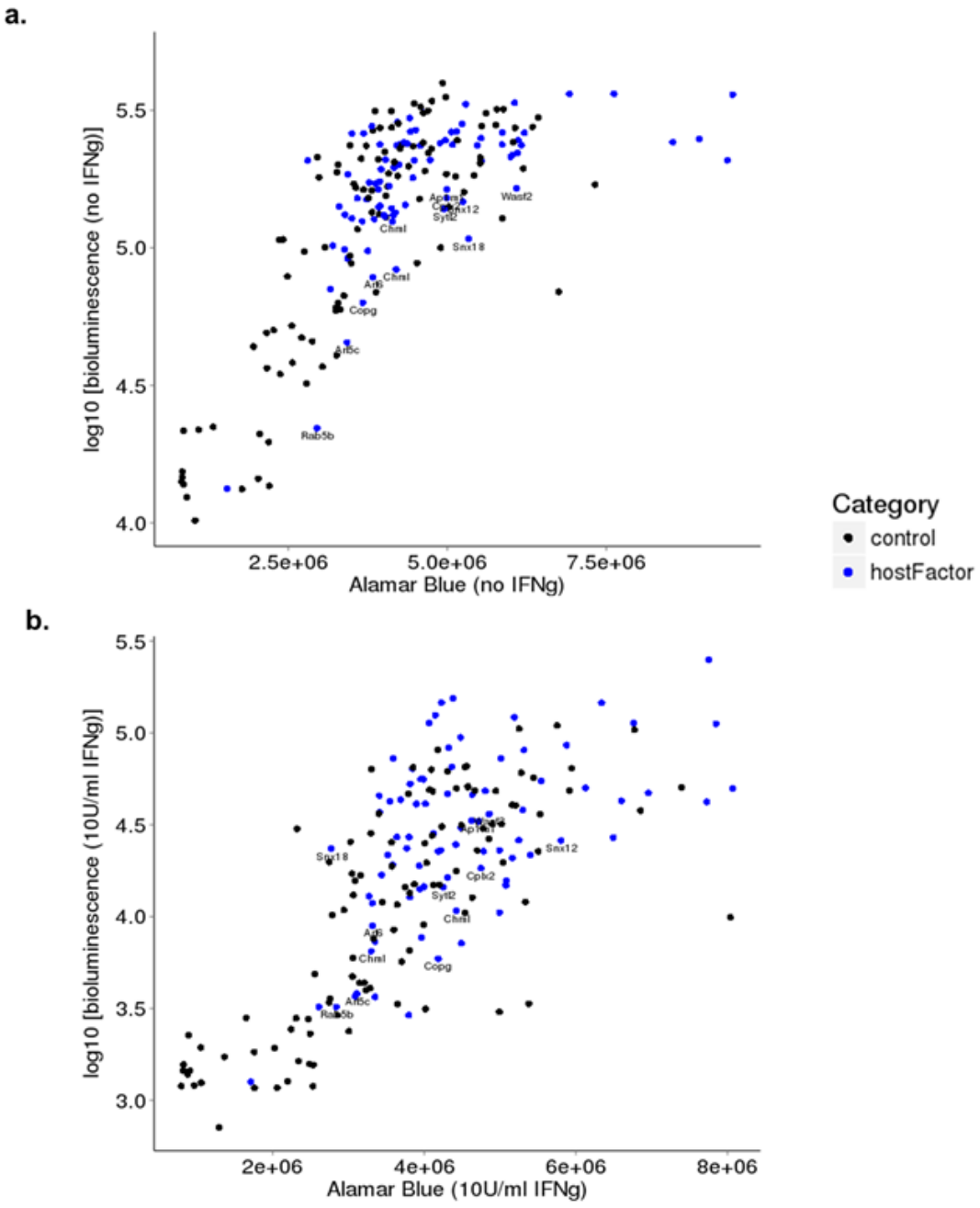

Figure 2-6. Candidate host factors validated in the secondary screen

WT BMMs were lentivirally transduced with shRNAs classified as hits in the primary screen, as well as control shRNAs. Only hits classified as candidate host factors are shown. Cells were infected with bioluminescent *L. pneumophila* and bioluminescence was measured at 2dpi. In a simultaneous assay, cell counts were measured using the Alamar Blue assay. Bacterial growth (bioluminescence) was log-transformed and plotted against cell counts (Alamar Blue) for assays done in IFNγ-stimulated (**a**) or resting (**b**) cells. Hits classified as validated are labeled with gene symbols.

Depletion of most IFNγ pathway candidate gene transcripts (red) enhances bacterial growth relative to controls (black) in the presence of IFNγ (**Fig. 2-7b**) but not in resting cells (**Fig. 2-7a**), indicating that restriction of *L. pneumophila* mediated by these candidates is IFNγ-specific. This is reflected in relatively higher ratios of log-transformed luminescence data in IFNγ treated *vs* untreated BMMs (**Fig. 2-7c**) compared to control and candidate host factor shRNA constructs.

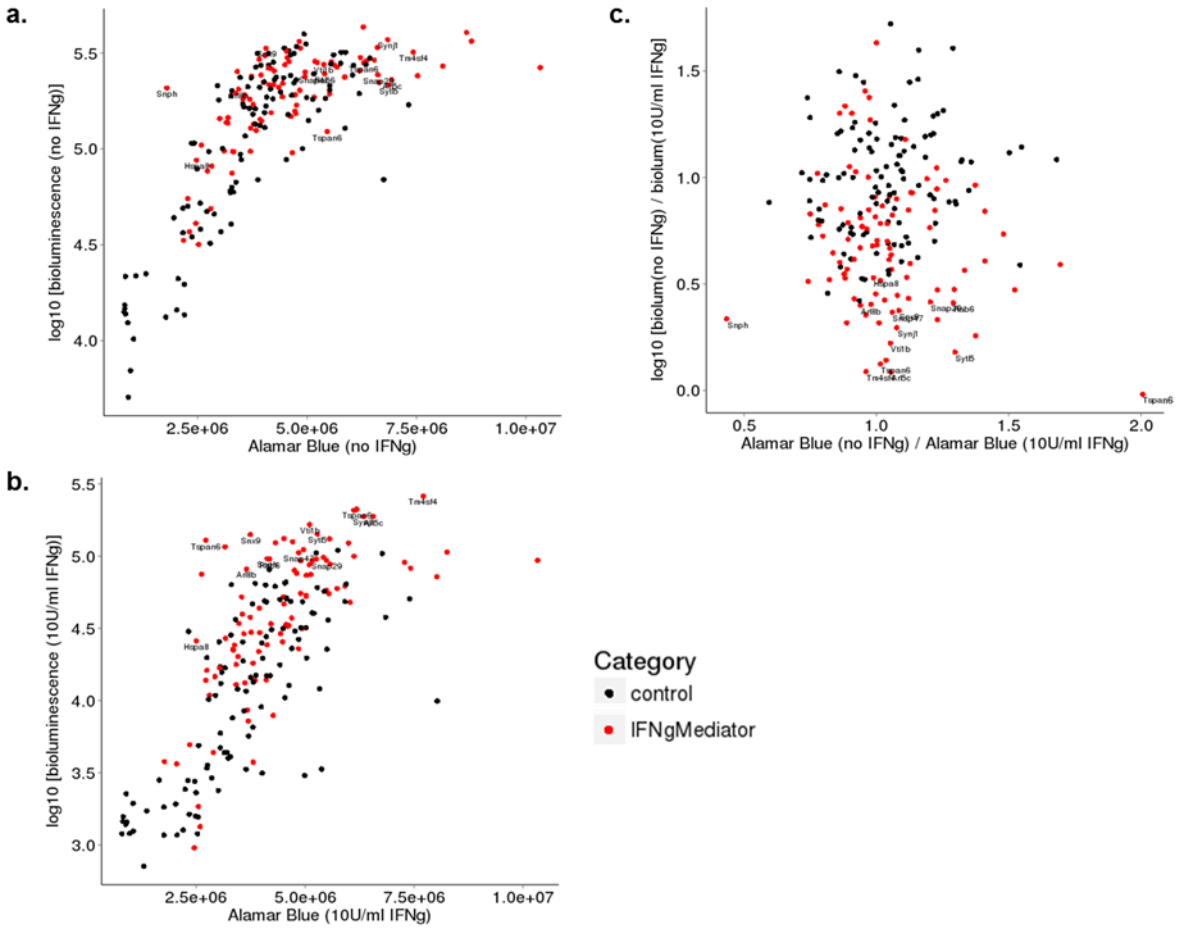

Figure 2-7. Candidate IFNγ mediators validated in the secondary screen

Screening was performed as in Fig. 2-6. Only hits classified as candidate IFNγ mediators are shown. host factors are shown. Bacterial growth (bioluminescence) was log-transformed and plotted against cell counts (Alamar Blue) for assays done in IFNγ-stimulated (**a**) or resting (**b**) cells. In (**c**), the log-transformed ratio of bioluminescence in IFNγ-stimulated *vs* resting BMMs is plotted against the ratio of cell count data. Hits classified as validated are labeled with gene symbols.

Candidate *L. pneumophila* host factors validated in the secondary screen

Among candidate *L. pneumophila* host factors (**Table 2-1**), none of the constructs targeting the ARF genes, SAR1B, or SEC22 was validated. Redundancy in the ARF gene family has previously been implicated in the lack of phenotypic changes in single-gene RNAi assays, and double knockdown of any two ARFs was required to induce changes in membrane trafficking in a human epithelial cell line [54]. The classification of ARF genes as candidate host factors in the primary screen with RAWγNO cells was either a false positive, or reflects biological differences between RAWγNO cells and BMMs.

Gene symbol	Gene name
Snx18	Sorting nexin18
Rab5b	Ras-related protein 5b
Wasf2	Wiskott-Aldrich syndrome protein family member 2
Arl5c	ADP-ribosylation factor-like 5C
Copg	Coatomer protein complex, subunit gamma
Chml	Choroideremia-like (Rab escort protein 2)
Arl6	ADP-ribosylation factor-like 6
Sytl2	Synaptotagmin-like 2
Snx12	Sorting nexin 12
Ap1m1	Adaptor-related protein complex 1, mu 1 subunit
Cplx2	Complexin-2

Table 2-1. Candidate host factors validated in the secondary screen

Novel candidate host factors identified in the secondary screen include sorting nexin 12 (SNX12), and sorting nexin 18 (SNX18), both members of the sorting nexin family of endosomal sorting proteins [55]. Like all sorting nexins, they contain a phox homology (PX) domain that binds membrane phosphoinositides. Like many sorting nexins, they also contain a Bin–Amphiphysin–Rvs (BAR) domain that can function in both sensing and induction of membrane curvature [56,57] and mediates key functions of endosome maturation [58]. Interestingly, recent data are consistent with a role for SNX12 in endosome maturation arrest by preventing the conversion of these early vesicles

into partially mature multivesicular bodies [59]. SNX18 participates in the budding of tubules at membranes enriched in PI(4,5)P2, which is characteristic of late endosomes [60]. Therefore, SNX12, and SNX18 are candidate *L. pneumophila* host factors in murine macrophages, possibly through limiting the tubulation and/or delivery of late endosomes to the LCV.

Candidate IFNγ effectors or pathway members identified in the secondary screen

Among the ~26 genes confirmed as hits in the secondary RNAi screen (**Table 2-2**), we used literature curation to select a list of ~15 genes most likely to satisfy the primary hypothesis: that the candidate is involved in targeting vesicles to the early bacterial phagosome downstream of IFNγ stimulation. This processed involved excluding genes that were likely to play a role in lysosome biogenesis or phagocytic uptake of bacteria. Among the remaining candidates, we selected seven for further analysis based on consistency of phenotype and biological interest (TSPAN6, SNAP29, SNAP47, HSPA8, VTI1B, ARL8B, AP3S1).

Gene symbol	Gene name	Endo-cytosis	ER-Golgi	Golgi / secretory	Lysosomal biogenesis
Tspan6	**Tetraspanin 6**				
Arl5c	**ADP-ribosylation factor-like 5C**				
Tm4sf4	**Transmembrane 4 L six family member 4**				
Rab1b	Ras-related protein 1		Yes		
Dnm2	Dynamin 2	Yes		Yes	
Sytl5	**Synaptotagmin-like 5**				
Arf4	ADP-ribosylation factor 4		Yes		
Vti1b	**vesicle transport through interaction with t-SNAREs 1B**				
Snx1	Sorting nexin 1				Yes
Synj1	**Synaptojanin 1**				
Ap1s2	Adaptor-related protein complex 1, sigma 2 subunit			Yes	
Arfrp1	ADP-ribosylation factor related protein 1		Yes	Yes	
Copz1	Coatomer protein complex, subunit zeta 1		Yes		
Ap3s1	Adaptor-related protein complex 3, sigma 1 subunit			Yes	Yes
Rab18	Ras-related protein 18			Yes	
Snph	Syntaphilin				
Arl13b	ADP-ribosylation factor-like 13b			Yes	
Cltc	Clathrin heavy chain	Yes		Yes	
Snx9	Sorting nexin 9	Yes			
Snap47	**Synaptosomal-associated protein, 47kDa**				
Stam	Signal transducing adaptor molecule (SH3 domain and ITAM motif) 1			Yes	
Rab2a	Ras-related protein 2a			Yes	
Arl8b	**ADP-ribosylation factor-like 8b**				
Rab6	**Ras-related protein 6**				
Snap29	**Synaptosomal-associated protein, 29kDa**				
Hspa8	**Heat shock 70kDa protein 8**				

Table 2-2. Candidate IFNγ mediators validated in the secondary screen.
Proteins with described roles in endocytosis, ER-Golgi transport, secretion, or lysosomal biogenesis are noted; these were excluded from the final candidate list.

TSPAN6

Tetraspanin 6 (TSPAN6), a member of the poorly described tetraspanin family of membrane proteins, was a significant hit in the IFNγ pathway screen. Two shTspan6 constructs were associated with a significant increase in bacterial growth in IFNγ-activated cells compared to cells transduced with control shRNA. Inspection of the shRNA sequences revealed that the two hit constructs overlap by all but one nucleotide, and are therefore essentially equivalent.

We first attempted to validate the shRNA-mediated depletion of Tspan6 mRNA in RAWγNOcells. The first two sets of PCR primers tested did not detect Tspan6 transcript in these

cells. We generated an additional ten primer sets and tested them in BMMs, RAWγNO cells, and mouse organ lysates in spleen, liver, and lung. All primers tested detected Tspan6 transcript in primary cells (BMMs and organ lysates). Only four primer sets detected transcript in RAWγNO cells, consistent with a mutation or splice variant of Tspan6 in RAWγNO cells.

Using the four qPCR primers common to both RAWγNO cells and primary cells, expression of Tspan6 mRNA was quantified in shTpan6-transduced cells. Results were highly variable, with 25%-80% transcript remaining, depending on which primer sets were used and on whether the cells were resting or IFNγ-stimulated. The low levels of signal indicating Tspan6 transcript levels detected by qPCR were concerning for a low signal-to-noise ratio, so we proceeded to Tspan6 knockdown validation at the post-translational level. Western blotting confirmed the depletion of TSPAN6 in RAWγNOcells (**Fig. 2-8a**).

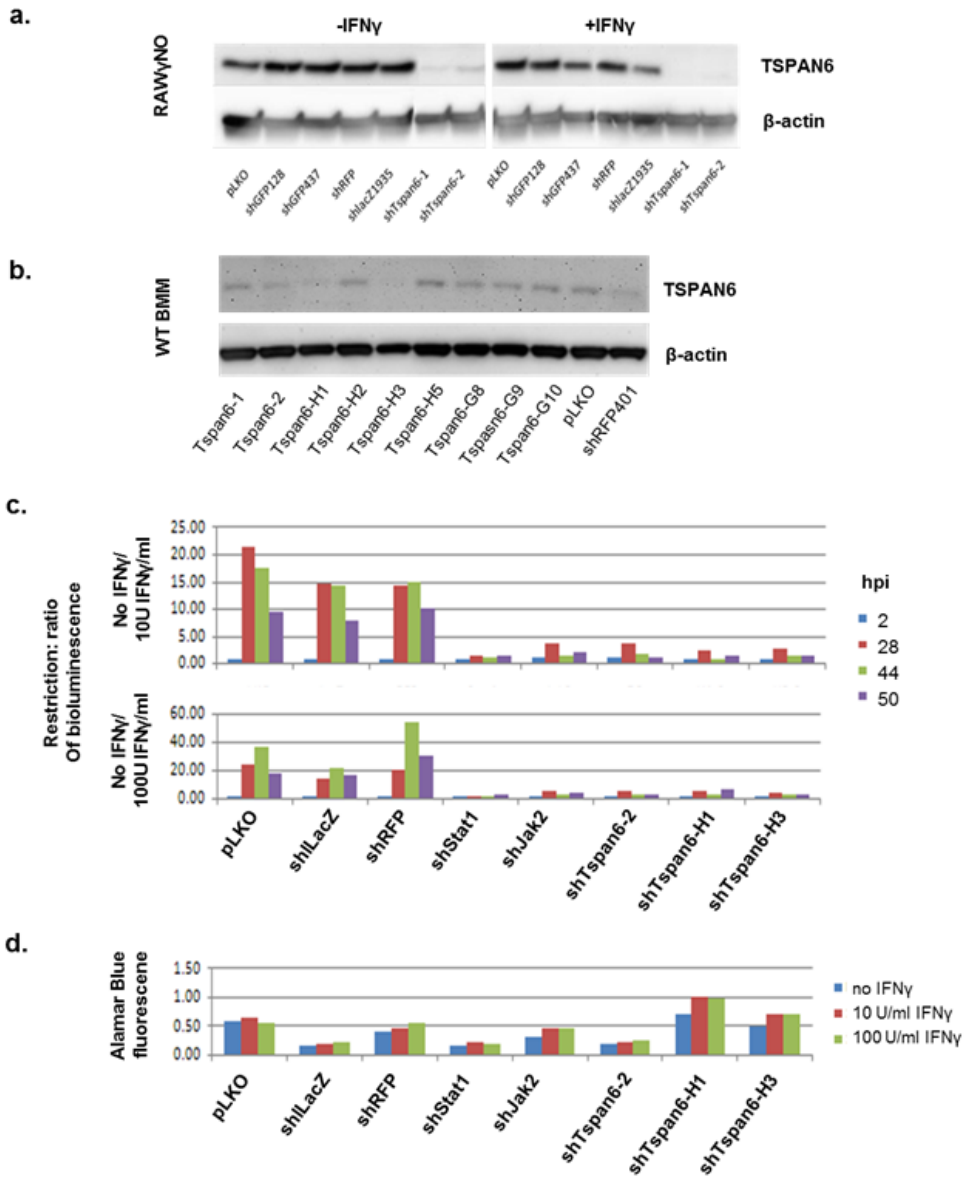

Figure 2.8. Validation of candidate IFNγ mediator TSPAN6

a. Western blot analysis of TSPAN6 expression in RAWγNO cells transduced with shTspan6 constructs classified as hits in the primary screen (shTspan6-1, shTspan6-2) or control shRNAs and mock-stimulated (**left**) or stimulated with IFNγ (**right**) for 24h.

b. Western blot analysis of TSPAN6 expression in WT BMMs transduced with shTspan6, including seven additional shRNAs not tested in the primary screen, or control shRNAs.

c. IFNγ-induced restriction of *L. pneumophila* in WT BMMs transduced with shTspan6-2 and positive (shStat1, shJak2) and negative control shRNA. Restriction is calculated as the ratio of bioluminescence in resting *vs* IFNγ-stimulated cells.

d. Alamar Blue assay of WT BMMs corresponding to data in (**c**)

Because each shRNA construct is associated with unique off-target effects, eight additional shRNAs targeting Tspan6, unrelated in sequence to the original five tested in the screen, were obtained from the RNAi Consortium. Two of these constructs (shTspan6-H1, H3) were selected based on TSPAN6 depletion in BMMs by Western blot (**Fig. 2-8b**). This experiment tested the two shRNA constructs (shTspan6-1, 2) used in the primary screen as well. Surprisingly, despite the nearly complete sequence overlap between shTspan6-1 and shTspan6-2, shTspan6-1 did not reduce TSPAN6 expression in BMMs and was not used in further studies. Transduction with shTspan-1, shTspan-H1, shTspan-H3 significantly reduced the IFNγ-mediated restriction of *L. pneumophila* in BMMs when compared with controls (**Fig. 2-8c**), in cells stimulated at either 10 U/ml or 100U/ml of IFNγ. However, the new shRNA constructs shTspan6-H1 and shTspan6-H3 also led to a dramatic increase in cell counts (**Fig. 2-8d**), a phenotype observed with shTspan6-1 in the primary screen as well.

To determine whether TSPAN6 expression is regulated by IFNγ, we prepared Western blots using lysates from RAWγNOcells treated with IFNγ at a series of timepoints. IFNγ treatment induced the expression of TSPAN6 within 4 hours of stimulation (**Fig. 2-9a).** However, neither IFNγ stimulation nor *L. pneumophila* infection affected the expression of TSPAN6 in BMMs.

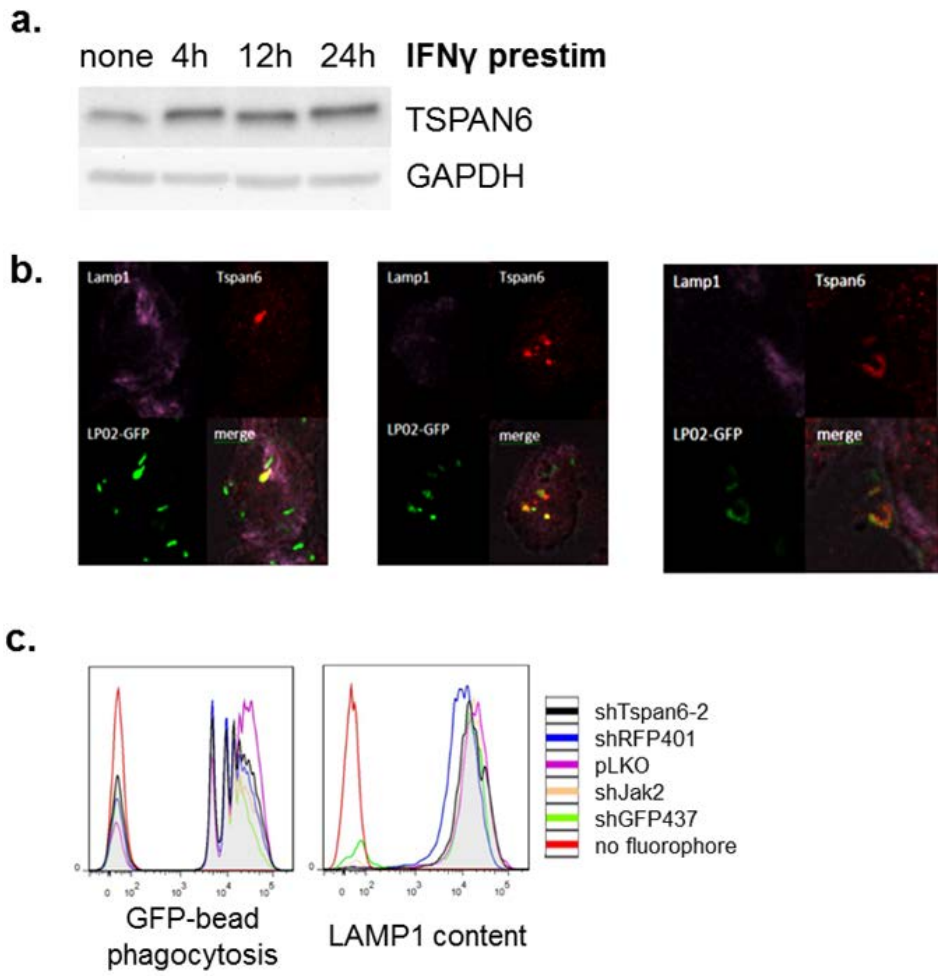

Figure 2-9. Functional characterization of candidate IFNγ mediator TSPAN6

- **a.** Western blot analysis of TSPAN6 in RAWγNO cells following treatment with IFNγ
- **b.** Immunofluorescence analysis of TSPAN6 in RAWγNO cells stimulated with IFNγ, infected with GFP-expressing *L. pneumophila*, and fixed at 30min after infection reveals colocalization of TSPAN6 with *L. pneumophila* phagosomes. LAMP1 is used as a counter-stain.
- **c.** Flow cytometry analysis of the uptake of GFP-labeled beads (**left**) and LAMP1 immunofluorescence (**right**) in IFNγ-stimulated RAWγNO cells transduced with shTspan6-2 or control shRNA.

IFNγ mediator proteins can impact vesicle trafficking at the LCV either directly, by physically interacting with bacterial phagosomes, or indirectly. We used GFP-expressing *L. pneumophila* and immunofluoresecence microscopy to determine whether TSPAN6 colocalizes with

bacterial phagosomes, and whether this localization is dependent on IFNγ. Immunofluorescence staining of TSPAN6 in RAWγNO reveals a punctate cytosolic pattern. RAWγNO cells infected with GFP-labeled, flagellin-deficient *L. pneumophila* strain LP02 delFlaA pAM239 [61] were fixed at 0min, 30min, 1hr, 2hr, and 4hr after infection, and stained with antibodies to TSPAN6 and LAMP1, a lysosome/late endosome marker protein that accumulates on maturing phagosomes. Surprisingly, TSPAN6 colocalized with LCVs at 30min after infection in IFNγ-stimulated cells (**Fig. 2-9b**). LAMP1 was not recruited to LCVs at this time. Colocalization was not observed at other timepoints, nor in resting cells. We were able to confirm this result in one but not two more repetitions of the experiment. Thus, we conclude that the potential association of TSPAN6 with the LCV is transient and possibly dependent on IFNγ stimulation.

An alternative hypothesis to explain the increase in bacterial growth in shTspan6-transduced, IFNγ-stimulated cells is that TSPAN6 enhances phagocytic uptake in an IFNγ-dependent manner. We used flow cytometry to analyze IFNγ-stimulated RAWγNOcells that had been incubated with fluorescently tagged latex beads, then washed with Trypan blue to quench fluorescence of free or surface-attached bacteria or beads. No significant difference was noted among the fluorescence intensity distributions of cells transduced with control shRNA or shTspan6-1 (**Fig. 2-9c, left**). These results suggest that enhanced bacterial uptake was not responsible for increased bacterial growth in shTspan6-transduced, IFNγ-stimulated cells. We note, however, that phagocytic capability is cargo-dependent, and beads may not provide phagocytes with relevant activation signals.

Another alternative hypothesis to explain the phenotype observed in TSPAN6 can explain decreased IFNγ-induced bacterial restriction was a defect in lysosomes and other compartments that phagosomes must fuse with in order to mature, rather than a defect in proper trafficking of these organelles to the phagolysosomal compartment. We used flow cytometry to quantify the staining intensity of LAMP1 as a proxy for lysosomal density. LAMP1 staining distribution was equivalent in

cells transduced with control shRNA and with shTspan6 (**Fig. 2-9c, right**), which suggests (but does not prove) that TSPAN6 does not play a role in lysosomal biogenesis.

SNAP29

The SNAP29 protein is a member of the SNAREs family of proteins that form connections between the membranes of fusing intracellular vesicles. SNAP29 plays a role in endocytic recycling in fibroblasts [62] and the lipid- loading and membrane fusion of lamellar granules in the epidermis [63,64]. A recent study of SNAP29 in phagocytic immune cells (mouse BM-derived mast cells and a rat basophil cell line) found that native Snap29 was transiently recruited to *E. coli* phagosomes 1-3 hours after infection, and overexpression of SNAP29 accelerated the killing of phagocytosed bacteria [65]. The Snap29 gene is one of several genes disrupted in the rare neurocutaneous syndrome cerebral dysgenesis, neuropathy, ichthyosis and keratoderma (CEDNIK) [63,66], but symptoms of immunodeficiency have not been observed in CEDNIK patients (E. Sprecher, personal communication).

Depletion of SNAP29 transcript in BMMs was confirmed using qPCR (19-70% transcript remaining). Analysis of protein expression level of SNAP29 showed that shRNA-mediated depletion of SNAP29 protein in RAWγNOcells was transient; after a fourfold reduction in transcript at 5d after lentiviral infection, protein expression was restored 6d after lentiviral infection (**Fig. 2-10a**).

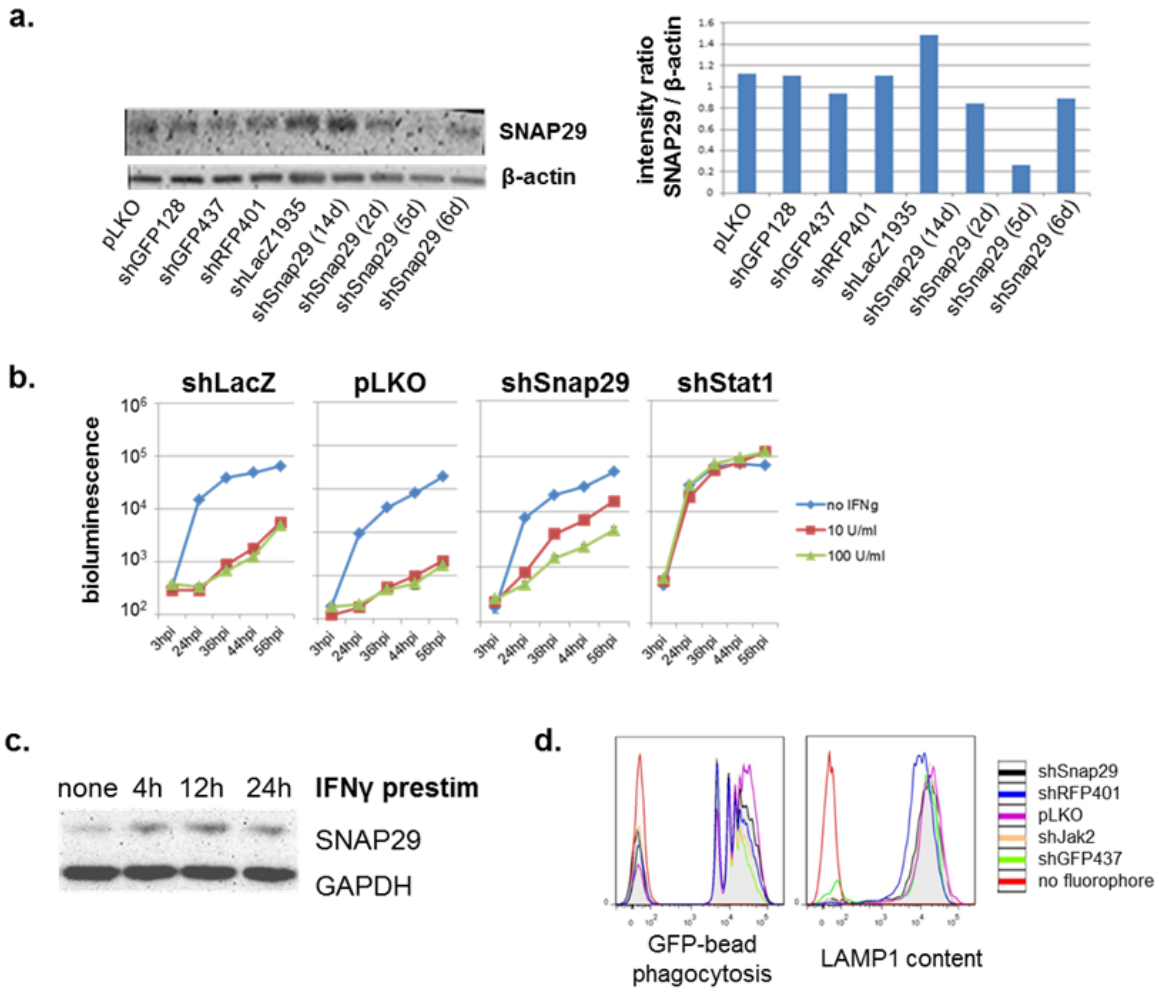

Figure 2-10. Validation and functional characterization of candidate IFNγ mediator SNAP29

a. Western blot analysis of SNAP29 levels in RAWγNO cells lysed at the timepoints indicated after lentiviral transduction with shSnap29, or at 5d after transduction with control shRNAs (**left**). SNAP29 levels were normalized to β-actin levels (**right**).

b. Growth curves of bioluminescent *L. pneumophila* in RAWγNO transduced with shSnap29, the negative control shLacZ or the lentiviral vector pLKO, or the positive control shStat1, and stimulated with the indicated concentration of IFNγ prior tobacterial infection.

c. Western blot analysis of SNAP29 levels in RAWγNO cells following stimulation with IFNγ and lysed at the timepoints indicated.

d. Flow cytometry analysis of the uptake of GFP-labeled beads (**left**) and LAMP1 immunofluorescence (**right**) in IFNγ-stimulated RAWγNO cells transduced with shSnap29 or control shRNA.

To determine whether SNAP29 expression is regulated by IFNγ, we prepared Western blots using lysates from RAWγNOcells treated with IFNγ at a series of timepoints. IFNγ treatment induced the expression of SNAP29 within 4 hours of stimulation (**Fig. 2-10c**), similar to results obtained with TSPAN6 expression following stimulation.

Also similar to results with depletion of TSPAN6, depletion of SNAP29 using shRNA did not affect the uptake of fluorescent beads or the expression of LAMP1 in IFNγ-stimulated cells relative to cells transduced with control shRNA (**Fig. 2-10d**). Based on these results, our collaborator pursued the study of SNAP29 using macrophage-conditional SNAP29$^{-/-}$ mice.

While germline SNAP29 deficiency is embryonic lethal, a recently created macrophage-conditional SNAP29 deletion mutant enabled the direct testing of the requirement for SNAP29 in IFNγ-induced bacterial restriction. However, growth of *L. pneumophila* in resting and IFNγ-activated SNAP29-deficient BMMs was equivalent to growth in WT BMMs (J. Coers, personal communication), indicating that SNAP29 is dispensable in not required for this process.

SNAP47

SNAP47 is a ubiquitously expressed SNARE protein of unknown function [67]. qPCR was used to validate SNAP47 transcript depletion in BMMs, with 7-16% transcript remaining after lentiviral transduction and selection. Western blotting showed partial shRNA-mediated depletion of Snap47 protein in RAWγNO cells (**Figure 2-11a**).

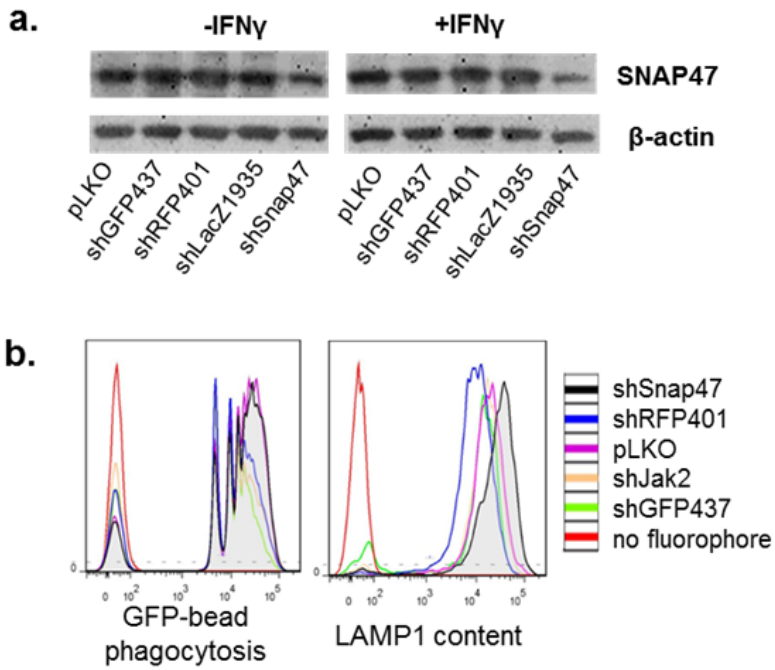

Figure 2-11. Validation and functional characterization of candidate IFNγ mediator SNAP47

a. Western blot analysis of SNAP47 expression in RAWγNO cells transduced with shSnap47 or control shRNAs and mock-stimulated (**left**) or stimulated with IFNγ (**right**) for 24h.

b. Flow cytometry analysis of the uptake of GFP-labeled beads (**left**) and LAMP1 immunofluorescence (**right**) in IFNγ-stimulated RAWγNO cells transduced with shSnap47 or control shRNA.

We next examined whether alternative hypotheses could explain the increased bacterial growth in shSnap47-transduced, IFNγ-activated macrophages. Surprisingly, depletion of SNAP47 by shRNA increased the uptake of fluorescent beads relative to two controls and to shJak2 (**Fig. 2-11b, left**). Notably, transduction with the pLKO control lentivirus similarly increased bead phagocytosis, with a significantly higher fraction of cells taking up three or more beads than cells transduced with shRFP, shGFP, or shJak2. Therefore, SNAP47 is a candidate inhibitor of phagocytosis.

Furthermore, shSnap47-transduced cells produced significantly more LAMP1 (**Fig. 2-11b, right**) than controls, suggesting derangement of the endolysosomal network in SNAP47-depleted

cells. Together, these data suggest profound effects of SNAP47 on vesicle trafficking throughout the phagolysosomal network.

VTI1B

The SNARE protein vesicle transport through interaction with t-SNAREs 1B (VTI1B) and its binding partner syntaxin 8 (STX8), both candidate members of the IFNγ-microbial restriction pathway in the screen, participate in a SNARE complex involved in late endosome-lysosome fusion in many cells, including macrophages [68,69]. We hypothesize that this complex may be involved in IFNγ-dependent targeting of lysosomal contents to the LCV, since LCVs acquire lysosomal markers in IFNγ-stimulated, but not resting macrophages [2].

Macrophages stimulated by LPS increase VTI1B expression, and release the cytokine TNFα in a vesicle trafficking process that requires VTI1B [70]. The requirement for VTI1B in the context of IFNγ stimulation has not been studied. However, TNFα is known to synergize with IFNγ-activated STAT1 homodimers at the promoters of key IFNγ-activated sequences (GAS) in the promoters of innate immune effectors such as NOS2 [71], suggesting that proteins such as VTI1B that facilitate TNFα signaling may play a positive role in the IFNγ response.

In addition, previous work in human epithelial cells has suggested a critical role for VTI1B in bacterial killing, showing that siRNA-mediated depletion of VTI1B suppressed the fusion of bacterial autophagosomes with lysosomes cells infected with Group A *Streptococcus* [72]. Intriguingly, domain analysis suggests that the VTI1B SNARE complex may be a target of the *L. pneumophila* secreted effector protein IcmG, which contains a cognate SNARE domain [73]. A previous study that tested this hypothesis found that purified IcmG blocked the fusion of liposomes bearing VTI1B/STX7/STX8 SNARE complexes with liposomes bearing the cognate SNARE VAMP8 [73].

We tested the hypothesis that VTI1B is required for IFNγ-induced restriction of *L. pneumophila* directly, using Vti1b$^{-/-}$, Vti1b$^{-/+}$, and WT mouse BMMs [74]. IFNγ-induced bacterial restriction increased, rather than decreased in Vti1b$^{-/-}$ BMMs compared to WT and Vti1b$^{-/+}$ BMMs (**Fig. 2-12a**). Therefore, VTI1B is not required for efficient restriction of *L. pneumophila* in response to IFNγ, contrary to what we expected from data in the primary and secondary screen.

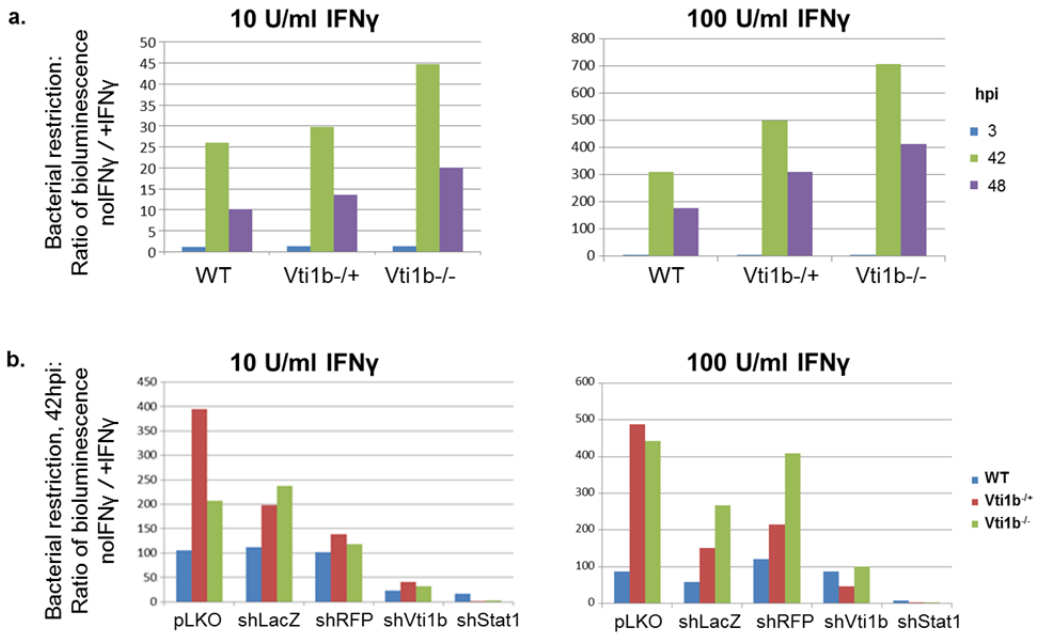

Figure 2-12. Validation of candidate IFNγ mediator VTI1B

- **a.** IFNγ-induced restriction of *L. pneumophila* in WT, Vti1b$^{-/+}$, and Vti1b$^{-/-}$ BMMs. Restriction is calculated as the ratio of bioluminescence in resting *vs* IFNγ-stimulated cells.
- **b.** IFNγ-induced restriction of *L. pneumophila* in WT, Vti1b$^{-/+}$, and Vti1b$^{-/-}$ BMMs transduced with shVti1b, or with positive (shStat1), and negative control shRNA, selected with puromycin, and stimulated with IFNγ at the indicated concentrations for 24 prior to bacterial infection. Restriction is calculated as the ratio of bioluminescence in resting *vs* IFNγ-stimulated cells, measured at 42hpi.

In order to determine why transduction with shVti1b decreases IFNγ-induced bacterial restriction, we subjected Vti1b$^{-/-}$, Vti1b $^{-/+}$, and WT BMMs to treatment with shVti1b or control

shRNA. Following puromycin selection and mock-stimulation or stimulation with IFNγ, BMMs were infected with bioluminescent *L. pneumophila*. IFNγ-mediated bacterial restriction was quantified as the ratio of measured bioluminescence in resting *vs* IFNγ-stimulated BMMs at each condition and timepoint. We found that transduction with shVti1b decreases bacterial restriction in BMMs of all genotypes (**Fig. 2-12b**). Therefore, we conclude that the phenotype observed in cells transduced with shRNA targeting Vti1b was caused by an off-target effect of the shRNA, rather than an effect of VTI1B depletion.

ARL8B

ARL8B is a regulator of lysosomal transport along microtubules [75,76], and was recently found to indirectly affect the trafficking of phagocytosed *Escherichia coli* to the lysosome in RAW264.7 cells by recruiting members of the homotypic fusion and vacuole protein sorting (HOPS) complex [36]. ARL8B is thought to be recruited by *S. typhimurium*, which proliferates in acidic phagolysosomes, to facilitate movement toward the cell periphery [77].

We obtained bone marrow from two independently derived strains of ARL8B-deficient mice, $Arl8b^{-/-(MMRRC)}$ and $Arl8b^{-/-(RRP119)}$, in order to directly test the hypothesis that ARL8B-mediated vesicle trafficking events are involved in IFNγ-induced restriction of *L. pneumophila*. Using BMMs from $Arl8b^{-/-(RRP119)}$ and $Arl8b^{-/+(RRP119)}$ mice, we did not observe a significant difference in IFNγ-dependent restriction of *L. pneumophila* compared to WT BMMs stimulated with either 10U/ml or 100U/ml IFNγ (**Fig. 2-13a)**. We did, however, observe a decrease in IFNγ-induced restriction of *L. pneumophila* by $Arl8b^{-/-(MMRRC)}$ BMMs relative to WT BMMs, especially in BMMs stimulated with 10U/ml IFNγ (**Fig. 2-13b**).

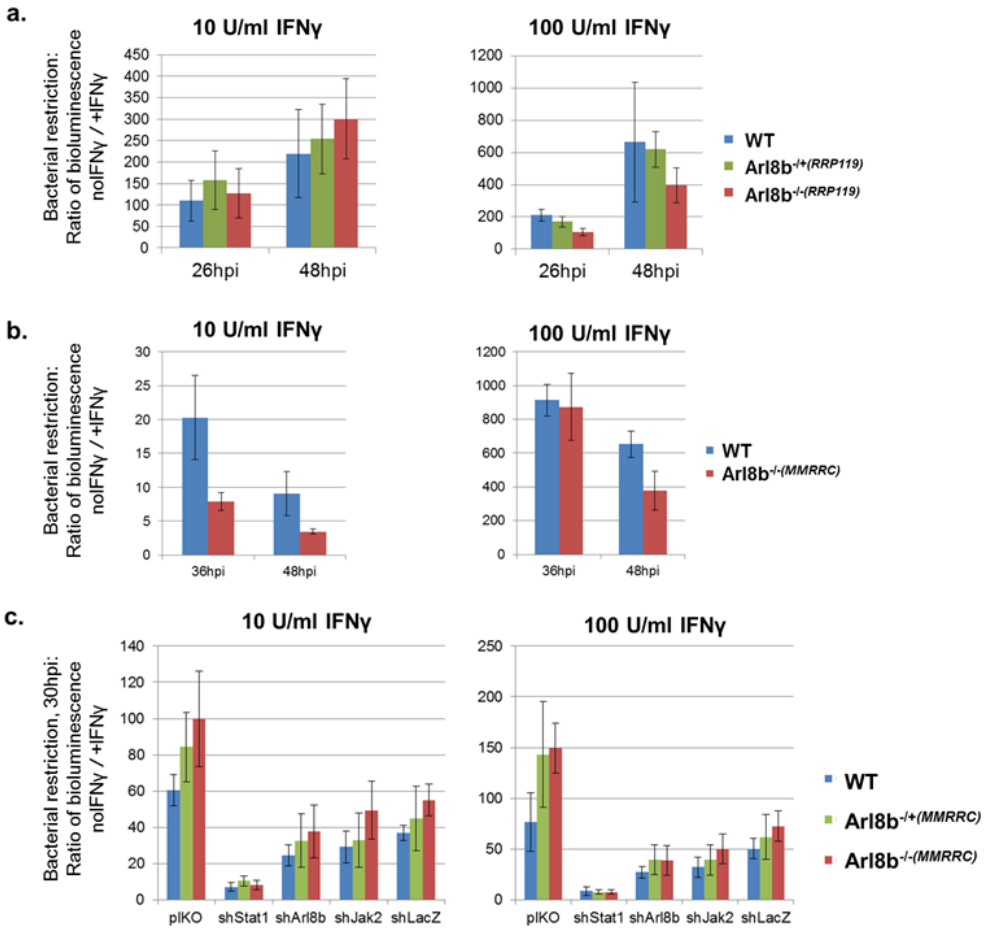

Figure 2-13. Validation of candidate IFNγ mediator ARL8B

Bacterial restriction is calculated as the ratio of Alamar Blue-normalized bioluminescence in resting *vs* IFNγ-stimulated cells at the concentrations of IFNγ and timepoints indicated.

- **a.** IFNγ-induced restriction of *L. pneumophila* in WT, Arl8b$^{-/+(RRP119)}$, and Arl8b$^{-/-(RRP119)}$ BMMs.
- **b.** IFNγ-induced restriction of *L. pneumophila* in WT and Arl8b$^{-/-(MMRRC)}$ BMMs.
- **c.** IFNγ-induced restriction of *L. pneumophila* in WT, Arl8b$^{-/+(MMRRC)}$, and Arl8b$^{-/-(MMRRC)}$ BMMs transduced with shArl8b or negative (pLKO, shLacZ) or positive (shStat1, shJak2) control shRNAs, selected with puromycin, and stimulated with IFNγ at the indicated concentrations for 24 prior to infection with *L. pneumophila*

In a second experiment with Arl8b$^{-/-(MMRRC)}$ BMMs as well as with Arl8b$^{-/+(MMRRC)}$ BMMs, cells were transduced with shRNA targeting ARL8B transcript or positive or negative controls, in order to assess whether the phenotype observed in the secondary screen was a result of shRNA-specific off-

target effects. In this experiment, we did not observe a significant difference in IFNγ-induced restriction of *L. pneumophila* among genotypes (**Fig. 2-13c**). The restriction induced by stimulation with 100U/ml IFNγ observed in cells transduced with shArl8b was comparable to restriction in cells transduced with the positive control shJak2 and nearly two-fold less than in cells transduced with negative control shLacZ, regardless of host genotype. It is not clear why the initial phenotype obtained with Arl8b$^{-/-(MMRRC)}$ BMMs did not reproduce; one possibility is an interaction of lentiviral infection in general that renders ARL8B redundant for IFNγ-mediated bacterial restriction and . These results suggest an off-target effect of the shArl8b construct that produced a hit in the screen.

AP3S1

Finally, we tested the candidate AP3S1 indirectly, by using BMMs derived from mice deficient in the essential AP3 complex member AP3B1. The AP3 complex, thought to reside on the cytosolic face of lysosomes, plays a role in the delivery of protein cargo to lysosomes, the biogenesis of lysosome-related organelles [78,79] and in the activation of TLR4 signaling from phagosomes in dendritic cells [80]. While AP3S1 was classified as a hit in the primary and secondary screens, three distinct shRNA constructs targeting the AP3 complex subunit AP3S2, as well as one shRNA targeting subunit AP3M2, were selected as candidates in the primary screen, prompting us to carry out a more complete investigation of the function of the AP3 complex in primary cells.

In three independent experiments using three pairs of WT and KO mice, we observed a significant defect in IFNγ-induced bacterial restriction in Ap3b1$^{-/-}$ BMMs. In BMMs stimulated with 10 U/ml IFNγ, AP3B1 deficiency led to a tenfold decrease in bacterial restriction capacity (**Fig. 2-14a**), though the phenotype was not significant when 100 U/ml IFNγ was used. We assume that full activation invokes pathways of bacterial restriction independent of AP3. The phenotype did not change when bacteria were opsonized by either IgG or mannose-binding lectin (MBL) instead of the regular serum proteins present in culture media (**Fig. 2-14a, b**), suggesting that the relevant action of

AP3 was independent of phagocytic receptors. However, in two following experiments using independent pairs of WT and KO mice, we were surprised to find no defect in IFNγ-induced bacterial restriction in Ap3b1$^{-/-}$ BMMs over a range of IFNγ concentrations.

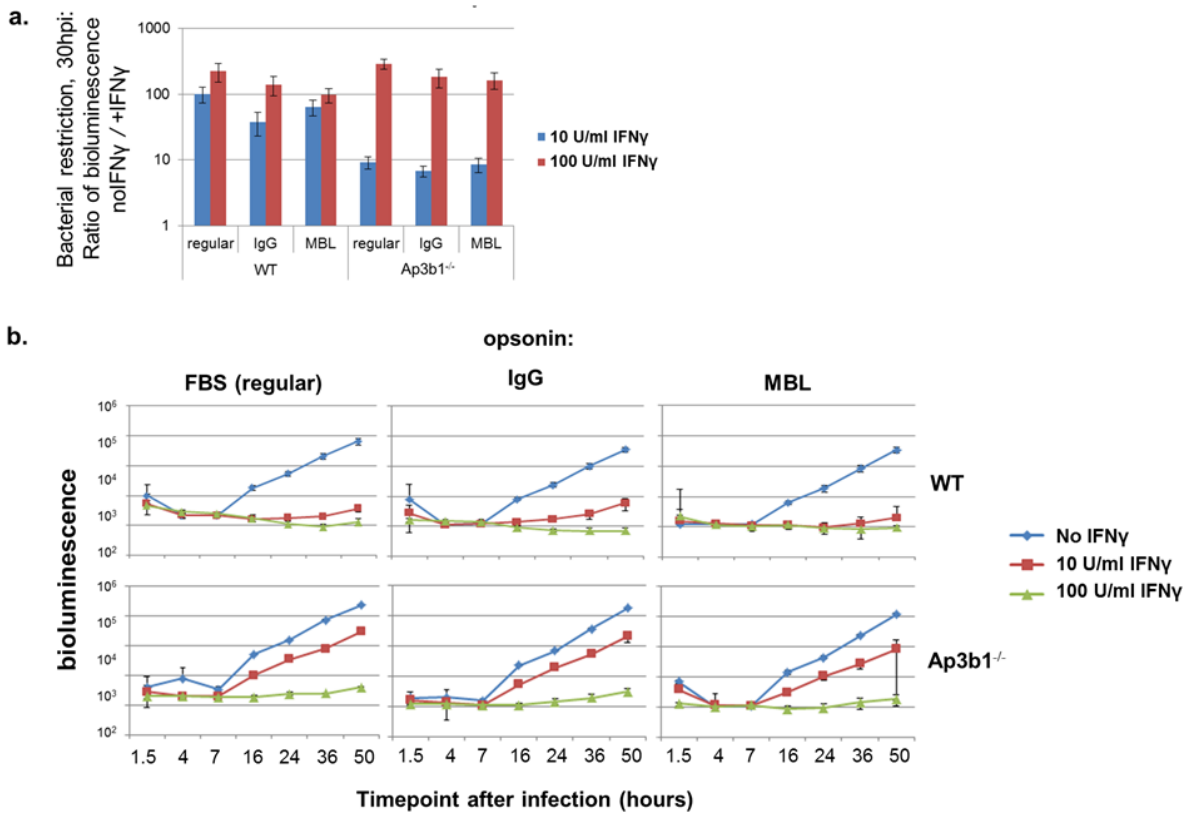

Figure 2-14. Validation of candidate IFNγ mediator AP3B1

a. IFNγ-induced restriction of *L. pneumophila* opsonized in serum (regular), IgG, or MBL in WT and Ap3b1$^{-/-}$ BMMs. Restriction is calculated as the ratio of bioluminescence in resting *vs* IFNγ-stimulated cells at 30hpi.

b. Growth curves of *L. pneumophila* corresponding to the experiment in (**a**)

DISCUSSION

Our goal was to use a targeted RNAi screen to illuminate vesicle trafficking mechanisms that facilitate bacterial restriction in IFNγ-activated macrophages. We used a high-throughput screening protocol to assess the effect of 1985 lentiviral shRNA constructs on cell count and on bacterial growth in resting and IFNγ-stimulated RAWγNOcells. In order to normalize bacterial growth to cell counts under each condition, we developed a generalizable computational method that was robust to outliers, imputed missing data points, and was independent of assumption bias that would otherwise be introduced using a regression model. 82 shRNA constructs classified as hits in the RAWγNO screen were tested in a secondary screen in primary macrophages as well.

Because bacterial growth was measured in resting as well as IFNγ-stimulated cells for every shRNA tested, analysis of the data in resting cells alone constituted a screen-within-a-screen that allowed us to predict host factors required for growth of *L. pneumophila* in RAWγNOcells.

To discover gene products that may be involved, we performed a primary screen in mouse RAWγNO macrophage-like cells. Using RNAi, we perturbed each of 380 genes in a curated set of vesicle trafficking-related genes, and then assessed the ability of these cells to respond to IFNγ by restricting the intracellular replication of *L. pneumophila*. Several hits from this screen were verified in a secondary screen in primary mouse macrophages. Recent work has focused on identifying 1-2 hits most likely to satisfy the primary hypothesis that the candidate is involved in targeting vesicles to the early bacterial phagosome downstream of IFNγ stimulation. We have also begun to rule out several alternative hypotheses to explain the observed IFNγ-dependent effect of hit genes on the bacterial phagosome.

To elucidate the relevance of these and other vesicle trafficking proteins suggested by our screen to IFNγ-mediated maturation of the bacterial phagosome in primary cells, we performed a secondary screen in BMMs of B6 mice. B6 BMMs have iNOS machinery, unlike the RAWγNOcells

used in the primary screen. However, B6 BMMs do not require production of NO for restriction of *L. pneumophila in vitro* [82].

TSPAN6 emerged as a prominent candidate. A relatively tiny protein (27.3kD), Tspan6 – like the other tetraspanins – likely functions via interactions with other proteins, likely through organization of membrane surfaces [83–85]. Therefore, it will be crucial to identify the binding partners of Tspan6 on the membranes of phagosomes, endolysosomal vesicles, or other vesicles, and to identify the dependence and nature of the interactions on intracellular bacterial infection and IFNγ stimulation.

The tetraspanin CD37 interacts with the Dectin-1 PRR and regulates production of IL-6 in macrophages [86], an effect that may be relevant in intracellular infections with the vacuolar parasite *Toxoplama gondii* [87]. A recent paper providing the only published data on TSPAN6 function so far suggests a role for this candidate in antiviral innate immunity [88]. The authors use overexpression and siRNA silencing of human Tspan6 transcript in 293T cells transfected with IFNβ, NFκB or interferon-sensitive response element (ISRE) antiviral response reporter constructs. TSPAN6 was found to be ubiquitinated upon MAVS activation, to localize to mitochondria, bind MAVS and inhibit its interaction with STING and the downstream effectors TRAF3 and IRF3.

The relevance of these findings to our work with TSPAN6 depends on whether the results extend to murine macrophages, and on the role of MAVS in both the macrophage-autonomous (IFNγ-independent) and the IFNγ-mediated response to *L. pneumophila*. It is possible that nucleic acid sensors are activated by bacterial infection, as *L. pneumophila* has been shown to leak bacterial DNA into the host cell cytosol [89]. Interestingly, *L. pneumophila* recruit mitochondria to LCVs in the early stages of infection. However, $MAVS^{-/-}$ BMMs permit only an insignificant increase in *L. pneumophila* replication [90], and MAVS deficiency does not affect bacterial infection *in vivo*. Furthermore, while some existing data support a MAVS-dependent IFNβ

response to *L. pneumophila* infection in vivo and in vitro [91,92], another study showed no effect of MAVS deficiency on IFNβ production in vitro [90].

Our hypothesis is that TSPAN6 *promotes* the IFNγ-dependent restriction of *L. pneumophila*, but may also *inhibit* antibacterial innate immunity in the absence of IFNγ. It is well-established that Type I IFN (stimulated in MAVS-dependent and most other innate immune sensing pathways) restricts *L. pneumophila* in vitro [42,93]. Therefore, our observation that shTspan6 reduces *L. pneumophila* growth in resting macrophages is consistent with a role for TSPAN6 in the inhibition of Type I IFN-mediated, MAVS-dependent responses to bacterial nucleic acids in the host cell cytosol.

Could TSPAN6 promote IFNγ-dependent immunity to *L. pneumophila* by inhibiting MAVS/Type I IFNγ signaling? Little is known about the interactions between Type I and Type II IFN responses in intracellular bacterial infection. In vivo, both types of IFN independently play important roles in restricting *L. pneumophila* infection, and doubly-deficient mice succumb rapidly. In vitro, IFNβ-mediated *L. pneumophila* restriction is limited in cells lacking the IFNγ-inducible protein IRGM [90]. Meanwhile, RIG-I deficiency does not affect the ability of mouse embryonic fibroblasts (MEFs) to restrict *L. pneumophila* in response to IFNγ [93]. In the context of other bacterial infections, examples exist in which Type I IFNs have either augmented the IFNγ response (*S. flexneri* in MEFs) [94] or detracted from it (*L monocytogenes* in macrophages and dendritic cells) [95].

A molecular basis for the impact of Type I IFN on the Type II response is based on competition for STAT1. Downstream of IFNγ receptor (IFNGR), Stat1 forms homodimers, known as gamma-activation factor (GAF) and binds IFNγ-activated sequences (GAS) when phosphorylated at both tyrosine 701 (Y701) and serine 727 (S727). However, phosphorylation of S709 by IKKε in the context of the antiviral response sterically hinders formation of GAF, instead favoring the

heterodimerization of STAT1 and STAT2 [96] to form the ISGF3 transcription complex together with IRF9.

The ability of macrophages to restrict intracellular bacteria in the absence of VTI1B is a significant negative result. VTI1B is a well-described and member of SNARE bundles involved in homotypic endosome-endosome fusion, late endosome-lysosome fusion [97] and autophagosome-lysosome fusion of both starvation-induced autophagosomes and those containing Group A streptococci [72]. We hypothesized, then, that Vti1b could be involved in either the delivery of late endosome-like vesicles to the late phagosome, or in fusion of the phagosome with lysosomes. The fact that Vti1b is dispensable for killing of *L. pneumophila* in IFNγ-activated cells indicates that (a) another SNARE or complex can substitute for VTI1b in fusion events between phagosomes containing *L. pneumophila* and late endosomes/lysosomes, or that (b) phagolysosomal fusion is not necessary for efficient restriction of *L. pneumophila* in response to IFNγ.

Lysotracker assays and acquisition of other endosomal (EEA1, VPS34, STX13, RILP, SNAPIN), autophagosomal (LC3, IRGMs, ATG proteins) and lysosomal markers can also be used to measure stages of phagosome maturation. Furthermore, biotin phagosome loading coupled with uptake of streptavidin-labeled beads or bacteria can monitor phagolysosome fusion in real time. Acquisition of lysosomal functional activities can likewise be measured over time using assays of protease, lipase, and beta-galactosidase activity.

Functional assays are readily performed to analyze bead-containing phagosomes, but a key challenge will be observing the bacterial phagosome which is not as readily isolated. Furthermore, given the potential effects of the *L. pneumophila* secreted factor IcmG on TSPAN6-mediated vesicle fusion, we recognize that measurement of IFNγ-mediated vesicle trafficking effects may be even more clear when live *L. pneumophila* are absent.

MATERIALS AND METHODS

Mice

B6 mice and Ap3b1$^{-/-}$ (*pearl*) mice were from Jackson Laboratories. Bone marrow derived from Arl8b$^{-/-(RRP119)}$ and Arl8b$^{-/-(MMRRC)}$ mice was provided by Salil Garg (Brenner Lab). Bone marrow derived from Vti1b$^{-/-}$, Vti1b$^{-/+}$, and matched control WT mice was provided by Dr. Gabriele Fischer von Mollard.

Cell lines and bacterial strains

RAWγNO cells were purchased from ATCC. *L. pneumophila* strain LP02 delFlaA *lux* was provided by Dr. Jörn Coers. *L. pneumophila* strain LP02 delFlaA pAM239 was provided by Dr. Ralph Isberg.

BMM isolation and culture

Bone marrow was collected from femurs and tibiae of 2-6 month old mice. Red blood cells were lysed using TAC RBC lysis buffer (Sigma). Cells were passed through a 70μm cell strainer and plated in RPMI-1640 medium, supplemented with 10% FBS, L-glutamine, penicillin/streptomycin, MEM nonessential amino acids, HEPES, sodium pyruvate, β-mercaptoethanol, and recombinant human MCSF (10 ng/ml, R&D Systems). For screening, cells were plated directly into 96-well assay plates. For other studies, cells were plated on non-tissue culture treated petri dishes, differentiated for 5d, washed with ice-cold PBS, incubated with PBS at 4°C for 30min, collected by repeated pipetting with PBS, and re-seeded at the densities indicated in complete supplemented media with MCSF. Cells were differentiated for a total of 7d prior to stimulation with IFNγ (Millipore) or infection.

Bacterial infection

L. pneumophila strains were maintained on N-(2-acetamido)-2-aminoethanesulfonic acid (ACES) buffered charcoal-yeast extract agar supplemented with FeNO3, cysteine, and thymidine. For experimental assays, *L. pneumophila* was grown in ACES-buffered yeast extract broth at 37°C to a density greater than 3 OD600. Bacteria were washed with PBS twice before infection. For experiments involving opsonization, bacteria were incubated for 1h with rotation at 37°C with 10 μg/ml recombinant human MBL (provided by Dr. Lynda Stuart) with 5mM CaCl2 or 0.4mg/ml murine IgG (Jackson Immunoresearch).

Primary screen in RAWγNO cell line macrophages

RAWγNOcells were seeded in duplicate in clear-bottom black or solid white 96-well plates at 1000 cells/well, incubated for 4h, then infected with 5ul of lentivirus created by cloning into the pLKO.1 lentiviral vector (RNAi Consortium).

A two-day selection process with 5μg/ml puromycin (Invitrogen) was initiated 2d after viral infection to eliminate cells uninfected with virus. 5d after viral infection, cells were mock-stimulated or stimulated with low (10U/ml) or high (100U/ml) concentrations of IFNγ. 6d after viral infection, cells in black plates were incubated with Alamar Blue (Life Technologies) for 3h, and fluorescence was then measured with a plate reader (Envision) to determine cell counts. Cells in white plates were infected with LP02 delFlaA *lux*, and luminescence was measured with the Envision plate reader at 24, 32, and 48h after infection. The screening set was divided into 4 batches, which were done in series.

Secondary screen in primary cells

Large-scale viral preps of lentivirus bearing shRNA were produced in 293T packaging cells. shRNA sequences were identical to the sequences that produced hits in the primary and secondary

screens and targeted the screen-hit constructs targeting Tspan6 (3 constructs), Snap29, Snap47 and Vti1b. Lentivirus was titrated in parallel with negative control virus containing shRNAs targeting GFP, RFP, LacZ or the empty vector. We observed that maximum cell survival following puromycin selection varied from among viruses. Therefore, we continued to quantify cells in each phenotypic assay and to normalize assay readouts to cell density. We also chose optimal viral volumes per well that resulted in similar cell densities and, as a secondary consideration, that maximized the bacterial restriction phenotype.

Bone marrow macrophage progenitor cells were prepared from B6 mice, seeded in duplicate in clear-bottom black or solid white 96-well plates at 1e5 cells/well, and cultured in the presence of MCSF for 3d before infection with 10ul of lentivirus (The RNAi Consortium). A two-day selection process with 4μg/ml puromycin was initiated 2d after viral infection to eliminate cells uninfected with virus. 5d after viral infection, cells were mock-stimulated or stimulated with IFNγ at 10U/ml. 6d after viral infection, cells in black clear-bottom plates were incubated with Alamar Blue for 3h, and fluorescence was then measured with the Envision plate reader. Cells in white plates were infected with LP02 delFlaA *lux*, and luminescence was measured with the Envision plate reader at 24 and 48h after infection.

The bacterial restriction phenotype assay was performed as follows. Murine BMMs grown in 96 well plates were stimulated by 24h treatment in IFNγ at 10 U/ml or 100 U/ml or grown in media alone. Cells were then spin-infected with *L. pneumophila* LP02 delFlaA *lux* in log-phase growth at an MOI of 20. This bacterial strain expresses the *lux* operon so that bacilli are constitutively bioluminescent. Bioluminescence was quantified in an Envision plate reader. Bacterial restriction was calculated as the ratio of normalized luminescence in resting cells to that in IFNγ-treated cells.

Screen Analysis: Log-transformation and plate normalization

All data were analyzed at the level of individual shRNA constructs, rather than genes. Data reflecting bacterial growth (luminescence) from each timepoint and data reflecting cell count (AlamarBlue) were independently quality-controlled, log-transformed and plate-normalized. Data replicates were first compared to identify and eliminate problematic plates and/or wells. Low-quality plates were eliminated from further analysis. Next, data were log-transformed in order to approach a normal distribution. For the purposes of log-transformation, zero values were converted to a constant value below the lowest nonzero output value generated by the plate reader. The data were then plate-normalized to adjust for systematic error on each plate as follows. For each plate, robust z-scores were determined for each well, using the in-house application RNAeyes (TRC). This program uses the formula: $RZ(i) = (x(i) - plateMedian)/plateMAD$, where RZ(i) is the calculated robust z-score for well (i), x(i) is the log-transformed data for well (i), plateMedian is the median of data for all non-empty wells on the plate, and plateMAD is the median absolute deviation (MAD) of those data, defined as the median of the absolute deviations from the data's median. Next, replicate data for each shRNA construct were combined using the geometric mean (average of log-transformed values), also within RNAeyes. The above analysis yielded one luminescence RZ score and one Alamar Blue RZ score for each shRNA construct. Normalization enabled us to pool data from all plates within a batch together for further analysis.

Normalization to Alamar Blue: calculation of the fit score

We are interested in shRNA constructs that have a significant effect on bacterial growth (luminescence) independent of its effect on cell growth (Alamar Blue). A strong correlation was seen between luminescence and Alamar Blue RZ scores within each batch, and at each timepoint. Luminescence RZ scores were therefore normalized to Alamar Blue RZ scores using a custom MATLAB script. Normalization to Alamar Blue was done independently for luminescence data from each batch and timepoint. First, for each condition/timepoint, luminescence RZ scores (y) were

plotted against Alamar Blue RZ scores (x), with each shRNA construct represented by a single point. A curve to best fit the correlation between the two types of data was calculated as follows. First, the moving average was used to estimate a rough fit curve. For each point, a window of 100 points to the left and right on the x-axis was used to compute a moving average of y-values. At the edges of the x-data, the window of the moving average decreased accordingly to fit within the boundaries of the x-values of the dataset while taking equal numbers of points from left and right along the x-axis. The calculated moving averages, when plotted against Alamar Blue on the x-axis, define a curve that is roughly fit to the data.

The initial fit-curve based on moving average is prone to outlier effects. To refine the fit-curve, a robust moving average was then computed on the basis of the initial moving average. The residual of each data point from the moving average was computed. Each residual was converted to a residual z-score by dividing by the standard deviation of all residuals from the curve. Points with statistically significant residual z-scores (with absolute value greater than 1.96) were labeled as "outliers." The moving average was then re-calculated on the basis of all non-outlier points. Moving average values for the missing outlier points were then intrapolated using a robust linear regression line through the [moving average values vs Alamar Blue] points for 10 non-outlier points to both left and right of the missing outlier. This yielded a refined moving average fit-curve for the data. Refinement by recalculating residuals and removing outliers from the calculation of the fit-curve was iterated a total of 5 times, at which point the fit-curves were observed to converge.

Next, the edge effect of the fit-curve was addressed. Since the span of the moving average, or the number of points to left and right used to calculate moving average for each point, decreases at the low (left) and high (right) edges of the x-data – down to zero at the leftmost and rightmost data point – these calculated values were discarded. To estimate a moving average for the leftmost 20 points, new values were extrapolated using a robust linear regression line through the [moving

average values vs Alamar] points of the next-leftmost 20 points. The rightmost 20 points were treated in an analogous fashion.

Last, the robust, edge-corrected fit-curve was smoothed using Lowess smoothing with a span of 201, in order to eliminate any high-frequency fluctuations without changing the overall position of shape of the curve.

To quantify the deviation of each point from the fit-curve, a fit score was calculated for each point in a manner identical to that used to identify outliers (above). The residual of each data point from the fit-curve was calculated. Each residual was converted to a fit-score by dividing by the standard deviation of all residuals from the curve. Negative fit scores represents points below the fit-curve; positive fit scores correspond to points above the curve.

Since each residual was normalized by the standard deviation of the set of residuals in the batch, data from all batches (for each condition and timepoint) could be combined and analyzed.

Replicate quality

Each RZ score was derived from data in duplicate. It is possible that false hits may result from an outlying data point that is not confirmed by its replicate. To identify shRNA constructs with highly variable replicate data, the residual of each data replicate (log-transformed) to the fit-curve point was calculated for each shRNA. The standard deviation of the residuals of the replicates was calculated as a measure of variability among replicates.

shRNA construct quality

Data regarding knockdown efficiency was available from the TRC for 51% (1953) of shRNA constructs in the experimental set. Of these, 63% (600) were classified as “good” quality data. Knockdown efficiency experiments were mostly in Hepa cells. Any shRNA constructs for which “good” quality knockdown data indicate a knockdown efficiency of less than 69% were not eligible

to be considered as hits. The threshold was set high because knockdown efficiency may vary among cell types.

Candidate selection

For the IFNγ mediator screen, fit scores from the primary condition and timepoint of 100U/ml IFNγ, 2dpi data were used to rank hits. Fit scores from the intermediate condition of 10U/ml IFNγ, 2dpi data were used to confirm hits. Fit scores were sorted in descending order, because points above the curve represent potential hits, with bacterial survival higher than expected in the presence of IFNγ.

In order to qualify as a hit for secondary screening, shRNA constructs were selected on the following criteria: primary fit score > 1.5, intermediate fit score > 1.2. This yielded 95 shRNA construct hits.

For the host factor screen, fit scores from the primary condition and timepoint of no IFNγ, 2dpi data were used to rank hits. Fit scores from the intermediate condition of no IFNγ, 1dpi-late data were used to confirm hits In Batches II-IV. Since the 1dpi-late timepoint was not assayed in Batch I, the 1dpi-early timepoint was used instead for this batch only.

shRNA constructs classified as hits for further screening in the host factor screen satisfied the following criteria: primary fit score < -1.4 (all batches), intermediate fit score <-0.75 (Batch I), intermediate fit score < -1.1 (Batches II-IV).

Hits from the host factor screen were required to satisfy the additional criterion of replicate quality score <0.8, indicating low variation between duplicate data. This criterion was used because wells with abnormally low bacterial luminescence due to experimental error were likely to produce false positives. This step yielded 77 shRNA construct hits (Batches II-IV) and 7 shRNA construct hits (Batch I).

mRNA isolation and qPCR measurement

For experiments in 96-well plates, cells were lysed and polyA+ RNA was prepared using the Turbocapture mRNA kit (Qiagen); mRNA was then reverse transcribed with the Sensiscript RT kit (Qiagen). For cells grown in 6-well plates, total RNA was extracted using the RNeasy kit (Qiagen) following the procedure for adherent cells and reverse transcribed with the High Capacity cDNA Reverse Transcription kit (Applied Biosystems). Real time quantitative PCR reactions were performed on the LightCycler 480 system (Roche) with FastStart Universal SYBR Green Master Mix (Roche). Every reaction was run in triplicate and outliers were excluded. GAPDH was used as an endogenous control for normalization.

Western blotting

Protein was purified from lysates of RAWγNOcells grown in six-well plates, infected with control or candidate-targeting lentivirus, and selected for puromycin resistance. Cells were washed three times in PBS and lysed in RIPA buffer (Boston Bioproducts) with protease inhibitor (Roche). Lysates were purified by centrifugation and suspended in SDS buffer with 10mM dithiothreitol (DTT). Proteins were separated by electrophoresis on a Bis-Tris 4-12% polyacrylamide gel (Novex), transferred to a nitrocellulose membrane, blocked with 5% milk in Tris-buffered saline with Tween (TBST), and incubated overnight at 4°C with primary antibodies in 5% nonfat dry milk in TBST. Membranes were washed, incubated with secondary antibody in 5% bovine serum albumin (BSA) in TBST for one hour at room temperature, washed again, and incubated with for 5min with luminol reagent (Pierce). Antibodies were from Abcam (β-actin, TSPAN6), Cell Signaling Technologies (β-tubulin, GAPDH), Jackson Immunoresearch (HRP-conjugated secondary antibodies), Santa Cruz (SNAP29), and Synaptic Systems (SNAP47).

Flow cytometry analysis

Bead phagocytosis assays were performed using Dragon Green latex microsphere beads (Bangs Laboratories) opsonized in 0.4 mg/ml rabbit IgG (Jackson Immunoresearch) for 1hr with rotation at 37°C, added to macrophages at an MOI of 1, and centrifuged for 10m. LAMP1 quantification was performed using an APC-conjugated monoclonal anti-LAMP1 antibody (BioLegend). Flow cytometry was performed using a FACSDiva (Becton-Dickinson).

Immunofluorescence microscopy

Cells were seeded onto 8-well glass chamber slides (Nunc) at 2e4 cells/chamber, washed three times with PBS, and fixed with 4% paraformaldehyde (Electron Microscopy Sciences) in PBS for ten minutes. Cells were permeabilized with 0.1% saponin and blocked with 5% goat or donkey serum (Jackson Immunoresearch) and 5% BSA (Cell Signaling Technologies). Primary antibody incubation was done overnight at 4°C. Cells were washed with PBS and incubated with Alexa-fluorophore conjugated secondary antibody (Life Technologies) for 1 hour in the dark. Cells were washed, mounted on coverslips, and imaged using a confocal microscope (Zeiss).

REFERENCES

1. Yates R, Hermetter A, Taylor G, Russell D (2007) Macrophage activation downregulates the degradative capacity of the phagosome. Traffic Cph Den 8: 241–250. doi:10.1111/j.1600-0854.2006.00528.x.

2. Santic M, Molmeret M, Abu Kwaik Y (2005) Maturation of the Legionella pneumophila-containing phagosome into a phagolysosome within gamma interferon-activated macrophages. Infect Immun 73: 3166–3171. doi:10.1128/IAI.73.5.3166-3171.2005.

3. Kim B-H, Shenoy AR, Kumar P, Bradfield CJ, MacMicking JD (2012) IFN-inducible GTPases in host cell defense. Cell Host Microbe 12: 432–444. doi:10.1016/j.chom.2012.09.007.

4. Virreira Winter S, Niedelman W, Jensen KD, Rosowski EE, Julien L, et al. (2011) Determinants of GBP recruitment to Toxoplasma gondii vacuoles and the parasitic factors that control it. PloS One 6: e24434. doi:10.1371/journal.pone.0024434.

5. Tiwari S, Choi H-P, Matsuzawa T, Pypaert M, MacMicking J (2009) Targeting of the GTPase Irgm1 to the phagosomal membrane via PtdIns(3,4)P(2) and PtdIns(3,4,5)P(3) promotes immunity to mycobacteria. Nat Immunol 10: 907–917. doi:10.1038/ni.1759.

6. Bernstein-Hanley I, Coers J, Balsara ZR, Taylor GA, Starnbach MN, et al. (2006) The p47 GTPases Igtp and Irgb10 map to the Chlamydia trachomatis susceptibility locus Ctrq-3 and mediate cellular resistance in mice. Proc Natl Acad Sci U S A 103: 14092–14097. doi:10.1073/pnas.0603338103.

7. Coers J, Bernstein-Hanley I, Grotsky D, Parvanova I, Howard JC, et al. (2008) Chlamydia muridarum evades growth restriction by the IFN-gamma-inducible host resistance factor Irgb10. J Immunol Baltim Md 1950 180: 6237–6245.

8. Saka HA, Valdivia R (2012) Emerging roles for lipid droplets in immunity and host-pathogen interactions. Annu Rev Cell Dev Biol 28: 411–437. doi:10.1146/annurev-cellbio-092910-153958.

9. Zhao YO, Khaminets A, Hunn JP, Howard JC (2009) Disruption of the Toxoplasma gondii parasitophorous vacuole by IFNgamma-inducible immunity-related GTPases (IRG proteins) triggers necrotic cell death. PLoS Pathog 5: e1000288. doi:10.1371/journal.ppat.1000288.

10. Ling YM (2006) Vacuolar and plasma membrane stripping and autophagic elimination of Toxoplasma gondii in primed effector macrophages. J Exp Med 203: 2063–2071. doi:10.1084/jem.20061318.

11. Kim B-H, Shenoy A, Kumar P, Das R, Tiwari S, et al. (2011) A family of IFN-γ-inducible 65-kD GTPases protects against bacterial infection. Science 332: 717–721. doi:10.1126/science.1201711.

12. Yamamoto M, Okuyama M, Ma JS, Kimura T, Kamiyama N, et al. (2012) A cluster of interferon-γ-inducible p65 GTPases plays a critical role in host defense against Toxoplasma gondii. Immunity 37: 302–313. doi:10.1016/j.immuni.2012.06.009.

13. Bekpen C, Hunn JP, Rohde C, Parvanova I, Guethlein L, et al. (2004) The interferon-inducible p47 (IRG) GTPases in vertebrates: loss of the cell autonomous resistance mechanism in the human lineage. Genome Biol 6. Available: http://dx.doi.org/10.1186/gb-2005-6-11-r92.

14. Gazzinelli RT, Mendonça-Neto R, Lilue J, Howard J, Sher A (2014) Innate resistance against Toxoplasma gondii: an evolutionary tale of mice, cats, and men. Cell Host Microbe 15: 132–138. doi:10.1016/j.chom.2014.01.004.

15. Zhou H, DeLoid G, Browning E, Gregory DJ, Tan F, et al. (2012) Genome-wide RNAi screen in IFN-γ-treated human macrophages identifies genes mediating resistance to the intracellular pathogen Francisella tularensis. PloS One 7: e31752. doi:10.1371/journal.pone.0031752.

16. Mishra BB, Moura-Alves P, Sonawane A, Hacohen N, Griffiths G, et al. (2010) Mycobacterium tuberculosis protein ESAT-6 is a potent activator of the NLRP3/ASC inflammasome: Inflammasome activation during M. tuberculosis infection. Cell Microbiol 12: 1046–1063. doi:10.1111/j.1462-5822.2010.01450.x.

17. Kim JH, Chan C, Elwell C, Singer MS, Dierks T, et al. (2013) Endosulfatases SULF1 and SULF2 limit Chlamydia muridarum infection. Cell Microbiol 15: 1560–1571. doi:10.1111/cmi.12133.

18. Lombardo F, Ghani Y, Kafatos FC, Christophides GK (2013) Comprehensive genetic dissection of the hemocyte immune response in the malaria mosquito Anopheles gambiae. PLoS Pathog 9: e1003145. doi:10.1371/journal.ppat.1003145.

19. Sundaramurthy V, Barsacchi R, Samusik N, Marsico G, Gilleron J, et al. (2013) Integration of chemical and RNAi multiparametric profiles identifies triggers of intracellular mycobacterial killing. Cell Host Microbe 13: 129–142. doi:10.1016/j.chom.2013.01.008.

20. De Arras L, Laws R, Leach SM, Pontis K, Freedman JH, et al. (2013) Comparative Genomics RNAi Screen Identifies Eftud2 as a Novel Regulator of Innate Immunity. Genetics 197: 485–496. doi:10.1534/genetics.113.160499.

21. Lee MN, Roy M, Ong S-EE, Mertins P, Villani A-CC, et al. (2013) Identification of regulators of the innate immune response to cytosolic DNA and retroviral infection by an integrative approach. Nat Immunol 14: 179–185. doi:10.1038/ni.2509.

22. Kumar D, Nath L, Kamal MA, Varshney A, Jain A, et al. (2010) Genome-wide analysis of the host intracellular network that regulates survival of Mycobacterium tuberculosis. Cell 140: 731–743. doi:10.1016/j.cell.2010.02.012.

23. Misselwitz B, Dilling S, Vonaesch P, Sacher R, Snijder B, et al. (2011) RNAi screen of Salmonella invasion shows role of COPI in membrane targeting of cholesterol and Cdc42. Mol Syst Biol 7: 474. doi:10.1038/msb.2011.7.

24. Genovesio A, Giardini MA, Kwon Y-J, de Macedo Dossin F, Choi SY, et al. (2011) Visual genome-wide RNAi screening to identify human host factors required for Trypanosoma cruzi infection. PloS One 6: e19733. doi:10.1371/journal.pone.0019733.

25. Sharma M, Machuy N, Böhme L, Karunakaran K, Mäurer AP, et al. (2011) HIF-1α is involved in mediating apoptosis resistance to Chlamydia trachomatis-infected cells. Cell Microbiol 13: 1573–1585. doi:10.1111/j.1462-5822.2011.01642.x.

26. Philips JA, Rubin EJ, Perrimon N (2005) Drosophila RNAi screen reveals CD36 family member required for mycobacterial infection. Science 309: 1251–1253. doi:10.1126/science.1116006.

27. Thornbrough JM, Hundley T, Valdivia R, Worley MJ (2012) Human genome-wide RNAi screen for host factors that modulate intracellular Salmonella growth. PloS One 7: e38097. doi:10.1371/journal.pone.0038097.

28. Akimana C, Al-Khodor S, Abu Kwaik Y (2010) Host factors required for modulation of phagosome biogenesis and proliferation of Francisella tularensis within the cytosol. PloS One 5: e11025. doi:10.1371/journal.pone.0011025.

29. Derré I, Pypaert M, Dautry-Varsat A, Agaisse H (2007) RNAi screen in Drosophila cells reveals the involvement of the Tom complex in Chlamydia infection. PLoS Pathog 3: 1446–1458. doi:10.1371/journal.ppat.0030155.

30. Dorer MS, Kirton D, Bader JS, Isberg RR (2006) RNA interference analysis of Legionella in Drosophila cells: exploitation of early secretory apparatus dynamics. PLoS Pathog 2. Available: http://dx.doi.org/10.1371/journal.ppat.0020034.

31. Qin Q-M, Pei J, Ancona V, Shaw BD, Ficht TA, et al. (2008) RNAi screen of endoplasmic reticulum-associated host factors reveals a role for IRE1alpha in supporting Brucella replication. PLoS Pathog 4: e1000110. doi:10.1371/journal.ppat.1000110.

32. Pielage JF, Powell KR, Kalman D, Engel JN (2008) RNAi screen reveals an Abl kinase-dependent host cell pathway involved in Pseudomonas aeruginosa internalization. PLoS Pathog 4: e1000031. doi:10.1371/journal.ppat.1000031.

33. Ulvila J, Vanha-aho L-M, Kleino A, Vähä-Mäkilä M, Vuoksio M, et al. (2011) Cofilin regulator 14-3-3zeta is an evolutionarily conserved protein required for phagocytosis and microbial resistance. J Leukoc Biol 89: 649–659. doi:10.1189/jlb.0410195.

34. Tzircotis G, Braga VMM, Caron E (2011) RhoG is required for both FcγR- and CR3-mediated phagocytosis. J Cell Sci 124: 2897–2902. doi:10.1242/jcs.084269.

35. Kinchen JM, Doukoumetzidis K, Almendinger J, Stergiou L, Tosello-Trampont A, et al. (2008) A pathway for phagosome maturation during engulfment of apoptotic cells. Nat Cell Biol 10: 556–566. doi:10.1038/ncb1718.

36. Garg S, Sharma M, Ung C, Tuli A, Barral DC, et al. (2011) Lysosomal trafficking, antigen presentation, and microbial killing are controlled by the Arf-like GTPase Arl8b. Immunity 35: 182–193. doi:10.1016/j.immuni.2011.06.009.

37. Moffat J, Grueneberg DA, Yang X, Kim SY, Kloepfer AM, et al. (2006) A lentiviral RNAi library for human and mouse genes applied to an arrayed viral high-content screen. Cell 124: 1283–1298. doi:10.1016/j.cell.2006.01.040.

38. Root DE, Hacohen N, Hahn WC, Lander ES, Sabatini DM (2006) Genome-scale loss-of-function screening with a lentiviral RNAi library. Nat Methods 3: 715–719. doi:10.1038/nmeth924.

39. Coers J, Monahan C, Roy C (1999) Modulation of phagosome biogenesis by Legionella pneumophila creates an organelle permissive for intracellular growth. Nat Cell Biol 1: 451–453. doi:10.1038/15687.

40. Mintz CS, Chen JX, Shuman HA (1988) Isolation and characterization of auxotrophic mutants of Legionella pneumophila that fail to multiply in human monocytes. Infect Immun 56: 1449–1455.

41. Ren T, Zamboni DS, Roy CR, Dietrich WF, Vance RE (2006) Flagellin-deficient Legionella mutants evade caspase-1- and Naip5-mediated macrophage immunity. PLoS Pathog 2. Available: http://dx.doi.org/10.1371/journal.ppat.0020018.

42. Coers J, Vance RE, Fontana MF, Dietrich WF (2007) Restriction of Legionella pneumophila growth in macrophages requires the concerted action of cytokine and Naip5/Ipaf signalling pathways. Cell Microbiol 9: 2344–2357. doi:10.1111/j.1462-5822.2007.00963.x.

43. Summersgill JT, Powell LA, Buster BL, Miller RD, Ramirez JA (1992) Killing of Legionella pneumophila by nitric oxide in gamma-interferon-activated macrophages. J Leukoc Biol 52: 625–629.

44. Lowenstein CJ, Alley EW, Raval P, Snowman AM, Snyder SH, et al. (1993) Macrophage nitric oxide synthase gene: two upstream regions mediate induction by interferon gamma and lipopolysaccharide. Proc Natl Acad Sci U S A 90: 9730–9734.

45. The RNAi Consortium (n.d.) RNAeyes. Available: http://www.broadinstitute.org/rnai/public/software/misc.

46. Vieira OV, Botelho RJ, Rameh L, Brachmann SM, Matsuo T, et al. (2001) Distinct roles of class I and class III phosphatidylinositol 3-kinases in phagosome formation and maturation. J Cell Biol 155: 19–25. doi:10.1083/jcb.200107069.

47. Hardy P-O, Diallo TO, Matte C, Descoteaux A (2009) Roles of phosphatidylinositol 3-kinase and p38 mitogen-activated protein kinase in the regulation of protein kinase C-alpha activation in interferon-gamma-stimulated macrophages. Immunology 128: e652–660. doi:10.1111/j.1365-2567.2009.03055.x.

48. Gold ES, Underhill DM, Morrissette NS, Guo J, McNiven MA, et al. (1999) Dynamin 2 is required for phagocytosis in macrophages. J Exp Med 190: 1849–1856.

49. Robinson CG, Roy CR (2006) Attachment and fusion of endoplasmic reticulum with vacuoles containing Legionella pneumophila. Cell Microbiol 8: 793–805. doi:10.1111/j.1462-5822.2005.00666.x.

50. Kagan JC, Roy CR (2002) Legionella phagosomes intercept vesicular traffic from endoplasmic reticulum exit sites. Nat Cell Biol 4: 945–954. doi:10.1038/ncb883.

51. Scales SJ, Pepperkok R, Kreis TE (1997) Visualization of ER-to-Golgi transport in living cells reveals a sequential mode of action for COPII and COPI. Cell 90: 1137–1148.

52. Zhang T, Wong SH, Tang BL, Xu Y, Hong W (1999) Morphological and functional association of Sec22b/ERS-24 with the pre-Golgi intermediate compartment. Mol Biol Cell 10: 435–453.

53. Kagan JC, Stein M-PP, Pypaert M, Roy CR (2004) Legionella subvert the functions of Rab1 and Sec22b to create a replicative organelle. J Exp Med 199: 1201–1211. doi:10.1084/jem.20031706.

54. Volpicelli-Daley LA, Li Y, Zhang C-J, Kahn RA (2005) Isoform-selective effects of the depletion of ADP-ribosylation factors 1-5 on membrane traffic. Mol Biol Cell 16: 4495–4508. doi:10.1091/mbc.E04-12-1042.

55. Teasdale RD, Loci D, Houghton F, Karlsson L, Gleeson PA (2001) A large family of endosome-localized proteins related to sorting nexin 1. Biochem J 358: 7–16.

56. Suarez A, Ueno T, Huebner R, McCaffery JM, Inoue T (2014) Bin/Amphiphysin/Rvs (BAR) family members bend membranes in cells. Sci Rep 4: 4693. doi:10.1038/srep04693.

57. Van Weering JRT, Verkade P, Cullen PJ (2010) SNX-BAR proteins in phosphoinositide-mediated, tubular-based endosomal sorting. Semin Cell Dev Biol 21: 371–380. doi:10.1016/j.semcdb.2009.11.009.

58. Van Weering JRT, Verkade P, Cullen PJ (2012) SNX-BAR-mediated endosome tubulation is co-ordinated with endosome maturation. Traffic Cph Den 13: 94–107. doi:10.1111/j.1600-0854.2011.01297.x.

59. Pons V, Ustunel C, Rolland C, Torti E, Parton RG, et al. (2012) SNX12 role in endosome membrane transport. PloS One 7: e38949. doi:10.1371/journal.pone.0038949.

60. Håberg K, Lundmark R, Carlsson SR (2008) SNX18 is an SNX9 paralog that acts as a membrane tubulator in AP-1-positive endosomal trafficking. J Cell Sci 121: 1495–1505. doi:10.1242/jcs.028530.

61. Li Z, Solomon JM, Isberg RR (2005) Dictyostelium discoideum strains lacking the RtoA protein are defective for maturation of the Legionella pneumophila replication vacuole. Cell Microbiol 7: 431–442. doi:10.1111/j.1462-5822.2004.00472.x.

62. Rapaport D, Lugassy Y, Sprecher E, Horowitz M (2010) Loss of SNAP29 impairs endocytic recycling and cell motility. PloS One 5. Available: http://dx.doi.org/10.1371/journal.pone.0009759.

63. Sprecher E, Akemi I-Y, Mordechai M-K, Rapaport D, Goldsher D, et al. (2005) A mutation in SNAP29, coding for a SNARE protein involved in intracellular trafficking, causes a novel neurocutaneous syndrome characterized by cerebral dysgenesis, neuropathy, ichthyosis, and palmoplantar keratoderma. Am J Hum Genet 77: 242–251. doi:10.1086/432556.

64. Li Q, Frank M, Akiyama M, Shimizu H, Ho S-YY, et al. (2011) Abca12-mediated lipid transport and Snap29-dependent trafficking of lamellar granules are crucial for epidermal morphogenesis in a zebrafish model of ichthyosis. Dis Model Mech 4: 777–785. doi:10.1242/dmm.007146.

65. Wesolowski J, Caldwell V, Paumet F (2012) A novel function for SNAP29 (synaptosomal-associated protein of 29 kDa) in mast cell phagocytosis. PloS One 7. Available: http://dx.doi.org/10.1371/journal.pone.0049886.

66. Fuchs-Telem D, Stewart H, Rapaport D, Nousbeck J, Gat A, et al. (2011) CEDNIK syndrome results from loss-of-function mutations in SNAP29. Br J Dermatol 164: 610–616. doi:10.1111/j.1365-2133.2010.10133.x.

67. Holt M, Varoqueaux F, Wiederhold K, Takamori S, Urlaub H, et al. (2006) Identification of SNAP-47, a novel Qbc-SNARE with ubiquitous expression. J Biol Chem 281: 17076–17083. doi:10.1074/jbc.M513838200.

68. Luzio JP, Pryor PR, Bright NA (2007) Lysosomes: fusion and function. Nat Rev Mol Cell Biol 8: 622–632. doi:10.1038/nrm2217.

69. Offenhäuser C, Lei N, Roy S, Collins BM, Stow JL, et al. (2011) Syntaxin 11 binds Vti1b and regulates late endosome to lysosome fusion in macrophages. Traffic Cph Den 12: 762–773. doi:10.1111/j.1600-0854.2011.01189.x.

70. Murray RZ, Wylie FG, Khromykh T, Hume DA, Stow JL (2005) Syntaxin 6 and Vti1b form a novel SNARE complex, which is up-regulated in activated macrophages to facilitate exocytosis of tumor necrosis Factor-alpha. J Biol Chem 280: 10478–10483. doi:10.1074/jbc.M414420200.

71. Liew FY, Li Y, Millott S (1990) Tumor necrosis factor-alpha synergizes with IFN-gamma in mediating killing of Leishmania major through the induction of nitric oxide. J Immunol Baltim Md 1950 145: 4306–4310.

72. Furuta N, Fujita N, Noda T, Yoshimori T, Amano A (2010) Combinational soluble N-ethylmaleimide-sensitive factor attachment protein receptor proteins VAMP8 and Vti1b mediate fusion of antimicrobial and canonical autophagosomes with lysosomes. Mol Biol Cell 21: 1001–1010. doi:10.1091/mbc.E09-08-0693.

73. Paumet F, Wesolowski J, Garcia-Diaz A, Delevoye C, Aulner N, et al. (2009) Intracellular bacteria encode inhibitory SNARE-like proteins. PloS One 4: e7375. doi:10.1371/journal.pone.0007375.

74. Atlashkin V, Kreykenbohm V, Eskelinen E-L, Wenzel D, Fayyazi A, et al. (2003) Deletion of the SNARE vti1b in mice results in the loss of a single SNARE partner, syntaxin 8. Mol Cell Biol 23: 5198–5207.

75. Bagshaw RD, Callahan JW, Mahuran DJ (2006) The Arf-family protein, Arl8b, is involved in the spatial distribution of lysosomes. Biochem Biophys Res Commun 344: 1186–1191. doi:10.1016/j.bbrc.2006.03.221.

76. Hofmann I, Munro S (2006) An N-terminally acetylated Arf-like GTPase is localised to lysosomes and affects their motility. J Cell Sci 119: 1494–1503. doi:10.1242/jcs.02958.

77. Kaniuk NA, Canadien V, Bagshaw RD, Bakowski M, Braun V, et al. (2011) Salmonella exploits Arl8B-directed kinesin activity to promote endosome tubulation and cell-to-cell transfer. Cell Microbiol 13: 1812–1823. doi:10.1111/j.1462-5822.2011.01663.x.

78. Chapuy B, Tikkanen R, Mühlhausen C, Wenzel D, von Figura K, et al. (2008) AP-1 and AP-3 mediate sorting of melanosomal and lysosomal membrane proteins into distinct post-Golgi trafficking pathways. Traffic Cph Den 9: 1157–1172. doi:10.1111/j.1600-0854.2008.00745.x.

79. Dell'Angelica EC, Ohno H, Ooi CE, Rabinovich E, Roche KW, et al. (1997) AP-3: an adaptor-like protein complex with ubiquitous expression. EMBO J 16: 917–928. doi:10.1093/emboj/16.5.917.

80. Blasius AL, Arnold CN, Georgel P, Rutschmann S, Xia Y, et al. (2010) Slc15a4, AP-3, and Hermansky-Pudlak syndrome proteins are required for Toll-like receptor signaling in plasmacytoid dendritic cells. Proc Natl Acad Sci U S A 107: 19973–19978. doi:10.1073/pnas.1014051107.

81. Hmama Z, Sendide K, Talal A, Garcia R, Dobos K, et al. (2004) Quantitative analysis of phagolysosome fusion in intact cells: inhibition by mycobacterial lipoarabinomannan and rescue by an 1alpha,25-dihydroxyvitamin D3-phosphoinositide 3-kinase pathway. J Cell Sci 117: 2131–2140. doi:10.1242/jcs.01072.

82. Akamine M, Higa F, Haranaga S, Tateyama M, Mori N, et al. (2007) Interferon-gamma reverses the evasion of Birc1e/Naip5 gene mediated murine macrophage immunity by Legionella pneumophila mutant lacking flagellin. Microbiol Immunol 51: 279–287.

83. Charrin S, le Naour F, Silvie O, Milhiet P-E, Boucheix C, et al. (2009) Lateral organization of membrane proteins: tetraspanins spin their web. Biochem J 420: 133–154. doi:10.1042/BJ20082422.

84. Berditchevski F, Odintsova E (2007) Tetraspanins as regulators of protein trafficking. Traffic Cph Den 8: 89–96. doi:10.1111/j.1600-0854.2006.00515.x.

85. Hemler ME (2005) Tetraspanin functions and associated microdomains. Nat Rev Mol Cell Biol 6: 801–811. doi:10.1038/nrm1736.

86. Meyer-Wentrup F, Figdor CG, Ansems M, Brossart P, Wright MD, et al. (2007) Dectin-1 interaction with tetraspanin CD37 inhibits IL-6 production. J Immunol Baltim Md 1950 178: 154–162.

87. Yan J, Wu B, Huang B, Huang S, Jiang S, et al. (2014) Dectin-1-CD37 association regulates IL-6 expression during Toxoplasma gondii infection. Parasitol Res. doi:10.1007/s00436-014-3946-1.

88. Wang Y, Tong X, Omoregie E, Liu W, Meng S, et al. (2012) Tetraspanin 6 (TSPAN6) negatively regulates retinoic acid-inducible gene I-like receptor-mediated immune signaling in a ubiquitination-dependent manner. J Biol Chem 287: 34626–34634. doi:10.1074/jbc.M112.390401.

89. Ge J, Gong Y-NN, Xu Y, Shao F (2012) Preventing bacterial DNA release and absent in melanoma 2 inflammasome activation by a Legionella effector functioning in membrane trafficking. Proc Natl Acad Sci U S A 109: 6193–6198. doi:10.1073/pnas.1117490109.

90. Lippmann J, Müller HC, Naujoks J, Tabeling C, Shin S, et al. (2011) Dissection of a type I interferon pathway in controlling bacterial intracellular infection in mice. Cell Microbiol 13: 1668–1682. doi:10.1111/j.1462-5822.2011.01646.x.

91. Chiu Y-H, Macmillan J, Chen Z (2009) RNA polymerase III detects cytosolic DNA and induces type I interferons through the RIG-I pathway. Cell 138: 576–591. doi:10.1016/j.cell.2009.06.015.

92. Monroe K, McWhirter S, Vance R (2009) Identification of host cytosolic sensors and bacterial factors regulating the type I interferon response to Legionella pneumophila. PLoS Pathog 5. Available: http://dx.doi.org/10.1371/journal.ppat.1000665.

93. Plumlee C, Lee C, Beg A, Decker T, Shuman H, et al. (2009) Interferons direct an effective innate response to Legionella pneumophila infection. J Biol Chem 284: 30058–30066. doi:10.1074/jbc.M109.018283.

94. Jehl S, Nogueira C, Zhang X, Starnbach M (2012) IFNγ inhibits the cytosolic replication of Shigella flexneri via the cytoplasmic RNA sensor RIG-I. PLoS Pathog 8. Available: http://dx.doi.org/10.1371/journal.ppat.1002809.

95. Rayamajhi M, Humann J, Penheiter K, Andreasen K, Lenz L (2010) Induction of IFN-alphabeta enables Listeria monocytogenes to suppress macrophage activation by IFN-gamma. J Exp Med 207: 327–337. doi:10.1084/jem.20091746.

96. Ng S-LL, Friedman BA, Schmid S, Gertz J, Myers RM, et al. (2011) IκB kinase epsilon (IKK(epsilon)) regulates the balance between type I and type II interferon responses. Proc Natl Acad Sci U S A 108: 21170–21175. doi:10.1073/pnas.1119137109.

97. Antonin W, Holroyd C, Fasshauer D, Pabst S, Von Mollard G, et al. (2000) A SNARE complex mediating fusion of late endosomes defines conserved properties of SNARE structure and function. EMBO J 19: 6453–6464. doi:10.1093/emboj/19.23.6453.

Chapter 3: IRF3 inhibits IFNγ-mediated restriction of intracellular pathogens

Introduction
Results
Discussion
Materials and Methods
References

ABSTRACT

Macrophages use an array of innate immune sensors to detect intracellular pathogens and to tailor effective antimicrobial responses. During infection with some pathogenic vacuolar bacteria and parasites, however, extrinsic activation with the cytokine interferon gamma (IFNγ) is often required as well to tip the scales of the host-pathogen balance toward host protection and bacterial restriction. Prior work has uncovered positive and negative interactions among intersecting signaling pathways, but the effect of innate pathogen sensing on the persistence and activity of the antibacterial IFNγ-activated state is largely unknown. We show that in the absence of continued IFNγ stimulation, the key innate sensing transcription factor IRF3 suppresses the IFNγ-induced antimicrobial state in macrophages infected with the intracellular bacterium *Legionella pneumophila* and the protozoan parasite *Trypanosoma cruzi*. Surprisingly, this activity is independent of cytosolic nucleic acid sensors that activate IRF3 through the signaling adaptors STING or MAVS. Furthermore, this repression is independent of Type I IFNs usually activated downstream of IRF3. Still, IRF3 deficiency profoundly affects the transcriptional program of both IFNγ-activated and bacterially-infected macrophages.IRF3 suppresses the expression of nitric oxide synthase (iNOS), yet the significant increase in antimicrobial nitric oxide levels observed in infected $IRF3^{-/-}$ macrophages is not required for their enhanced antibacterial capacity. Gene expression analysis suggests other innate immune mechanisms, including iron restriction that may be involved in enhanced IFNγ-dependent pathogen restriction in $IRF3^{-/-}$ BMMs. Finally, we show that IFNγ-activated but not resting macrophages antagonize IRF3 effects by excluding the active form of IRF3 from the nucleus. These data are consistent with a cascade of inhibition, in which active IRF3 imperfectly excluded from the nucleus of IFNγ-activated macrophages suppresses IFNγ-induced effectors.

INTRODUCTION

Interferon gamma (IFNγ) is a potent activator of macrophage defense mechanisms that restrict intracellular pathogens, especially bacteria and parasites that subvert the host phagosome into a replicative vacuole. While IFNγ is produced extrinsically by NK, NKT, and T cells, macrophages also possess innate immune sensors that detect infection and stimulate cell-intrinsic defense. Previous studies suggest a synergy between several pathogen sensing pathways and IFNγ activation in macrophages at the level of signaling and transcription [1–3]. Despite our knowledge of microbial ligands, the sensors that detect them, and the pathways induced downstream, little is understood about whether and how these innate sensing pathways affect restriction of bacteria in macrophages activated by IFNγ.

Legionella pneumophila is a Gram-negative vacuolar bacterial pathogen of protozoan phagocytes that can opportunistically colonize mammalian macrophages and, in humans, lead to Legionnaire's disease or Pontiac fever. Several innate sensing pathways are known to mediate macrophage responses to *L. pneumophila*, including the inflammasome [4–8], Toll-like receptor (TLR) [9], and cytosolic DNA [8,10] and RNA [11] sensing pathways. Despite the vacuolar localization of *L. pneumophila*, there is evidence that bacterial nucleic acids and other pathogen ligands reach sensors throughout the cells via the specialized secretion system Dot/icm [12,13]. Infected macrophages with an intact NAIP5-NLRC4 inflammasome pathway undergo rapid pyroptosis upon exposure to bacterial flagellin. Resting macrophages that lack elements of the NAIP5 pathway or are infected with flagellin-deficient *L. pneumophila*, are permissive for bacterial growth. Macrophages activated by IFNγ, however, become restrictive.

We tested the hypothesis that innate sensing pathways synergize with the IFNγ-induced anti-bacterial state. We thus quantified IFNγ-induced restriction of intracellular bacteria in bone-marrow derived macrophages (BMMs) from mice deficient in key components of pathogen sensing

pathways. In our studies, we used a bacterial strain lacking flagellin to eliminate NAIP5/NLRC4-induced pyroptosis, allowing us to analyze the role of the TLR, DNA- and RNA-sensing pathways in IFNγ -mediated restriction.

RESULTS

To determine the effects of innate sensing on IFNγ-activated bacterial restriction, we first considered the roles of the Toll-like receptors (TLRs), membrane-associated sensors of bacterial cell wall components and nucleic acids. We used mice lacking both MYD88 and TRIF to eliminate signaling downstream of TLR ligand sensing. BMMs were pre-stimulated with IFNγ for 24hr, and media was completely replaced with IFNγ-free media during at the time of infection in order to temporally separate IFNγ signaling and bacterial sensing events, allowing observation of the effects of genetic perturbations on the maintenance of the IFNγ-activated state, IFNγ-free media was used to wash uninternalized bacteria 2h after infection (**Fig 3-1a**). Alternately, resting BMMs were infected with *L.p*. in IFNγ-free media and only stimulated with IFNγ-at the media change 2h after infection, a scenario that captures potential effects of genetic perturbations on the establishment (via signal transduction from the IFNγ receptor) as well as on the maintenance of the IFNγ-activated state (**Fig. 3-1b**).

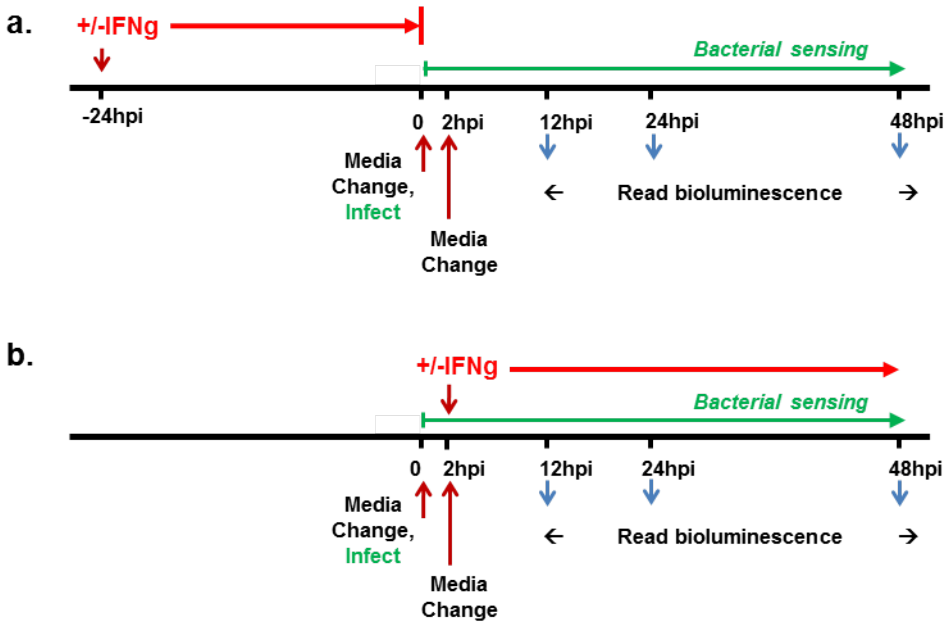

Figure 3-1. Schematic of the innate immune sensor/IFNγ pathway interaction assay
During infection, media is removed and replaced with media containing bacteria. Media is changed again 2h after infection to remove uninternalized bacteria. Bacterial growth is tracked over 48h by measuring bacterial bioluminescence.

- **a.** Pre-stimulation of macrophages with IFNγ, followed by removal of IFNγ prior to infection with bacteria, isolates the effects of sensing on the *maintenance* of the IFNγ-activated state
- **b.** Stimulation of macrophages with IFNγ *during* infection with bacteria involves the effects of sensing on the *establishment* of the IFNγ-activated state

TLR signaling through MYD88/TRIF synergizes with concurrent IFNγ signaling, but does not affect the maintenance of the IFNγ-activated state

BMMs were infected with LP02 delFlaA *lux*, a flagellin-deficient, constitutively bioluminescent strain of *L. pneumophila*. As expected, *L. pneumophila* exhibits logarithmic growth in resting B6 BMMs, but is highly restricted in BMMs prestimulated with IFNγ in a dose-dependent manner. We found that MYD88/TRIF deficiency did not significantly affect permissivity to *L. pneumophila* growth relative to WT in resting BMMs but enhanced growth in BMMs prestimulated with 10U/ml or 100U/ml IFNγ (**Fig. 3-2, top**), indicating that TLR signaling plays a nonredundant

role in the macrophage-intrinsic maintenance or the antibacterial activity of the IFNγ-activated state.

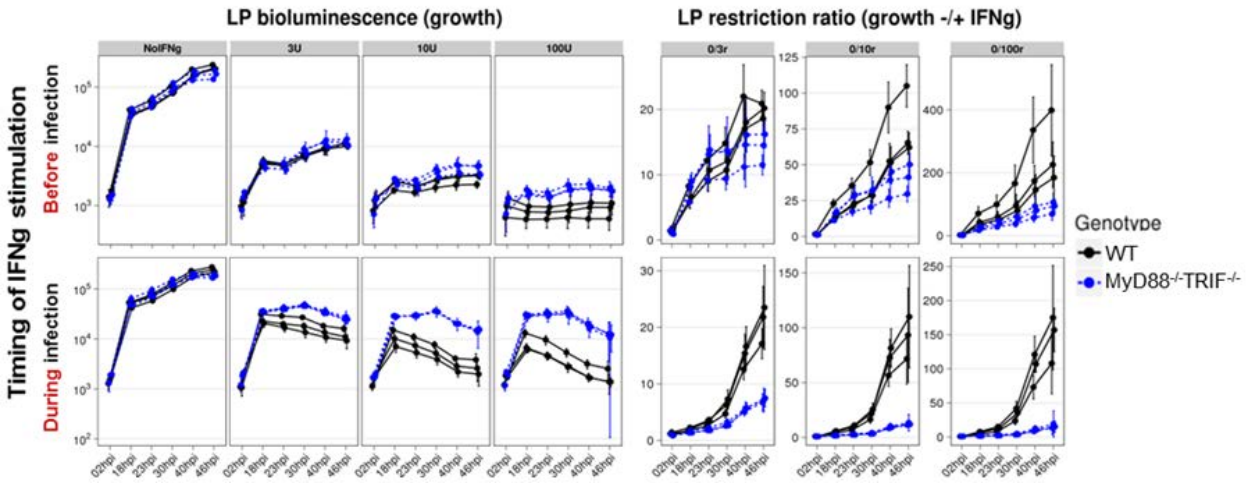

Figure 3-2. Contribution of MYD88 and TRIF to the establishment and maintenance of the IFNγ-activated state

Intracellular growth of *L. pneumophila* (**left**) in IFNγ-stimulated BMMs is enhanced in MyD88$^{-/-}$ and TRIF$^{-/-}$ BMMs (blue) compared to WT BMMs (black). IFNγ-dependent restriction of *L. pneumophila* (**right**) is decreased roughly twofold in MyD88/TRIF$^{-/-}$ BMMs prestimulated with IFNγ prior to infection (**top**), and over fivefold in MyD88/TRIF$^{-/-}$ BMMs stimulated with IFNγ during infection (**bottom**).

To verify the observation that TLR and IFNγ signaling pathways may interact synergistically when stimulated at the same time (as seen in many studies, for example [1]) we stimulated BMMs with IFNγ at 2h post-infection . Compared to WT BMMs, over fivefold reduction in IFNγ-activated bacterial restriction was observed in MyD88$^{-/-}$TRIF$^{-/-}$ BMMs (**Fig. 3-2**). We conclude that the TLR pathway can significantly synergize with IFNγ signaling to establish the anti-bacterial state of macrophages, but also facilitates the maintenance of a pre-established IFNγ-induced anti-bacterial state, albeit with a smaller effect on bacterial restriction.

The role of nucleic acid sensing in the restriction of bacteria by IFNγ-activated BMMs

We next asked whether intracellular nucleic acid sensing affects IFNγ-activated bacterial restriction. Previous work has identified the role of MAVS [11,13] and STING [10] in the Type I interferon macrophage response to *L. pneumophila* RNA and DNA, respectively. We found, however, that the capacity of IFNγ pre-stimulated BMMs to restrict *L. pneumophila* was unchanged in $MAVS^{-/-}$ or $STING^{-/-}$ BMMs at nearly all concentrations of IFNγ tested, with the exception of a decrease in bacterial restriction in $STING^{-/-}$ BMMs at 3U/ml (**Fig. 3-3, top**). Therefore, we found no evidence for a role for MAVS or STING-dependent sensing pathways in the maintenance of the IFNγ-activated state. In addition, bacterial growth and restriction in BMMs stimulated with IFNγ 2h after infection were not changed by lack of either STING or MAVS, indicating that neither adaptor is necessary for establishment of the IFNγ-activated state (**Fig. 3-3, bottom**).

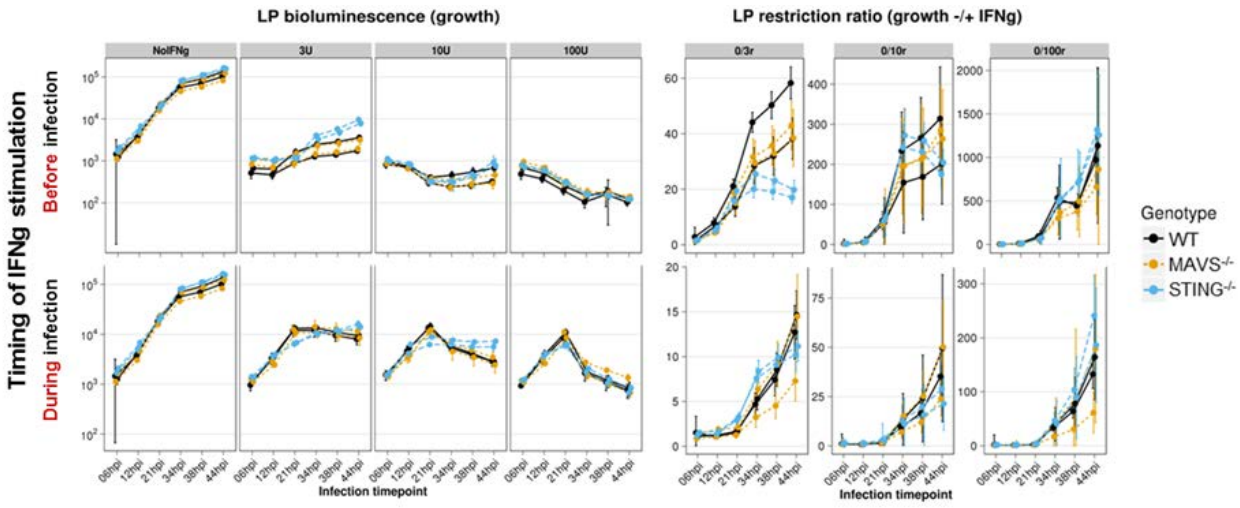

Figure 3-3. Contribution of STING, but not MAVS to the maintenance of the IFNγ -activated state

Intracellular growth of *L. pneumophila* (**left**) in IFNγ-stimulated BMMs is enhanced in STING$^{-/-}$ BMMs (blue) but not MAVS$^{-/-}$ BMMs (orange) compared to WT BMMs (black). IFNγ-dependent restriction of *L. pneumophila* (**right**) is decreased by 25-50% in STING$^{-/-}$ BMMs prestimulated with IFNγ (**top**), but not in BMMs stimulated with IFNγ during infection (**bottom**).

Given the possibility that multiple nucleic acid (DNA or RNA) sensing pathways may have to be ablated in the same mouse to observe changes in capacity for IFNγ-activated bacterial restriction, we next tested BMMs deficient in the phagolysosomal nuclease DNAse2 or the cytosolic DNase TREX1, both of which harbor an excess of immunostimulatory DNA [14–22]. *L. pneumophila* growth in resting BMMs was not significantly altered by lack of either nuclease. In IFNγ pre-stimulated BMMs, lack of DNAse2 impaired restriction (**Fig. 3-4a**), IFNγ while lack of TREX1 enhanced bacterial restriction compared to WT BMMs **(Fig. 3-4b**). Since the source (host or bacteria) of excess of immunostimulatory DNA is still not known, we cannot explain these divergent results. Thus, we conclude that while STING-independent DNA sensing pathways may still impact bacterial killing, STING and MAVS are not likely involved in modulating bacterial restriction induced by IFNγ.

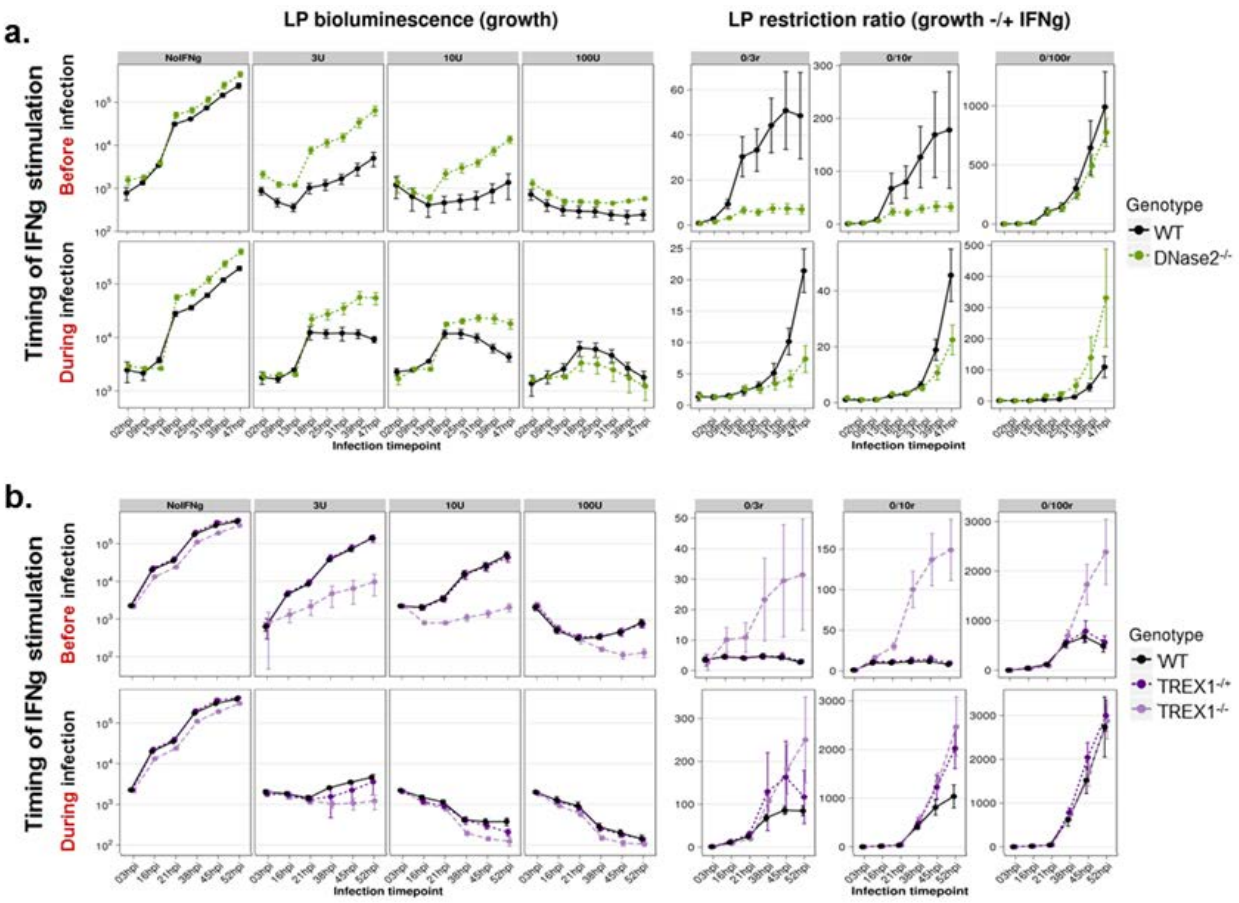

Figure 3-4. Opposing effects of DNAse2 and TREX1 nucleases on the IFNγ-activated state

Intracellular growth of *L. pneumophila* (left) in IFNγ-stimulated BMMs is enhanced in DNase2$^{-/-}$ BMMs (green) (**a**) but not TREX1$^{-/-}$ BMMs (violet) (**b**) compared to WT BMMs (black).

- **a.** IFNγ-dependent restriction of *L. pneumophila* (**right**) is decreased fivefold in DNase2$^{-/-}$ BMMs prestimulated with IFNγ (**top**), as well as in BMMs stimulated with IFNγ during infection (**bottom**), compared to WT BMMs.
- **b.** IFNγ-dependent restriction of *L. pneumophila* (**right**) is enhanced 20-fold in TREX1$^{-/-}$ BMMs prestimulated with IFNγ (**top**), and twofold in BMMs stimulated with IFNγ during infection (**bottom**), compared to WT BMMs.

IRF3 inhibits the maintenance and not the establishment of the IFNγ-activated state

Since loss of MYD88/TRIF, MAVS or STING did not impact IFNγ pre-stimulated bacterial restriction, we considered two transcription factors, IRF3 and IRF7, which are essential elements

downstream of many innate immune sensors (including the known non-inflammasome nucleic acid sensors). We found that resting IRF3$^{-/-}$IRF7$^{-/-}$ BMMs are slightly more permissive to *L. pneumophila* compared to WT BMMs. Surprisingly, lack of IRF3/7 significantly enhanced IFNγ-mediated restriction of bacteria (**Fig. 3-5a, top**), in contrast to our original hypothesis of synergy between innate sensing and IFNγ-mediated host defense.

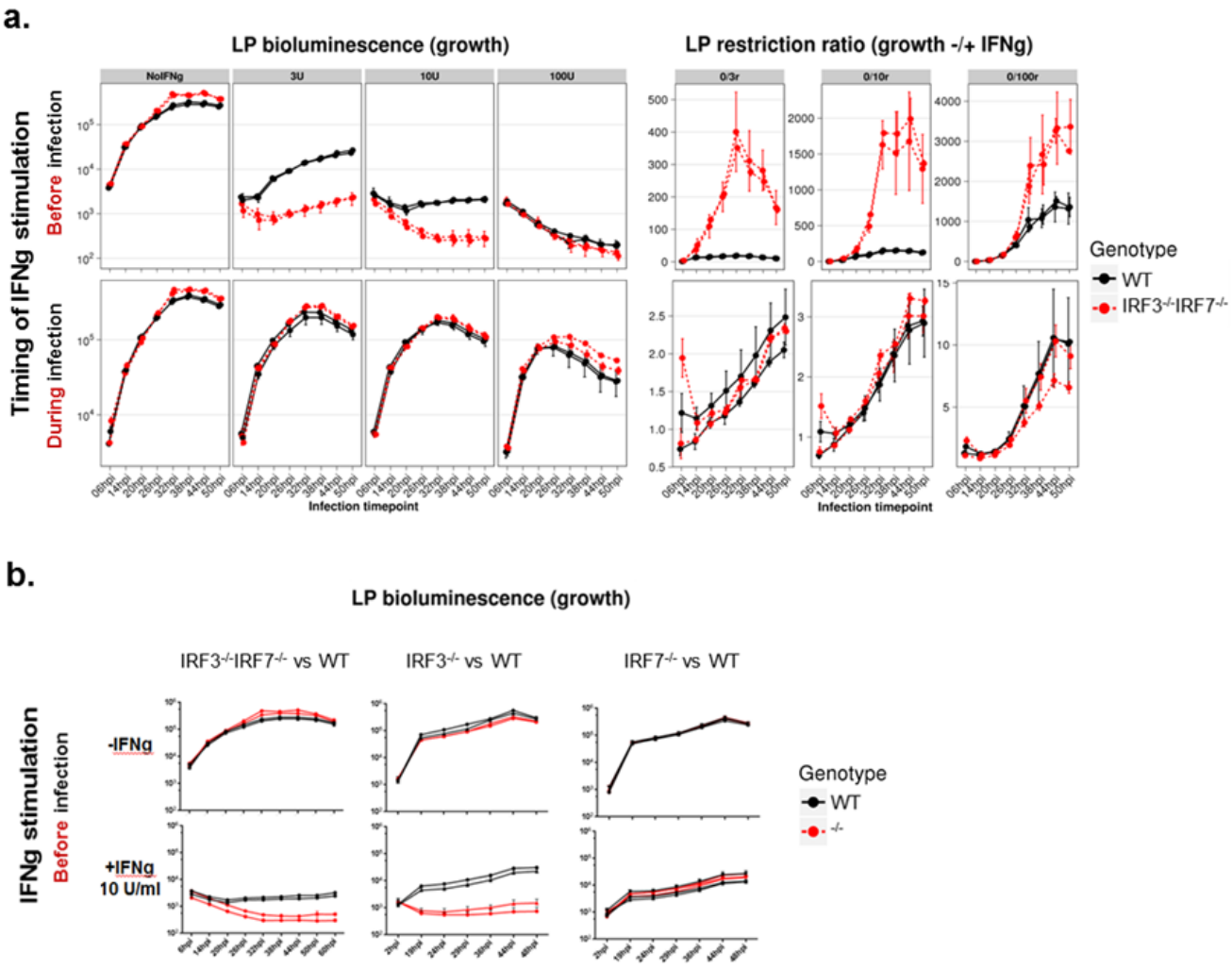

Figure 3-5. IRF3-mediated suppression of the IFNγ-activated state

a. IFNγ-dependent restriction of *L. pneumophila* (**right**) is enhanced tenfold in IRF3$^{-/-}$IRF7$^{-/-}$ BMMs prestimulated with IFNγ (**top**), but not in BMMs stimulated with IFNγ during infection (**bottom**), compared to WT BMMs.

b. Growth of *L. pneumophila* in IFNγ-stimulated BMMs is enhanced in IRF3$^{-/-}$IRF7$^{-/-}$ BMMs and IRF3$^{-/-}$ BMMs, but not IRF7$^{-/-}$ BMMs, compared to WT BMMs.

We next asked whether IRF3/7 also affect the establishment of the IFNγ-activated state by stimulating BMMs with IFNγ at 2h after infection. Under these conditions, IFNγ-mediated bacterial restriction was similar in WT and IRF3$^{-/-}$IRF7$^{-/-}$ BMMs (**Fig. 3-5a, bottom**), suggesting that IRF3-

mediated pathways involved in sensing of *L. pneumophila* affect the maintenance, but not the establishment of the IFNγ-activated state.

Further experiments with IRF3$^{-/-}$IRF7$^{-/-}$ BMMs showed that lack of IRF3 is wholly responsible for the enhanced bacterial restriction observed in IFNγ-activated IRF3$^{-/-}$IRF7$^{-/-}$ BMMs (**Fig. 3-5b**), while IRF7$^{-/-}$ BMMs are phenotypically identical to WT BMMs in this model of IFNγ-mediated bacterial restriction. Prolonged incubation with IFNγ was insufficient to overcome IRF3-dependent suppression of the IFNγ-mediated state (**Fig. 3-6**). Together, our results suggest that MAVS- and STING-independent sensing of *L. pneumophila* infection is likely to activate IRF3, which in turn robustly inhibits the maintenance of the IFNγ-activated state.

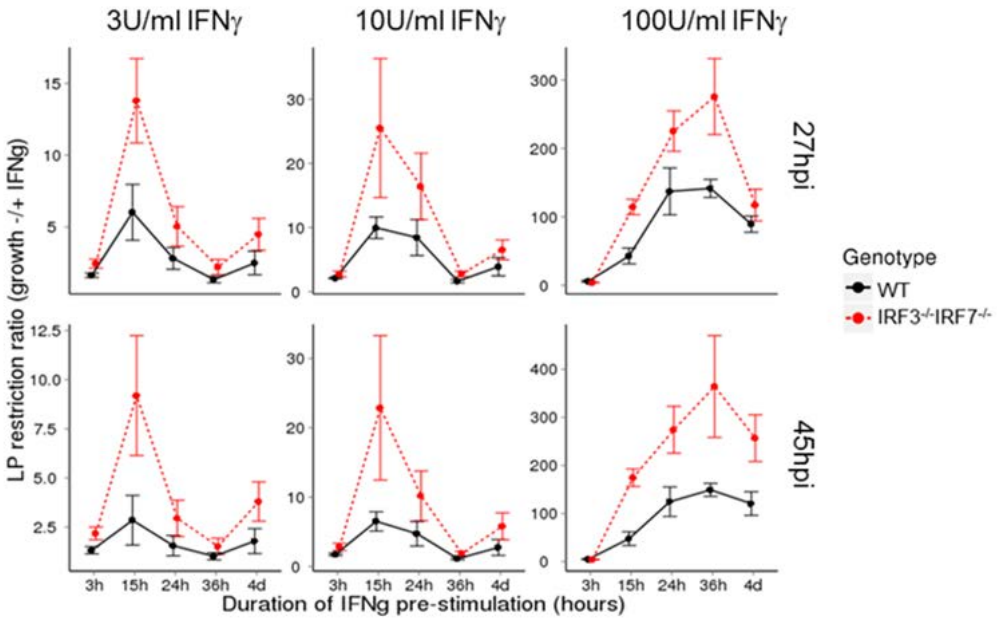

Figure 3-6. Relationship between the magnitude of IRF3-mediated suppression of IFNγ effector activity and the magnitude of effector activity

IFNγ-dependent restriction (y-axis) of *L. pneumophila* in BMMs pre-stimulated with IFNγ for the duration of time indicated (x-axis) was calculated as the ratio of bioluminescence in resting BMMs *vs* in BMMs stimulated with the indicated concentration of IFNγ, measured at the timepoints indicated.

IFNγ inhibits *L. pneumophila*-induced phosphorylation of IRF3

To test whether IRF3 is affected by infection of IFNγ, we monitored the activity of IRF3 based on its phosphorylation and dimerization in the nucleus and cytosol [23]. Within 1hr of infection by *L. pneumophila*, Ser385-phosphorylated IRF3 is strongly detected in the nucleus of control BMMs not treated with IFNγ, but surprisingly, is barely detectable in IFNγ pre-stimulated BMMs in either the nucleus (**Fig. 3-7a**) or cytosol (**Fig. 3-7b**). IFNγ-stimulated or resting, but uninfected BMMs do not accumulate IRF3-p in the nucleus (**Fig. 3-7c**) or cytoplasm (**Fig. 3-7d**). Thus, while infection can lead to phosphorylation (likely through an unidentified innate sensing mechanism), IFNγ appears to inhibit this phosphorylation, consistent with an antagonistic relationship between bacterial sensing and IFNγ in regulating the anti-bacterial state. A simple hypothesis is that IFNγ blocks IRF3 activation to reduce the inhibitory effect of IRF3, and that complete removal of IRF3 allows IFNγ to maximally induce bacterial restriction.

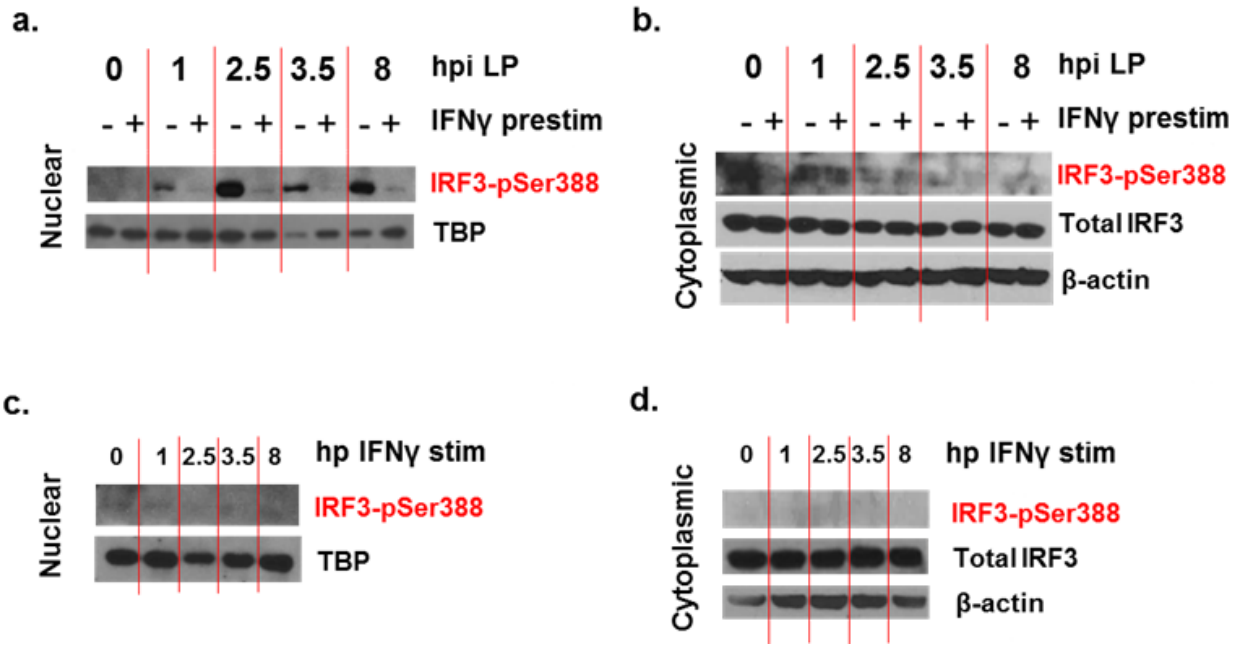

Figure 3-7. Activation of IRF3 in resting, but not IFNγ-activated BMMs upon infection with *L. pneumophila*

IRF3 phosphorylation at serine 388 was assessed by Western blot using lysates from resting or IFNγ-prestimulated WT BMMs infected with *L. pneumophila* and lysed at the timepoints indicated.

- **a.** Nuclear extracts from BMMs mock-stimulated or stimulated with IFNγ for 24h and infected with *L. pneumophila* for the duration of time indicated. The nuclear protein TBP is used as a loading control.
- **b.** Cytoplasmic extracts from BMMs as in (**a**). Total IRF3 is quantified as well. β-actin is used as a loading control.
- **c.** Nuclear extracts from BMMs stimulated with IFNγ for the duration of time indicated. The nuclear protein TBP is used as a loading control.
- **d.** Cytoplasmic extracts from BMMs as in (**c**). Total IRF3 is quantified as well. β-actin is used as a loading control.

TBK1 and IKKε phosphorylation profiles are not consistent with changes in IRF3 phosphorylation

To determine whether the known IRF3 kinases, IKKε and TBK1, are activated upon infection or modulated by IFNγ, we monitored their phosphorylation in cell lysates. We found that

IKKε and TBK1 are phosphorylated in response to *L. pneumophila* infection in both resting and IFNγ pre-stimulated BMMs. IKKε phosphorylation was, in fact, transiently higher in IFNγ pre-stimulated BMMs than in resting BMMs (**Fig. 3-8**). The observed exclusion of IRF3-pS385 from the nucleus in BMMs containing active forms of IKKε and TBK1 could be consistent with several different scenarios. First, IFNγ effectors could block the phosphorylation of IRF3 at Ser385 by activated IKKε and TBK1, either directly or by separating them spatially into different locations within the cell. Alternatively, IRF3-pS385 could be rapidly dephosphorylated in an IFNγ-dependent manner. Third, IFNγ-activated BMMs could block the translocation of IRF3-pS385 into the nucleus.

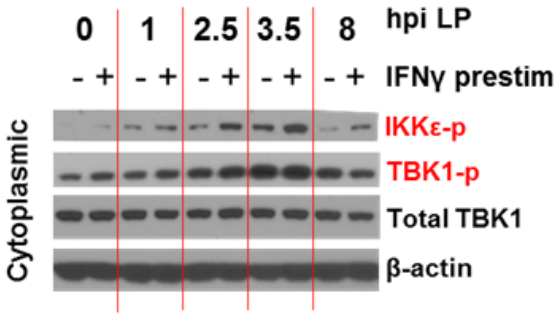

Figure 3-8. Activation of IKKε and TBK1 in resting and IFNγ-preactivated BMMs upon infection with *L. pneumophila*

Western blot analysis of IKKε and TBK1 phosphorylation. BMMs from resting or IFNγ-prestimulated WT BMMs were infected with *L. pneumophila* and lysed at the timepoints indicated.

To test the latter possibility, we had probed the corresponding cytoplasmic extracts of each sample for the presence of IRF3-pS385. Since phosphorylated IRF3 does not accumulate in the cytoplasm of IFNγ-activated BMMs (**Fig. 3-7b**), our evidence suggests that activated IKKε and TBK1 cannot stably phosphorylate IRF3 at Ser385 in IFNγ-activated BMMs.

Further supporting the lack of connection between IRF3 phosphorylation and phosphorylation of its known kinases, we found that deficiency in IKKε or knockdown of TBK1

could not phenocopy IRF3 deficiency. We note that we could not assess the ability of IKKε$^{-/-}$ BMMs treated with shTBK1 to phenocopy IRF3 deficiency, because of the confounding requirement for IKKε and TBK1 for efficient bacterial growth in resting BMMs (**Fig. 3-9**).

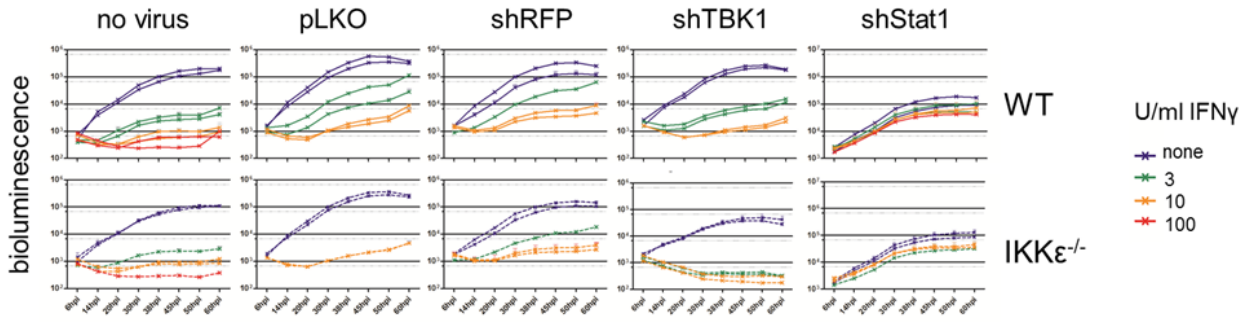

Figure 3-9. Contribution of IRF3 kinases to the maintenance of the IFNγ-activated state
WT or IKKε$^{-/-}$ BMMs were transduced with shTBK1, with control shRNA, or mock-transduced (no virus). Following puromycin selection, BMMs were re-seeded into 96-well plates at constant cell density and infected with *L. pneumophila*. Bioluminescence is proportional to bacterial growth.

Type I IFN does not inhibit the IFNγ-activated state during *L. pneumophila* infection of macrophages

We next considered how IRF3 may repress the IFNγ anti-bacterial state. We thus studied the role and induction of Type I IFNs, the most potent immune regulators induced by IRF3 activation. Even though we did not detect the presence of the Ser385-phosphorylated form thought to be required for Type I IFN induction in in the nuclei of IFNγ-prestimulated BMMs either before or after *L. pneumophila* infection, others have demonstrated that post-translational modifications are not easily correlated with the transcriptional activity of IRF3 [24]. Therefore, we pursued a series of independent assays to test the role of IRF3-mediated Type I IFN in repressing the anti-bacterial state.

While the targets of Type I and II interferons partially overlap [25–27], prior studies have shown that Type I and II IFN-stimulated pathways can reinforce [25,28–32] or antagonize [25,33–35] each other in a context-dependent manner. In the context of bacterial infection, prior work has uncovered only antagonizing effects of Type I IFN on IFNγ-dependent activation through a variety of mechanisms, including induction of antagonistic effectors [35] and downregulation of the IFNγ receptor [21]. We expected lack of the Type I IFN receptor, IFNAR, to phenocopy lack of IRF3, consistent with these reports, by enhancing IFNγ-activated bacterial restriction.

In resting BMMs, IFNAR deficiency conferred a slight increase in permissivity to growth of *L. pneumophila* (**Fig. 3-10a, top left**), consistent with prior observations [36]. Contrary to our expectations, and despite evidence that baseline signaling through IFNAR is required for a full-fledged response to IFNγ [37], IFNAR deficiency did not significantly affect IFNγ-dependent *L. pneumophila* restriction in BMMs stimulated prior to infection (**Fig. 3-10a, top right**). This result suggests that endogenous Type I IFN signaling in BMMs treated with IFNγ and infected with *L. pneumophila* did not alter the IFNγ-activated state. Consistent with this hypothesis, the ability of neither $IRF3^{-/-}$ nor WT IFNγ-activated BMMs to restrict *L. pneumophila* were affected when IFNAR receptors were blocked with a neutralizing antibody (**Fig. 3-10a, bottom**). Likewise, the establishment of the IFNγ-activated state was only minimally affected by loss or blocking of IFNAR (**Fig. 3-11**).

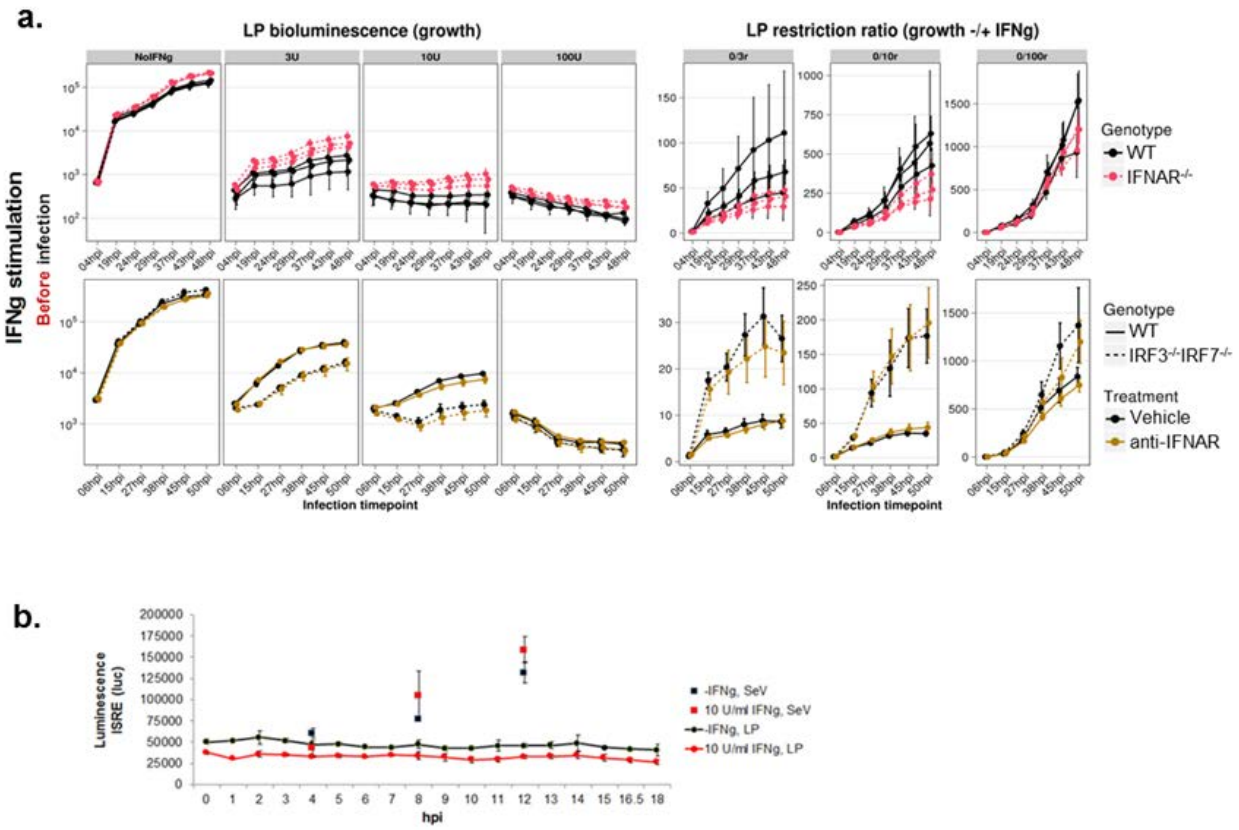

Figure 3-10. IRF3 mediates suppression of the IFNγ-activated state in macrophages independently of endogenous Type I interferons

a. Growth of *L. pneumophila* (**left**) in BMMs stimulated with IFNγ prior to infection is enhanced in IFNAR$^{-/-}$ BMMs (magenta) compared to WT BMMs (black). IFNγ-dependent restriction of *L. pneumophila* (**right**) is decreased by roughly 25-50% in IFNAR$^{-/-}$ BMMs pre-stimulated with IFNγ (**top**). Blocking IFNAR with a neutralizing antibody did not affect bacterial growth or restriction in pre-stimulated WT or IRF3$^{-/-}$IRF7$^{-/-}$ BMMs (**bottom**)

b. BMMs that were either resting or pre-stimulated with IFNγ produce Type I interferons in response to infection with Sendai virus but not *L. pneumophila*, as measured by an ISRE assay in p53$^{-/-}$ MEFs.

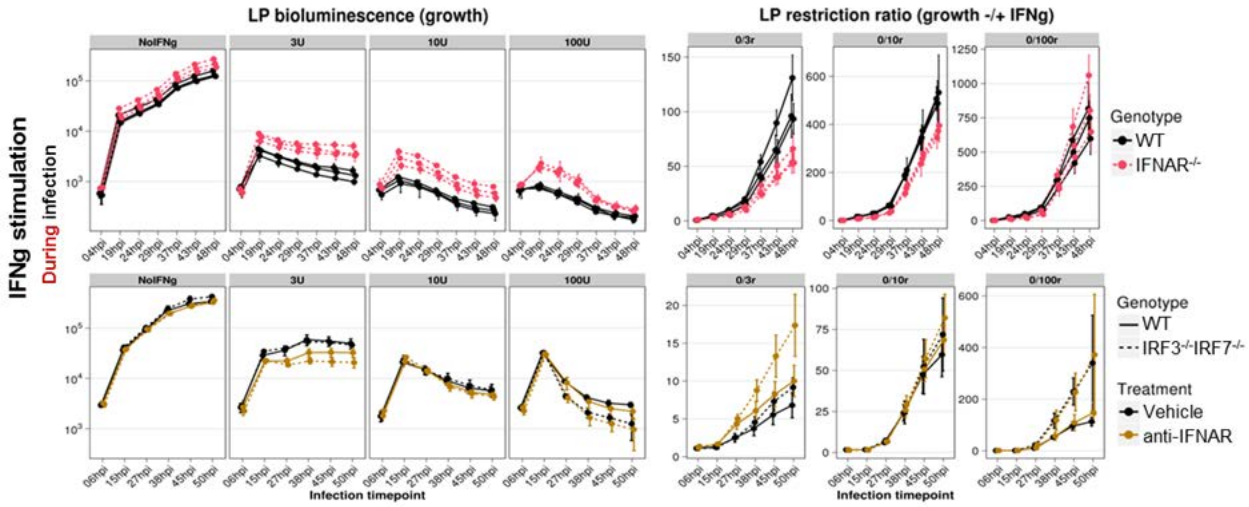

Figure 3-11. Involvement of endogenous signaling through IFNAR in establishment of the IFNγ-activated state in macrophages

Intracellular growth of *L. pneumophila* (**left**) in BMMs stimulated with IFNγ only during bacterial infection is enhanced in IFNAR$^{-/-}$ BMMs (magenta) compared to WT BMMs (black). IFNγ-dependent restriction of *L. pneumophila* (**right**) is decreased slightly in IFNAR$^{-/-}$ BMMs stimulated with IFNγ during infection (**top**). Blocking IFNAR with a neutralizing antibody did not affect bacterial growth or restriction in WT or IRF3$^{-/-}$IRF7$^{-/-}$ BMMs stimulated with IFNγ during infection (**bottom**)

These results suggest that IRF3-mediated repression of the IFNγ-activated state proceeds through a novel, Type I IFN-independent mechanism. In fact, we found that the level of endogenous production of Type I IFNs by WT BMMs during *L. pneumophila* infection is very low. Supernatants from *L. pneumophila*-infected WT BMMs were unable to activate ISRE-driven transcription in a reporter cell line, while supernatants from BMMs infected with Sendai virus at an MOI of 2 robustly activated the ISRE reporter (**Fig. 3-10b**). IFNβ transcript levels in *L. pneumophila* infected BMMs were less than 0.1% of those in Sendai virus-infected BMMs, and were not significantly affected by IFNγ pre-stimulation.

Even when added exogenously at high levels, Type I IFNs do not repress the IFNγ-activated state. In both WT and IRF3$^{-/-}$ BMMs prestimulated with IFNγ and infected with *L. pneumophila*,

stimulation with IFNβ 2 hours after infection appeared to potentiate IFNγ-mediated effectors, significantly enhancing bacterial restriction throughout the course of infection (**Fig. 3-12, top**). Exogenous IFNβ modestly enhanced bacterial restriction in resting, infected BMMs as well, but the effect was only significant at timepoints 38h after infection. Notably, the relative timing of IFNβ stimulation is critical to its effect on the IFNγ-activated state. In both WT and IRF3$^{-/-}$ BMMs stimulated with IFNγ 2h *after L. pneumophila* infection, simultaneous stimulation with exogenous IFNβ significantly *restricts* IFNγ-activated bacterial restriction (**Fig. 3-12, bottom),** likely by direct inhibition of IFNγ signaling [25] and subsequent establishment of the IFNγ-mediated state. In summary, while Type I and II interferons clearly interact to modulate the anti-bacterial state, Type I IFN signaling is not required for the inhibitory effect of IRF3 on the anti-bacterial state.

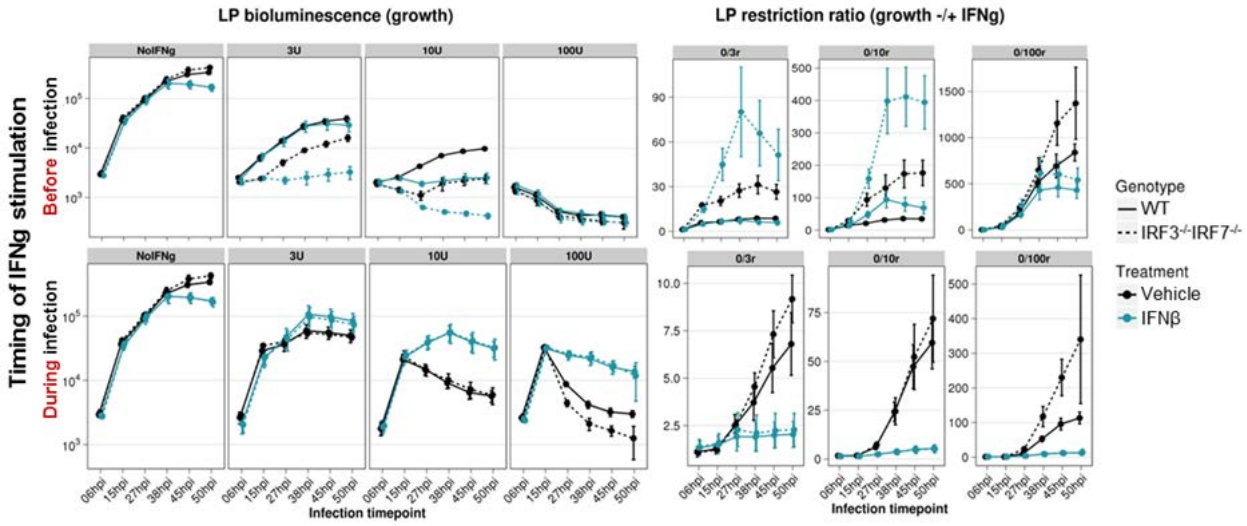

Figure 3-12. Opposite effects of exogenous Type I IFN on the establishment and maintenance of the IFNγ-activated state

(**Top**) Growth of *L. pneumophila* (**left**) in both WT and IRF3$^{-/-}$IRF7$^{-/-}$ BMMs pre-stimulated with IFNγ prior to bacterial infection is decreased in BMMs treated with exogenous IFNβ during infection (blue) compared to mock-treated BMMs (black), and IFNγ-dependent restriction of *L. pneumophila* (**right**) is significantly increased.

(**Bottom**) Treatment with exogenous IFNβ in BMMs stimulated with IFNγ only after bacterial infection increases bacterial growth (**left**) and decreases restriction (**right**).

IRF3/7 deficiency affects the transcriptional programs of resting, IFNγ-stimulated, and *L. pneumophila*-infected BMMs

To further investigate potential roles for IRF3-mediated alteration of gene expression, we used RNA-seq transcriptome analysis to explore potential targets of IRF3 responsible for inhibition of the IFNγ-activated state. IRF3 could affect IFNγ-mediated bacterial restriction via changes in the transcriptome either (a) indirectly, by inducing a repressor that destabilizes the IFNγ-activated state (as illustrated in the context of hepatitis [38]) or (b) directly, by inhibiting a promoter element or transcription factor that is necessary to maintain the IFNγ-activated state, a novel IRF3 function recently demonstrated in T cells, where it binds RORγT to inhibit its nuclear translocation and subsequent IL-17 induction [39].

We found a number of genes both repressed and induced in $IRF3^{-/-}IRF7^{-/-}$ BMMs in the context of activation with 10U/ml IFNγ followed by *L. pneumophila* infection. Of 28,416 genes measured, we chose the 8,885 whose maximum expression values fell within the 50^{th} percentile or higher of all expression values. Of these, 232 genes varied by 3-fold or more based on genotype within any of the categories representing IFNγ-stimulated and/or *L.pneumophila*-infected BMMs. Of these, the expression of 93 genes varied by 3-fold or more based on genotype in BMMs that were both IFNγ-stimulated and *L.pneumophila*-infected (**Fig. 3-13**) while 162 did not (**Fig. 3-14**). 43 genes were differentially expressed based on genotype in IFNγ-stimulated, infected BMMs only (**Fig. 3-13a**), including one gene previously identified as a direct antibacterial effector in macrophages, Lcn2 (lipocalin 2). The list of genes uniquely regulated by IRF3 only in IFNγ-stimulated, *L.pneumophila*-infected BMMs includes genes that encode transcription factors (LYL1, EGR3, EPAS1, BATF3, KRC, viral response and cytokine genes (OASL2, IFIT3, MX1, IL23a), GPCR ligands (NPY, NIACR), the p47 GTPase GM12250, and genes involved in apoptosis (CHEK2, NPTX1, SERPINB2, FAH) as well as non-apoptotic cell death (CD00IF). The

ten genes differentially regulated based on genotype only in infected BMMs, regardless of IFNγ stimulation, include the transcription factor PLAC8 and the IFNγ-inducible GTPase IFGGA2 (encoded by the gene Gm4951) (**Fig. 3-13b, top**). 28 genes differ in IFNγ-activated, *L.pneumophila*-infected BMMs as well as at baseline, these include the viral response gene (OASL1) as well as secreted factors including G-CSF (CSF3) and the acute-phase reactant SAA3 (**Fig. 3-13b**).

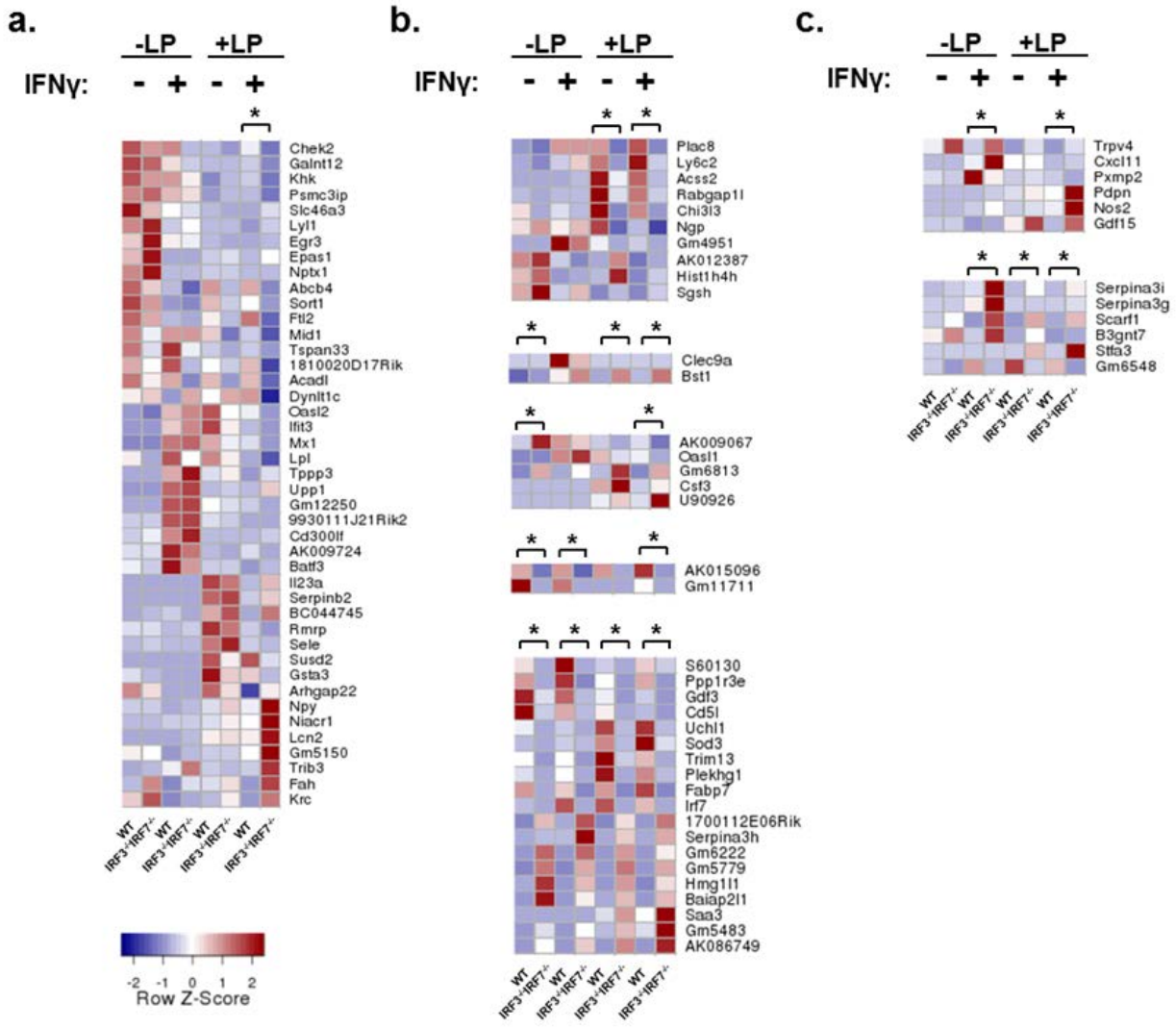

Figure 3-13. Effect of IRF3/7 deficiency on the transcriptomes of IFNγ-stimulated BMMs infected with *L. pneumophila*

Heatplots of row-normalized RNA-seq data from IRF3$^{-/-}$IRF7$^{-/-}$ and WT resting and IFNγ–prestimulated BMMs before and 12 hours after infection with *L. pneumophila*. Transcripts with maximum expression above the 50th abundance percentile were further filtered to include only transcripts with a fold-change of 3 or more between the two genotypes (indicated by *) in IFNγ-prestimulated and *L. pneumophila*-infected BMMs as well as (**a**) no other categories, (**b**) in infected BMMs, or at baseline, or (**c**) in IFNγ-stimulated BMMs, but not at baseline.

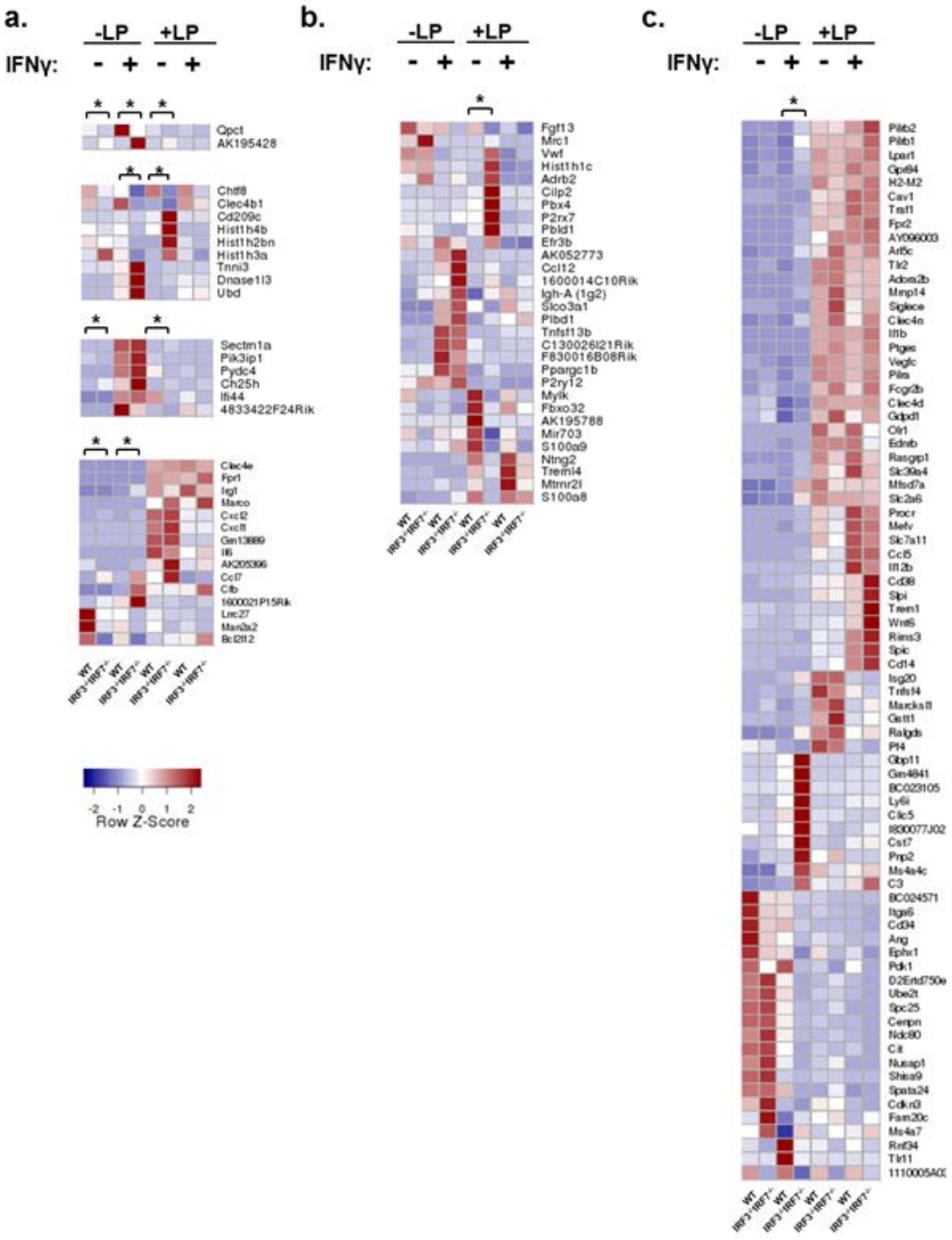

Figure 3-14. Effect of IRF3/7 deficiency on the transcriptomes of resting, IFNγ-stimulated, and *L. pneumophila*-infected BMMs

As in Fig. 3.13, except showing transcripts with a fold-change less than 3 between counts in the two genotypes in IFNγ-prestimulated and *L. pneumophila*-infected BMMs. Transcripts shown have a fold-change of 3 or greater (indicated by *) in (**a**) two or three categories, (**b**) in infected but not IFNγ-prestimulated BMMs only, and (**c**) IFNγ-prestimulated but uninfected BMMs.

We have assumed that IRF3-dependent effects result from IRF3 activity following infection with *L. pneumophila*, consistent with a potential role in bacterial sensing pathways. However, IRF3 deficiency also affects the establishment of an IFNγ-activated state, as evidenced by the large number of genes differentially expressed in uninfected IRF3$^{-/-}$ BMMs relative to WT BMMs following IFNγ stimulation but not at baseline (**Fig. 3-13c**). This list includes inducible nitric oxide synthase (NOS2) as well as chemokines (GDF15, CXCL11), scavenger receptors (SCARF1), and a cation channel that controls macrophage activation (TRPV4). Like the genes in **Fig. 3-13a-b**, the genes listed in **Fig. 3-13c** are potential elements of a transcription-mediated pathway by which IRF3 might suppress the IFNγ-activated state. However, the lack of IRF3-dependent phenotype in BMMs stimulated with IFNγ *during L. pneumophila* infection strongly suggests that the inhibitory effect of IRF3 on the IFNγ-activated state *that is relevant to restriction of L. pneumophila* affects the maintenance and function, not the establishment, of the IFNγ-activated state.

iNOS is upregulated but is not required for enhanced IFNγ-mediated restriction of bacteria in IRF3$^{-/-}$ BMMs

Inducible nitric oxide synthase (iNOS, NOS2) is one of the canonical mediators of the IFNγ-mediated response to intracellular bacteria and parasites [40]. Nos2 transcription was induced in macrophages synergistically by prestimulation with 10U/ml IFNγ and by *L. pneumophila* infection. Transcript levels in IFNγ-activated BMMs were approximately fivefold higher in IRF3$^{-/-}$ BMMs compared to WT BMMs before or after infection **(Fig. 3-13b)**. Therefore, we investigated the potential role of iNOS in the superior capacity of IRF3$^{-/-}$ BMMs to restrict intracellular bacteria.

Consistent with the trend in transcript levels, IRF3$^{-/-}$ BMMs stimulated with 100U/ml of IFNγ produced significantly more nitrite metabolites in response to bacterial infection than identically activated WT BMMs. At 10U/ml IFNγ, however, there was no significant difference

(**Fig. 3-15a**), likely due to post-transcriptional iNOS regulation, which has previously been described in murine macrophages [41,42]. This suggests that enhanced iNOS activity is dispensable for the enhanced IFNγ-activated antibacterial response in IRF3$^{-/-}$ BMMs. To investigate this in another way, we used both selective and nonselective iNOS inhibitors to treat BMMs during IFNγ stimulation and infection. Treatment with the inhibitors L-NIL and 1400W suppressed nitrite production by both WT and IRF3$^{-/-}$ BMMs, but did not affect restriction of *L. pneumophila* in either WT or IRF3$^{-/-}$ BMMs **(Fig. 3-16)**, consistent with the existence of an iNOS-independent mechanism of enhanced IFNγ-activated bacterial restriction in BMMs lacking IRF3.

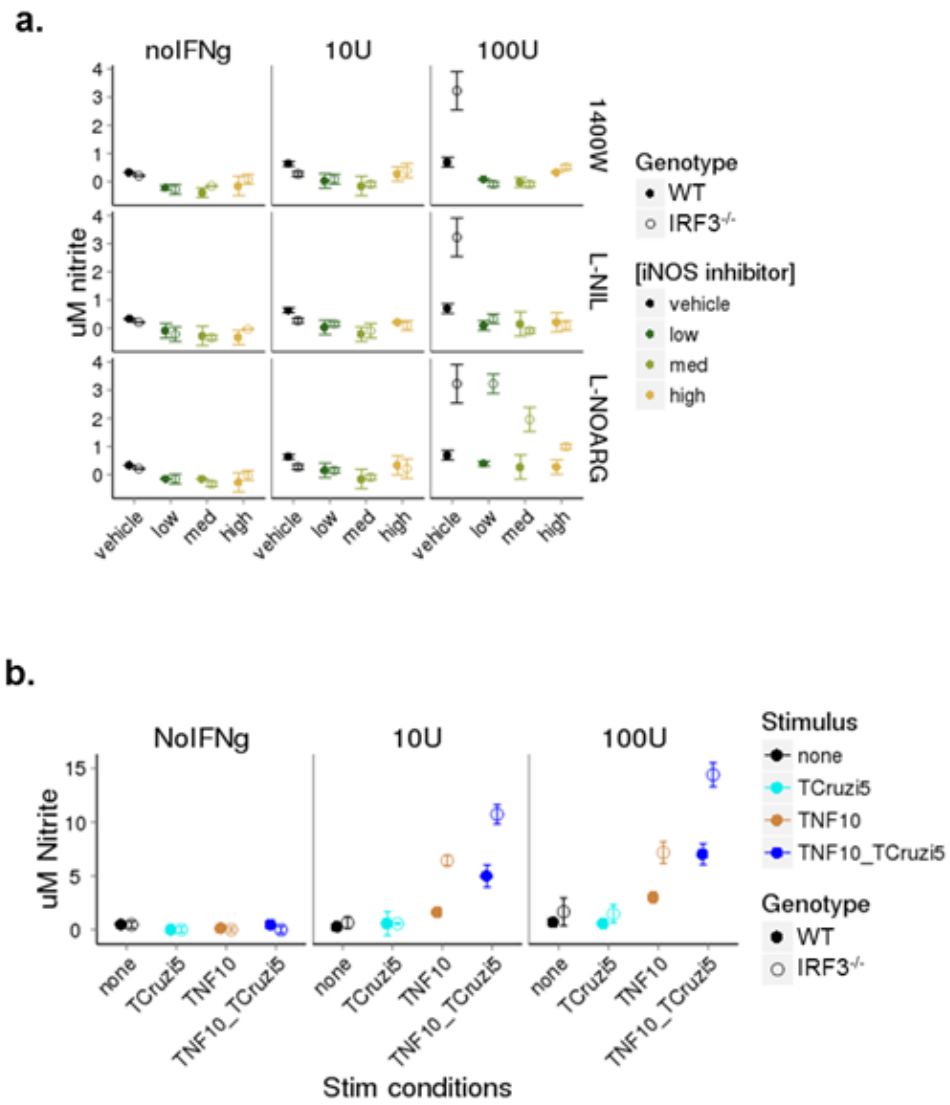

Figure 3-15. IRF3 suppresses IFNγ-induced NO production in the context of infection with bacterial or parasitic infection or TNFα costimulation

a. The Griess assay was used to detect nitric oxide byproducts produced by IRF3$^{-/-}$ and WT BMMs prestimulated with IFNγ and infected with *L. pneumophila* in the presence of DMSO or iNOS inhibitors L-NOARG, L-NIL or 1400W at concentrations 5-fold (low), 25-fold (medium), or 125-fold (high) above their published IC50

b. The Griess assay was used to detect nitric oxide byproducts produced by IRF3$^{-/-}$ and WT BMMs mock-treated (none), stimulated with 10U/ml TNFα (TNF10), infected with T. cruzi Brener strain trypomastigotes at an MOI of 5 (TCruzi5), or co-prestimulated with 10U/ml TNFα followed by T. cruzi infection (TNF10_TCruzi5).

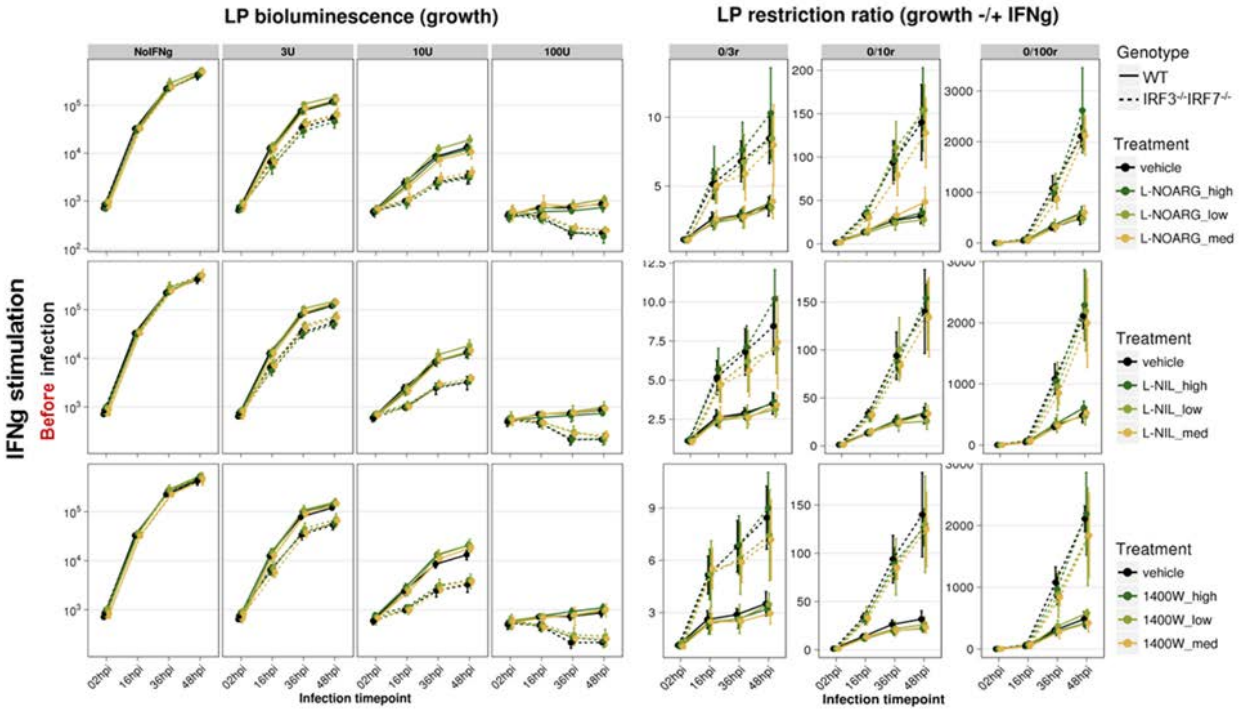

Figure 3-16. IRF3-mediated suppression of IFNγ-dependent restriction of *L. pneumophila* independently of iNOS inhibition

WT or IRF3$^{-/-}$IRF7$^{-/-}$ BMMs were stimulated with the indicated concentrations of IFNγ, then treated with the nitric oxide synthase inhibitors L-NOARG, L-NIL, or 1400W at three different concentrations before and during infection with *L. pneumophila*. Bacterial growth was observed by measuring bioluminescence. IFNγ-dependent bacterial restriction was calculated as the ratio of growth in resting BMMs *vs* in IFNγ-stimulated BMMs.

The role of iNOS in pathogen restriction varies with pathogen species, and has **b**een shown to be dispensable for the restriction of *L. pneumophila* in human monocytes [43]. Therefore, we asked whether iNOS activity was enhanced in IRF3$^{-/-}$ BMMs infected with the intracellular parasite *Trypanosoma cruzi*, which is restricted in an iNOS-dependent manner in IFNγ–activated macrophages [44]. iNOS-dependent restriction of *T. cruzi* is potentiated by co-stimulation with TNFα [45–47]. We found that IRF3$^{-/-}$ BMMs prestimulated with both IFNγ and TNFα produced significantly more nitrites than WT BMMs, and that infection with *T. cruzi* further increased the

amount of nitrites released while maintaining the effect of IRF3-dependent iNOS repression (**Fig. 3-15b**).

IRF3 suppresses IFNγ–activated defense mechanisms that delay the lysis of macrophages by the intracellular parasite *T. cruzi* in a Type I IFN-independent manner.

To assess the Type I interferon-independent effect of IRF3 on the IFNγ-mediated restriction of *T. cruzi*, we infected BMMs with this parasite using media containing IFNAR-blocking antibody. IFNγ and TNFα-costimulated IRF3$^{-/-}$ BMMs released significantly less parasites into cell supernatants at 5d after infection, but not afterward (**Fig. 3-17a**). Restriction of *T. cruzi* by IFNγ and TNFα-costimulated WT and IRF3$^{-/-}$ BMMs was only moderately suppressed by addition of an iNOS inhibitor before and during infection, indicating the presence of both iNOS dependent and independent antimicrobial mechanisms induced by IFNγ in both genotypes. We used microscopy to examine the fate of intracellular parasites at 3d and 5d after infection in BMMs that had been activated with 100U/ml IFNγ and 10U/ml TNFα and had not been treated with iNOS inhibitor. At 3d, the infection rate and average parasite burden per cell did not significantly different between genotypes (**Fig. 3-17b**). At 5d, however, the average cellular parasite burden was higher in WT than in IRF3$^{-/-}$ BMMs, concomitant with a drastic drop in cell density in WT BMMs only, probably due to the lysis of BMMs that release mature parasites as quantified in (**Fig. 3-17a**). We conclude that IRF3 suppresses an IFNγ-activated defense mechanism that delays the maturation and egress of *T. cruzi* parasites.

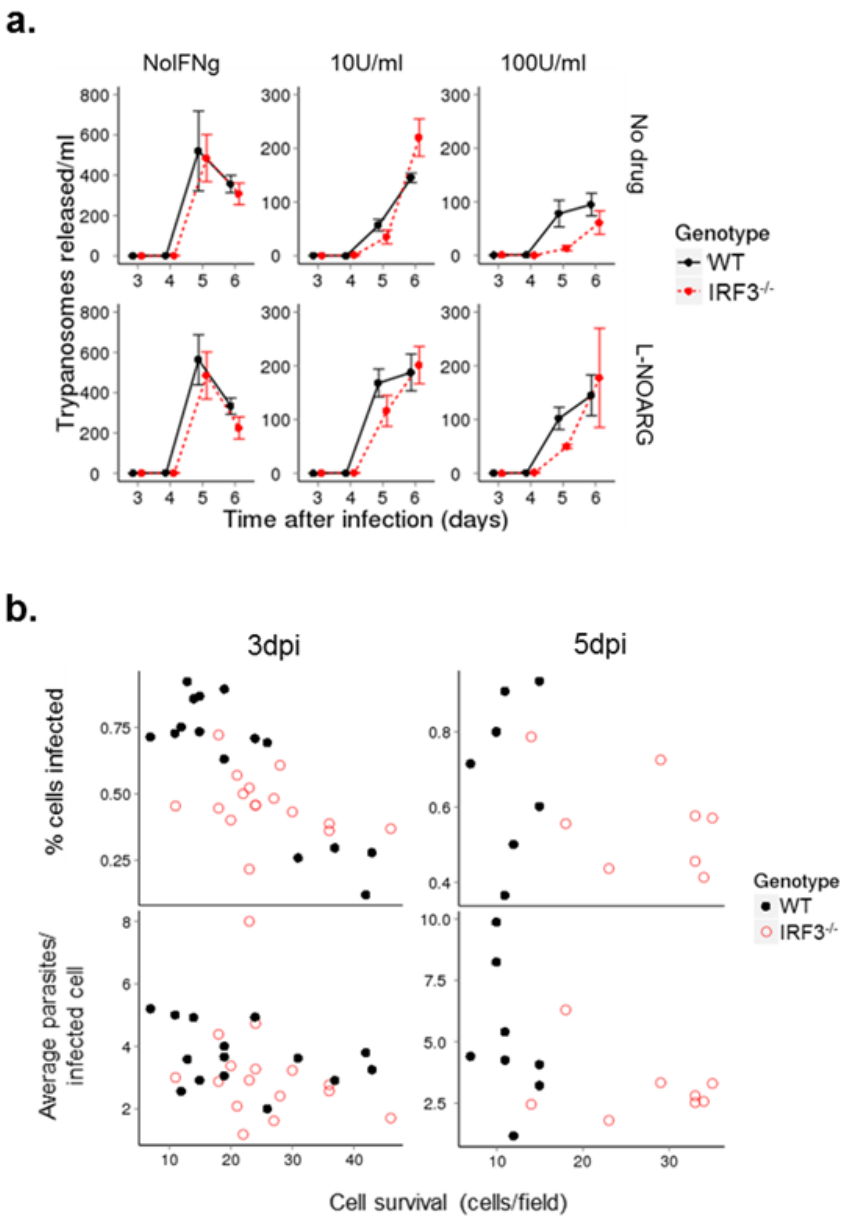

Figure 3-17. IRF3-mediated suppression of growth and lytic egress of *T. cruzi* from IFNγ and TNFα-stimulated BMMs

a. Trypanosomes released into supernatant from WT or IRF3$^{-/-}$ BMMs treated with IFNγ, TNFα and IFNAR-blocking antibody

b. Confocal images of fixed and stained infected BMMs were analyzed using CellProfiler to identify BMMs and parasites based on DAPI staining to quantify cell and parasite nuclei and Brightfield images to demarcate cell borders. Cell survival was quantified as the number of BMM nuclei per field.

Spatial distribution of IRF3 in *L. pneumophila*-infected or LPS-stimulated BMMs is consistent with IFNγ-mediated relocalization of IRF3

In order to gain insight into the activity of IRF3 in the context of intracellular infection, we performed immunofluorescence analysis of resting or IFNγ-stimulated WT BMMs after *L.pneumophila* infection, or after stimulation with LPS, which is known to drive IRF3 localization into the nucleus (**Fig. 3-18**). Consistent with the results of Western blot analysis in these cells (**Fig. 3-7**), IRF3 was observed in the nuclei of resting BMMs 2h after infection with *L. pneumophila*, as well as the nuclei of BMMs stimulated with LPS. IRF3 was partially excluded from the nuclei of BMMs stimulated with 10U/ml of IFNγ prior to infection or stimulation, but mostly localized to the nuclei of LPS-stimulated BMMs. IRF3 was more efficiently excluded from the nuclei of BMMs that had been stimulated with 10U/ml of IFNγ prior to infection or stimulation. Surprisingly, IRF3 staining in IFNγ-stimulated BMMs that had been either infected with *L. pneumophila* or stimulated with LPS displayed a prominent cytosolic speckling pattern that was not detected in BMMs that had not been stimulated with IFNγ. It it remains to be determined whether the observed speckles are specific for IRF3 or, perhaps, an unidentified, IFNγ-inducible cytosolic protein. If the staining is specific for IRF3, these results suggest that IRF3 is relocalized in an IFNγ-induced manner.

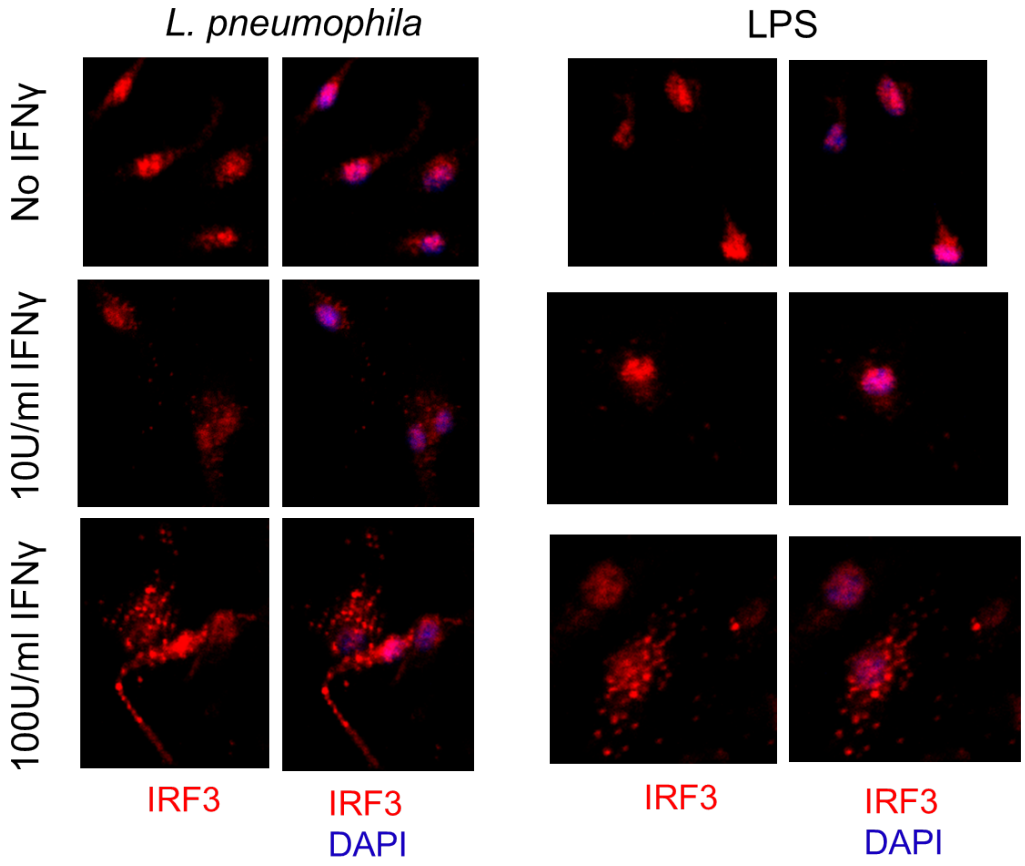

Figure 3-18. Spatial distribution of IRF3 in *L. pneumophila*-infected or LPS-stimulated BMMs consistent with IFNγ-mediated relocalization of IRF3

Immunofluorescence microscopy analysis of IRF3 localization in WT BMMs prestimulated with the indicated concentrations of IFNγ for 16h, then and fixed 2h after infection with *L. pneumophila* or stimulation with LPS.

DISCUSSION

Our studies of the role of innate sensing pathways in regulating the IFNγ-induced anti-bacterial state have led us to identify a role for IRF3 as a repressor of the IFNγ-activated state. This novel inhibitory pathway is not likely to depend on MYD88/TRIF, STING, MAVS or IFNAR for its effects, nor does it rely on iNOS for the enhancement of antibacterial effector activities. Many genes are dysregulated in IRF3$^{-/-}$ BMMs when compared to wild type macrophages that are treated with IFNγ and infected with bacteria, suggesting that IRF3 is a critical regulator of gene expression during establishment and maintenance of anti-bacterial state.

Most studies showing that IFNγ interacts with TLR sensors have identified synergies, consistent with our findings for concurrent IFNγ stimulation with infection, but different from the lack of effects in BMMs that are pre-stimulated with IFNγ. In one study, IFNγ-mediated restriction of the cytosolic bacterial pathogen *S. flexneri* in fibroblasts was dependent on the transcription factor IRF1 that upregulated the RIG-I RNA-sensing pathway [48], but did not suggest the antagonistic relationship that we found. On the other hand, there have been several studies showing that Type I IFNs can antagonize the actions of Type II IFNs, in the same direction as our findings. However, we could not find significant production of Type I IFNs in our system; and IFNAR deficiency did not lead to an increase in IFNγ activity.

One significant class of genes induced in IRF3$^{-/-}$ BMMs is related to iron restriction. Lipocalin 2 restricts iron availability in the vacuoles of pathogenic bacteria including *S. typhimurium* [49–51], *M. avium* [52], and *C. pneumoniae* [53], in some cases in an IFNγ-dependent manner [50], and is synergistically induced by IFNγ and *L. pneumophila* infection only in IRF3$^{-/-}$ IRF7$^{-/-}$ BMMs in our experiment. Therefore, IRF3 potentially masks an IFNγ-mediated effect at the phagosome. In addition, ferritin is strongly inhibited in IRF3$^{-/-}$ BMMs, restricting the import of iron from the external environment.

There are several major pathways of further study to investigate the results obtained. First, it is essential to validate the independence of the proposed mechanism on Type I interferons using $IRF3^{-/-}IFNAR^{-/-}$ mice. Then, comparison of gene expression in BMMs from these mice and from $IFNAR^{-/-}$ mice can elucidate which of the many genes that vary in $IRF3^{-/-}IRF7^{-/-}$ mice is relevant to the phenotype observed, and will help hone in on the proper effector functions to prioritize in further study.

Second, our work has identified a potential cascade of inhibition between IFNγ effectors and IRF3, visualized by the partial exclusion of IRF3 from the nuclei of IFNγ-stimulated BMMs stimulated by LPS or infected with *L. pneumophila*. This raises an important question: what other stimuli activate IRF3 in a manner that can be inhibited by IFNγ effectors?

Third, the ligands that activate IRF3 in the context of *L. pneumophila,* infection, together with the investigation of stimuli mentioned above, will help shed light on the role of the IRF3-mediated immunoregulatory mechanism. IFNγ-mediated responses can be harmful in the context of tissue damage, when uncontrolled inflammation and necrosis can be the cause of pathology rather than simply a bacterial defense, or in the context of infection with most viruses, in which macrophages are skewed toward different effector functions. Studies of *in vivo* infection in mice lacking IRF3 (and necessarily, to avoid confounding effects of Type I interferons, lacking IFNAR) will help investigate the role of IRF3-mediated suppression of IFNγ effectors in the context of bacterial infection. These mice may clear intracellular bacteria such as *L. pneumophila* readily, or they may succumb to exuberant nitric oxide response in the lung. Furthermore, the role of IRF3 in coinfection, especially with bacteria or parasites and viruses, can be addressed either *in vitro* or *in vivo*.

MATERIALS AND METHODS

Mice

IRF3$^{-/-}$ mice were provided by Dr. Meixiong Wu with permission from Dr. Tadatsugu Taniguchi. IRF7$^{-/-}$ mice were provided by Dr. Evelyn Kurt-Jones. IRF3$^{-/-}$IRF7$^{-/-}$ and IFNAR$^{-/-}$ mice were provided by Dr. Kate Fitzgerald. STING$^{-/-}$ mice were provided by Dr Glen Barber. Bone marrow derived from MAVS$^{-/-}$ mice was provided by Dr. Akiko Iwasaki. MyD88$^{-/-}$TRIF$^{-/-}$ mice were provided by Dr. Ruslan Medzitov. DNase2$^{-/-}$ mice were provided by Dr. Shigekazu Nagata. TREX1$^{-/-}$ mice were provided by Dr. Judy Lieberman. Age and sex-matched C57BL/6J mice were obtained from Jackson laboratories.

BMM isolation and culture

Bone marrow was collected from femurs and tibiae of 2-6 month old mice. Red blood cells were lysed using TAC RBC lysis buffer (Sigma). Cells were passed through a 70 μm cell strainer and plated on non-tissue culture treated petri dishes in RPMI-1640 medium, supplemented with 10% FBS, L-glutamine, penicillin/streptomycin, MEM nonessential amino acids, HEPES, sodium pyruvate, β-mercaptoethanol, heat-inactivated FBS, and human MCSF (10ng/ml, R&D Systems). BMMs were collected and reseeded into assay plates after 5 days of differentiation, and stimulated or infected after 7-12 days of differentiation. BMMs were seeded in 96-well plates at 4e4-5e4 BMM/well unless otherwise noted. Cytokines used to stimulate BMMs were from Millipore (IFNγ) or Peprotech (TNFα). BMMs were stimulated for 24h unless otherwise noted. iNOS inhibitors (L-NOARG, L-NIL, 1400W) were from Sigma.

Bacterial strains and parasites

L. pneumophila strain LP02 delFlaA *lux* was provided by Dr. Jörn Coers. *T. cruzi* strain

Brener trypomastigotes were provided by Dr. Ricardo Gazzinelli.

L. pneumophila and *T. cruzi* infections

L. pneumophila strains were maintained on N-(2-acetamido)-2-aminoethanesulfonic acid (ACES) buffered charcoal-yeast extract agar supplemented with FeNO3, cysteine, and thymidine. For experimental assays, *L. pneumophila* was grown in ACES-buffered yeast extract broth at 37°C to a density greater than 3 OD600. Bacteria were washed with PBS twice before infection. BMMs were infected at an MOI of 4 with bacteria resuspended in cell culture media. Infected BMMs were centrifuged for 10 minutes and incubated for 1.5-2 hours in a cell culture incubator. Media was removed and replaced with fresh supplemented media containing thymidine. Bioluminescence was measured over 2 days after infection using a plate reader (Envision).

For *T. cruzi* infection, IFNAR-neutralizing antibody (Leinco) was included in cell media from one day prior to infection onward. BMMs were infected with purified trypomastigotes at an MOI of 10 and incubated for 2 hours in a cell culture incubator. BMMs were washed three times with warm PBS, and media was removed and replaced with fresh media at 2h after infection as well as daily starting at 3d after infection. For extracellular parasite quantification, well contents were agitated briefly and 20ul of supernatant was applied to a Neubauer hemocytometer. Motile trypanosomes were counted manually. For intracellular parasite quantification, cells were washed three times with PBS, fixed with 4% paraformaldehyde, permeabilized with 0.25% Triton-X, stained with 4',6-diamidino-2-phenylindole (DAPI), and imaged using a confocal microscope (Olympus). BMMs and parasites were quantified using a custom automated image analysis pipeline in CellProfiler [54] on the basis of Brightfield image (BMM traces) and DAPI staining (BMM nuclei and parasite nuclei/kinetoplastids).

For quantification of nitrite/nitrate byproducts of NO synthesis in infected or stimulated BMMs, the Griess assay (Promega) was used according to the kit instructions.

Western blotting

Protein was purified from lysates of BMMs grown in six-well plates, infected with control or candidate-targeting lentivirus, and selected for puromycin resistance. Cells were washed three times in PBS and lysed in RIPA buffer (Boston Bioproducts) with protease inhibitor (Roche). Lysates were purified by centrifugation and suspended in SDS buffer with 10mM dithiothreitol (DTT). Proteins were separated by electrophoresis on a Bis-Tris 4-12% polyacrylamide gel (Novex), transferred to a nitrocellulose membrane, blocked with 5% milk in Tris-buffered saline with Tween (TBST), and incubated overnight at 4°C with primary antibodies in 5% nonfat dry milk in TBST or, for phospho-protein antibodies, in 5% bovine serum albumin (BSA) in TBST. Membranes were washed, incubated with secondary antibody in 5% BSA in TBST for one hour at room temperature, washed again, and incubated with for 5min with luminol reagent (Pierce). Antibodies were from Abcam (β-actin), Cell Signaling Technologies (IRF3, IRF3pS388), Jackson Immunoresearch (HRP-conjugated secondary antibodies), and Santa Cruz (TBP).

Immunofluorescence microscopy

BMMs were seeded onto 8-well glass chamber slides (Nunc), washed three times with PBS, and fixed with 4% paraformaldehyde (Electron Microscopy Sciences) in PBS for ten minutes. Cells were permeabilized with 0.25% Triton-X and blocked with 5% goat or donkey serum (Jackson Immunoresearch) and 5% BSA (Cell Signaling Technologies). Primary antibody incubation was done overnight at 4°C. Cells were washed with PBS and incubated with Alexa-fluorophore conjugated secondary antibody (Life Technologies) for 1 hour in the dark. Cells were washed, counterstained with DAPI, mounted on coverslips, and imaged using a confocal microscope (Olympus).

RNA-seq

Total RNA was prepared using RNeasy columns (Qiagen). RNA-seq libraries were prepared under the supervision of Max Mumbach as described previously [55]. Briefly, poly-A mRNA was captured using selection beads (Oligo-dT Dynabeads, Life Technologies). mRNA was fragmented using zinc chloride (Ambion), and 3' ends were dephosphorylated prior to ligation of RNA adapters (Illumina) using T4 RNA ligase (New England Biosciences). Reverse transcription was performed using reverse transcriptase (Agilent) ,ssDNA was removed using ExoSap-IT (Affymetrix), and ssRNA was removed using acetic acid and sodium hydroxide. DNA adapters (Illumina) were ligated using T4 RNA ligase (New England Biosciences). PCR was performed with barcoded primers (Illumina) and Phusion DNA polymerase (New England Biosciences) to identify and amplify libraries. Sequencing was performed using a HiSeq machine (Illumina) and data normalization was performed as described previously [55] using the TMM method in R. Further analysis was performed using custom scripts in R. Heatmaps were generated by normalizing each row (gene) and plotting using the heatmap2 function in R.

REFERENCES

1. Schroder K, Sweet M, Hume D (2006) Signal integration between IFNgamma and TLR signalling pathways in macrophages. Immunobiology 211: 511–524. doi:10.1016/j.imbio.2006.05.007.

2. Gough D, Levy D, Johnstone R, Clarke C (2008) IFNgamma signaling-does it mean JAK-STAT? Cytokine Growth Factor Rev 19: 383–394. doi:10.1016/j.cytogfr.2008.08.004.

3. Hu X, Chakravarty SD, Ivashkiv LB (2008) Regulation of interferon and Toll-like receptor signaling during macrophage activation by opposing feedforward and feedback inhibition mechanisms. Immunol Rev 226: 41–56. doi:10.1111/j.1600-065X.2008.00707.x.

4. Akhter A, Gavrilin M, Frantz L, Washington S, Ditty C, et al. (2009) Caspase-7 activation by the Nlrc4/Ipaf inflammasome restricts Legionella pneumophila infection. PLoS Pathog 5. Available: http://dx.doi.org/10.1371/journal.ppat.1000361.

5. Molofsky A, Byrne B, Whitfield N, Madigan C, Fuse E, et al. (2006) Cytosolic recognition of flagellin by mouse macrophages restricts Legionella pneumophila infection. J Exp Med 203: 1093–1104. doi:10.1084/jem.20051659.

6. Ren T, Zamboni D, Roy C, Dietrich W, Vance R (2006) Flagellin-deficient Legionella mutants evade caspase-1- and Naip5-mediated macrophage immunity. PLoS Pathog 2. Available: http://dx.doi.org/10.1371/journal.ppat.0020018.

7. Zamboni DS, Kobayashi KS, Kohlsdorf T, Ogura Y, Long E, et al. (2006) The Birc1e cytosolic pattern-recognition receptor contributes to the detection and control of Legionella pneumophila infection. Nat Immunol 7: 318–325. doi:10.1038/ni1305.

8. Ge J, Gong Y-N, Xu Y, Shao F (2012) Preventing bacterial DNA release and absent in melanoma 2 inflammasome activation by a Legionella effector functioning in membrane trafficking. Proc Natl Acad Sci U S A 109: 6193–6198. doi:10.1073/pnas.1117490109.

9. Akamine M, Higa F, Arakaki N, Kawakami K, Takeda K, et al. (2005) Differential roles of Toll-like receptors 2 and 4 in in vitro responses of macrophages to Legionella pneumophila. Infect Immun 73: 352–361. doi:10.1128/IAI.73.1.352-361.2005.

10. Lippmann J, Müller HC, Naujoks J, Tabeling C, Shin S, et al. (2011) Dissection of a type I interferon pathway in controlling bacterial intracellular infection in mice. Cell Microbiol 13: 1668–1682. doi:10.1111/j.1462-5822.2011.01646.x.

11. Monroe K, McWhirter S, Vance R (2009) Identification of host cytosolic sensors and bacterial factors regulating the type I interferon response to Legionella pneumophila. PLoS Pathog 5. Available: http://dx.doi.org/10.1371/journal.ppat.1000665.

12. Stetson D, Medzhitov R (2006) Recognition of cytosolic DNA activates an IRF3-dependent innate immune response. Immunity 24: 93–9103. doi:10.1016/j.immuni.2005.12.003.

13. Chiu Y-H, Macmillan J, Chen Z (2009) RNA polymerase III detects cytosolic DNA and induces type I interferons through the RIG-I pathway. Cell 138: 576–591. doi:10.1016/j.cell.2009.06.015.

14. Yang Y-GG, Lindahl T, Barnes DE (2007) Trex1 exonuclease degrades ssDNA to prevent chronic

checkpoint activation and autoimmune disease. Cell 131: 873–886. doi:10.1016/j.cell.2007.10.017.

15. Stetson D, Ko J, Heidmann T, Medzhitov R (2008) Trex1 prevents cell-intrinsic initiation of autoimmunity. Cell 134: 587–598. doi:10.1016/j.cell.2008.06.032.

16. Yan N, Regalado-Magdos A, Stiggelbout B, Lee-Kirsch M, Lieberman J (2010) The cytosolic exonuclease TREX1 inhibits the innate immune response to human immunodeficiency virus type 1. Nat Immunol 11: 1005–1013. doi:10.1038/ni.1941.

17. Hasan M, Koch J, Rakheja D, Pattnaik A, Brugarolas J, et al. (2013) Trex1 regulates lysosomal biogenesis and interferon-independent activation of antiviral genes. Nat Immunol 14: 61–71. doi:10.1038/ni.2475.

18. Morita M, Stamp G, Robins P, Dulic A, Rosewell I, et al. (2004) Gene-targeted mice lacking the Trex1 (DNase III) 3'–\textgreater5' DNA exonuclease develop inflammatory myocarditis. Mol Cell Biol 24: 6719–6727. doi:10.1128/MCB.24.15.6719-6727.2004.

19. Pereira-Lopes S, Celhar T, Sans-Fons G, Serra M, Fairhurst A-M, et al. (2013) The exonuclease trex1 restrains macrophage proinflammatory activation. J Immunol Baltim Md 1950 191: 6128–6135. doi:10.4049/jimmunol.1301603.

20. Kawane K, Ohtani M, Miwa K, Kizawa T, Kanbara Y, et al. (2006) Chronic polyarthritis caused by mammalian DNA that escapes from degradation in macrophages. Nature 443: 998–991002. doi:10.1038/nature05245.

21. Ablasser A, Hemmerling I, L S-B, Jonathan, Behrendt R, Roers A, et al. (2014) TREX1 Deficiency Triggers Cell-Autonomous Immunity in a cGAS-Dependent Manner. J Immunol Baltim Md 1950. Available: http://dx.doi.org/10.4049/jimmunol.1400737.

22. Ahn J, Gutman D, Saijo S, Barber GN (2012) STING manifests self DNA-dependent inflammatory disease. Proc Natl Acad Sci U S A 109: 19386–19391. doi:10.1073/pnas.1215006109.

23. Fitzgerald K, McWhirter S, Faia K, Rowe D, Latz E, et al. (2003) IKKepsilon and TBK1 are essential components of the IRF3 signaling pathway. Nat Immunol 4: 491–496. doi:10.1038/ni921.

24. Noyce R, Collins S, Mossman K (2009) Differential modification of interferon regulatory factor 3 following virus particle entry. J Virol 83: 4013–4022. doi:10.1128/JVI.02069-08.

25. Ng S-L, Friedman B, Schmid S, Gertz J, Myers R, et al. (2011) IκB kinase epsilon (IKK(epsilon)) regulates the balance between type I and type II interferon responses. Proc Natl Acad Sci U S A 108: 21170–21175. doi:10.1073/pnas.1119137109.

26. Sanda C, Weitzel P, Tsukahara T, Schaley J, Edenberg HJ, et al. (2006) Differential gene induction by type I and type II interferons and their combination. J Interferon Cytokine Res Off J Int Soc Interferon Cytokine Res 26: 462–472. doi:10.1089/jir.2006.26.462.

27. Decker T, Kovarik P, Meinke A (1997) GAS elements: a few nucleotides with a major impact on cytokine-induced gene expression. J Interferon Cytokine Res Off J Int Soc Interferon Cytokine Res 17: 121–134.

28. Peng T, Zhu J, Hwangbo Y, Corey L, Bumgarner RE (2008) Independent and cooperative antiviral

actions of beta interferon and gamma interferon against herpes simplex virus replication in primary human fibroblasts. J Virol 82: 1934–1945. doi:10.1128/JVI.01649-07.

29. Tan H, Derrick J, Hong J, Sanda C, Grosse WM, et al. (2005) Global transcriptional profiling demonstrates the combination of type I and type II interferon enhances antiviral and immune responses at clinically relevant doses. J Interferon Cytokine Res Off J Int Soc Interferon Cytokine Res 25: 632–649. doi:10.1089/jir.2005.25.632.

30. Zhang X-NN, Liu J-XX, Hu Y-WW, Chen H, Yuan Z-HH (2005) Hyper-activated IRF-1 and STAT1 contribute to enhanced interferon stimulated gene (ISG) expression by interferon alpha and gamma co-treatment in human hepatoma cells. Biochim Biophys Acta 1759: 417–425. doi:10.1016/j.bbaexp.2006.08.003.

31. Changotra H, Jia Y, Moore TN, Liu G, Kahan SM, et al. (2009) Type I and type II interferons inhibit the translation of murine norovirus proteins. J Virol 83: 5683–5692. doi:10.1128/JVI.00231-09.

32. Abadie A, Besançon F, Wietzerbin J (2004) Type I interferon and TNFalpha cooperate with type II interferon for TRAIL induction and triggering of apoptosis in SK-N-MC EWING tumor cells. Oncogene 23: 4911–4920. doi:10.1038/sj.onc.1207614.

33. Yoshida R, Murray H, Nathan C (1988) Agonist and antagonist effects of interferon alpha and beta on activation of human macrophages. Two classes of interferon gamma receptors and blockade of the high-affinity sites by interferon alpha or beta. J Exp Med 167: 1171–1185. doi:10.1084/jem.167.3.1171.

34. Rayamajhi M, Humann J, Penheiter K, Andreasen K, Lenz L (2010) Induction of IFN-alphabeta enables Listeria monocytogenes to suppress macrophage activation by IFN-gamma. J Exp Med 207: 327–337. doi:10.1084/jem.20091746.

35. Teles R, Graeber T, Krutzik S, Montoya D, Schenk M, et al. (2013) Type I interferon suppresses type II interferon-triggered human anti-mycobacterial responses. Science 339: 1448–1453. doi:10.1126/science.1233665.

36. Coers J, Vance RE, Fontana MF, Dietrich WF (2007) Restriction of Legionella pneumophila growth in macrophages requires the concerted action of cytokine and Naip5/Ipaf signalling pathways. Cell Microbiol 9: 2344–2357. doi:10.1111/j.1462-5822.2007.00963.x.

37. Gough D, Messina N, Hii L, Gould J, Sabapathy K, et al. (2010) Functional crosstalk between type I and II interferon through the regulated expression of STAT1. PLoS Biol 8. Available: http://dx.doi.org/10.1371/journal.pbio.1000361.

38. Chow E, Castrillo A, Shahangian A, Pei L, O'Connell R, et al. (2006) A role for IRF3-dependent RXRalpha repression in hepatotoxicity associated with viral infections. J Exp Med 203: 2589–2602. doi:10.1084/jem.20060929.

39. Ysebrant de Lendonck L, Tonon S, Nguyen M, Vandevenne P, Welsby I, et al. (2013) Interferon regulatory factor 3 controls interleukin-17 expression in CD8 T lymphocytes. Proc Natl Acad Sci U S A 110: E3189–E3197. doi:10.1073/pnas.1219221110.

40. MacMicking J, Xie QW, Nathan C (1997) Nitric oxide and macrophage function. Annu Rev

Immunol 15: 323–350. doi:10.1146/annurev.immunol.15.1.323.

41. Vodovotz Y, Bogdan C, Paik J, Xie QW, Nathan C (1993) Mechanisms of suppression of macrophage nitric oxide release by transforming growth factor beta. J Exp Med 178: 605–613.

42. Söderberg M, Raffalli-Mathieu F, Lang MA (2002) Inflammation modulates the interaction of heterogeneous nuclear ribonucleoprotein (hnRNP) I/polypyrimidine tract binding protein and hnRNP L with the 3'untranslated region of the murine inducible nitric-oxide synthase mRNA. Mol Pharmacol 62: 423–431.

43. Neumeister B, Bach V, Faigle M, Northoff H (2001) Induction of iNOS in human monocytes infected with different Legionella species. FEMS Microbiol Lett 202: 31–38. doi:10.1111/j.1574-6968.2001.tb10776.x.

44. Gazzinelli R, Oswald I, Hieny S, James S, Sher A (1992) The microbicidal activity of interferon-gamma-treated macrophages against Trypanosoma cruzi involves an L-arginine-dependent, nitrogen oxide-mediated mechanism inhibitable by interleukin-10 and transforming growth factor-beta. Eur J Immunol 22: 2501–2506. doi:10.1002/eji.1830221006.

45. Muñoz-Fernández M, Fernández M, Fresno M (1992) Synergism between tumor necrosis factor-alpha and interferon-gamma on macrophage activation for the killing of intracellular Trypanosoma cruzi through a nitric oxide-dependent mechanism. Eur J Immunol 22: 301–307. doi:10.1002/eji.1830220203.

46. Silva JS, Vespa GN, Cardoso MA, Aliberti JC, Cunha FQ (1995) Tumor necrosis factor alpha mediates resistance to Trypanosoma cruzi infection in mice by inducing nitric oxide production in infected gamma interferon-activated macrophages. Infect Immun 63: 4862–4867.

47. Muñoz-Fernández MA, Fernández MA, Fresno M (1992) Activation of human macrophages for the killing of intracellular Trypanosoma cruzi by TNF-alpha and IFN-gamma through a nitric oxide-dependent mechanism. Immunol Lett 33: 35–40.

48. Jehl S, Nogueira C, Zhang X, Starnbach M (2012) IFNγ inhibits the cytosolic replication of Shigella flexneri via the cytoplasmic RNA sensor RIG-I. PLoS Pathog 8. Available: http://dx.doi.org/10.1371/journal.ppat.1002809.

49. Nairz M, Theurl I, Ludwiczek S, Theurl M, Mair SM, et al. (2007) The co-ordinated regulation of iron homeostasis in murine macrophages limits the availability of iron for intracellular Salmonella typhimurium. Cell Microbiol 9: 2126–2140. doi:10.1111/j.1462-5822.2007.00942.x.

50. Nairz M, Fritsche G, Brunner P, Talasz H, Hantke K, et al. (2008) Interferon-gamma limits the availability of iron for intramacrophage Salmonella typhimurium. Eur J Immunol 38: 1923–1936. doi:10.1002/eji.200738056.

51. Fritsche G, Nairz M, Libby SJ, Fang FC, Weiss G (2012) Slc11a1 (Nramp1) impairs growth of Salmonella enterica serovar typhimurium in macrophages via stimulation of lipocalin-2 expression. J Leukoc Biol 92: 353–359. doi:10.1189/jlb.1111554.

52. Halaas O, Steigedal M, Haug M, Awuh JA, Ryan L, et al. (2010) Intracellular Mycobacterium avium intersect transferrin in the Rab11(+) recycling endocytic pathway and avoid lipocalin 2 trafficking to the lysosomal pathway. J Infect Dis 201: 783–792. doi:10.1086/650493.

53. Bellmann-Weiler R, Schroll A, Engl S, Nairz M, Talasz H, et al. (2013) Neutrophil gelatinase-associated lipocalin and interleukin-10 regulate intramacrophage Chlamydia pneumoniae replication by modulating intracellular iron homeostasis. Immunobiology 218: 969–978. doi:10.1016/j.imbio.2012.11.004.

54. Kamentsky L, Jones TR, Fraser A, Bray M-A, Logan DJ, et al. (2011) Improved structure, function and compatibility for CellProfiler: modular high-throughput image analysis software. Bioinforma Oxf Engl 27: 1179–1180. doi:10.1093/bioinformatics/btr095.

55. Schwartz S, Agarwala SD, Mumbach MR, Jovanovic M, Mertins P, et al. (2013) High-resolution mapping reveals a conserved, widespread, dynamic mRNA methylation program in yeast meiosis. Cell 155: 1409–1421. doi:10.1016/j.cell.2013.10.047.

Chapter 4: Discussion

Summary of Findings
Analysis and Implications
Future Directions
References

SUMMARY OF FINDINGS

Vesicle trafficking screen

In Chapter 2, we discussed a targeted RNAi screen to find candidate *L. pneumophila* host factors and IFNγ mediators among genes in a curated vesicle trafficking set. Primary screening in the RAWγNO murine macrophage cell line assayed 380 genes using a lentiviral RNAi library of approximately 5 shRNA constructs per gene, measuring the effect of each construct on both bacterial growth and on cell survival and proliferation. We developed a novel, unbiased computational analysis pipeline to identify constructs that significantly increased or decreased observed bacterial growth relative to the growth expected at similar cell counts. 73 candidate host factors and 84 candidate IFNγ mediators were tested in a secondary screen using bone marrow derived macrophages (BMMs). Of these, 9 candidate host factors and 26 candidate IFNγ mediators were manually classified as validated on the basis of bacterial growth in BMMs relative to cell count. We pursued further validation and functional characterization for several of the candidate IFNγ mediators.

Knockout mice were used where available to validate the phenotypes observed in cells depleted of candidate transcripts using shRNA. Further assays measured the regulation of proteins levels in response to IFNγ treatment, the effects of transcript depletion on phagocytosis or on the levels of lysosomal marker proteins, and the cellular localization of candidate proteins relative to the bacterial phagosome. Using knockout mice, we discovered that ARL8B, VTI1B, and AP3B1 are not required for IFNγ-mediated restriction of *L. pneumophila* in BMMs. The candidate TSPAN6 is a potential member of this pathway, though the relevant results were not always reproducible, and the hypothesis requires further testing. In particular, the expression of TSPAN6 in BMMs appears to be low, and the specificity of anti-TSPAN6 antibody remains to be confirmed.

Effect of innate immune sensing on IFNγ-activated restriction of intracellular pathogens

In Chapter 3, we describe work investigating the effect of innate pathogen sensing on the IFNγ-activated state, culminating in the identification of the transcription factor IRF3 as a suppressor of IFNγ effectors through a mechanism independent of Type I interferons (IFNs). Using BMMs derived from wildtype (WT) and knockout mice, we used cells that were strictly pre-stimulated with IFNγ prior to, but not during exposure to bacteria in order to assess the contribution of sensing pathway members on the maintenance, but not the establishment, of the IFNγ-activated state. We found that the TLR pathway adaptor proteins MYD88 and/or TRIF facilitate both the establishment and maintenance of the IFNγ-activated state, while the nucleic acid sensing adaptor STING facilitates the maintenance of the IFNγ-activated state, and the nucleic acid sensing adaptor MAVS does not have a significant effect on either. Meanwhile, the transcription factors IRF3 and/or IRF7, which are activated downstream of the nucleic acid sensing pathways that signal through STING and MAVS, suppress the maintenance of the IFNγ-activated state, unlike these upstream adaptors. IRF3 and IRF7 are not required for the establishment of the IFNγ-activated state, suggesting that the JAK-STAT signaling pathway downstream of IFNγ receptor (IFNGR) engagement is functionally intact in $IRF3^{-/-}IRF7^{-/-}$ BMMs. Further work revealed that IRF3, but not IRF7 was responsible for the phenotype in $IRF3^{-/-}IRF7^{-/-}$ macrophages.

Our results revealed that IRF3 is activated by phosphorylation and localizes to the nucleus of *L. pneumophila*-infected BMMs, but that activated IRF3 is not detected in either the nucleus or cytoplasm of IFNγ-activated BMMs following infection, despite the activation of IRF3 kinases IKKε and TBK1. Meanwhile, immunofluorescence analysis revealed a speckled cytosolic pattern of IRF3 staining in IFNγ-activated, but not resting BMMs following infection with *L. pneumophila* or treatment with lipopolysaccharide (LPS), suggesting that IFNγ effectors relocalize IRF3 -- even as IRF3 directly or indirectly suppresses IFNγ effectors.

Several lines of evidence suggest that the mechanism by which IRF3 suppresses IFNγ effectors is independent of Type I interferons, a class of proteins that make up one of the major transcriptional targets of IRF3 and one of the canonical mediators of the IRF3-dependent antiviral response. First, deficiency in the Type I IFN receptor (IFNAR) does not phenocopy deficiency in IRF3; in fact, IFNAR appears to make a small but non-redundant positive contribution to the maintenance of the IFNγ-mediated state. Second, ablation of IFNAR signaling with a neutralizing antibody does not reduce the relative enhancement in IFNγ-mediated bacterial restriction observed in $IRF3^{-/-}$ BMMs relative to WT BMMs. Third, the levels of Type I IFNs induced by resting or IFNγ-activated BMMs following *L. pneumophila* infection are low, based on qPCR quantification of transcription of IFNβ and lack of detection of any Type I IFNs by ISRE reporter cells.

We investigated the mechanism by which $IRF3^{-/-}$ IFNγ-activated BMMs more efficiently restrict *L. pneumophila* when compared to WT IFNγ-activated BMMs. Using WT BMMs or BMMs deficient in IRF3 and IRF7, we measured gene expression before and after infection with *L. pneumophila* in both resting and IFNγ-activated BMMs using RNAseq. After excluding genes with insignificant expression levels across all conditions, 232 transcripts were found to be differentially expressed by threefold or more as a result of IRF3/IRF7 deficiency in IFNγ-stimulated or *L. pneumophila*-infected BMMs. The data revealed that IRF3/IRF7 profoundly affect the transcriptome of BMMs following *L. pneumophila* infection, but also after IFNγ stimulation and in the resting state, with both distinct and overlapping gene sets affected under each combination of conditions.

The inducible nitric oxide (NO) synthase (iNOS, otherwise known as NOS2), a well-described IFNγ effector, was present among the 93 genes preferentially induced in $IRF3^{-/-}IRF7^{-/-}$ BMMs relative to WT BMMs following both IFNγ stimulation and *L. pneumophila* infection. Indeed, IRF3/IRF7 deficiency resulted in roughly five times more Nos2 transcription under these conditions. On the post-transcriptional level, following IFNγ stimulation and *L. pneumophila* infection, the observed concentration of nitrite byproducts of NO production by $IRF3^{-/-}$ BMMs was

two-fold greater than by WT BMMs. Preferential IFNγ-dependent nitrite production in IRF3$^{-/-}$ BMMs was not unique to BMMs infected with *L. pneumophila*, but was also observed following stimulation with LPS, TNFα, or after infection with the protozoan parasite *Trypanosoma cruzi*. However, ablation of NOS2 activity with chemical inhibitors did not change levels of IFNγ-mediated bacterial restriction in either IRF3$^{-/-}$ or WT BMMs.

NOS2 activity is known to play a nonredundant role in the IFNγ-mediated restriction of intracellular *T. cruzi*. While IFNγ-stimulated IRF3$^{-/-}$ BMMs bear the same net parasite burden as WT BMMs, we found that the lysis of IRF3$^{-/-}$ BMMs that accompanies *T. cruzi* egress is substantially delayed relative to WT BMMs in a NOS2-dependent Type I IFN-independent manner.

ANALYSIS AND IMPLICATIONS

Vesicle trafficking screen

RNAi screening of the vesicle trafficking gene set in the context of *L. pneumophila* infection of BMMs did not yield any consistently validated and characterized IFNγ mediators. However, general observations from this RNAi screen may be relevant to the process of other screening experiments as well. Furthermore, negative results obtained are significant in their own right.

Technical issues in the RNAi screening process

First, both the primary and the secondary screens exhibited a large amount of noise, or variation among negative control shRNA constructs in both the cell count and bacterial growth observed. Still, we were able to distinguish strong hits above the noise by using a large number of negative controls. However, the screen lacked a robust set of positive controls, which are another critical element of good screen design [1]. In fact, while the positive control construct shJak2 was

classified as a screening hit in the primary screen, it fell beyond the cutoff in the secondary screen because of high overlap with negative control data. Does this fact invalidate the hit classification strategy used in the secondary screen? Without more data points, this is difficult to conclude, since the single shJak2 construct used as a positive control could have unique, idiosyncratic off-target effects in BMMs. The use of more well-validated positive controls, such as multiple shRNA constructs targeting both Jak2 and Stat1, would increase the statistical power of the screen and help decrease false positive hit identification.

Second, a majority of the shRNA constructs classified as hits in the primary screen using RAWγNO cells were not validated in the secondary screen using BMMs. While this narrowing of candidates is expected by design, it is important to note that false negatives can stem from experimental error or from different thresholds in hit selection, as opposed to real biological differences between cell line and primary macrophages. Even true biological differences can lead to false negatives or positives, if they impact significant off-target effects of shRNA that confound the data observed. Finally, the strategy of screening in WT BMMs could have led to false negatives as well. One obvious biological difference between host cells in the two screens is that primary BMMs produce NO, while RAWγNO cells do not. Disabling NOS2 in the secondary screen could have allowed us to better replicate the conditions in the primary screen and to lower the rate of false negatives. While NO is a redundant player in IFNγ-mediated *L. pneumophila* restriction in BMMs [2], iNOS inhibition using a chemical inhibitor may have been sufficient to reveal additional pathways disabled by shRNA in the IFNγ mediator arm of the secondary screen.

Another issue affecting the shRNA screen was the relative lack of candidate genes for which more than a single shRNA construct yielded a hit phenotype. In the primary screen, 63 of 74 *L. pneumophila* host factor candidates and 73 of 84 IFNγ mediator candidates were classified as hits based on data obtained with only a single shRNA construct. Of the 22 genes classified as candidates based on multiple shRNA constructs in either arm of the screen, only two were also validated by

multiple constructs in the secondary screen. One of these, the candidate *L. pneumophila* host factor choroideremia-like protein (CHML), has been studied in human phagocytic cells, and its described function does not suggest a potential role as a bacterial host factor [3]. In particular, siRNA-mediated depletion of Chml transcript in human cells suppressed phagosome acidification and maturation, and reduced the clearance of phagocytic cargo [4], the opposite of what would be expected from our screen. The second multiple-shRNA candidate in the screen, the potential IFNγ mediator TSPAN6, was represented by two shRNA constructs that were later found to be redundant at all but a single nucleotide. Thus, genes classified as hits by multiple targeting constructs were largely absent from this screen, which may have been partially responsible for the difficulty validating the candidates identified.

Redundancy is a hallmark of the intracellular life cycle of *L. pneumophila*. Among 270 or more effectors secreted through the Dot-Icm secretion system, only one (SdhA) has been shown to play a non-redundant role in intracellular survival within macrophages [5–7], and many macrophage host factors have been identified as redundant as well [8,9]. However, at least two individual host factors (SAR1 and ARF1) have been shown to be uniquely required for optimal intracellular growth of *L. pneumophila* [9]. Notably, several *L. pneumophila* effector proteins have been shown to bind host factors with remarkably high binding affinity [10,11], suggesting that complete host factor protein ablation rather than incomplete shRNA-mediated depletion of protein expression may have been be required in order to identify other essential host factors.

Host defense mechanisms are often highly redundant as well [12]. Many parallel pathways exist to deal with the large variety of bacterial and protozoan intracellular pathogens that infect macrophages, as outlined in Chapter 1. In addition to NO production, primary BMMs may have other, redundant IFNγ-inducible bacterial restriction mechanisms that cannot be discovered by a single-gene knockout approach.

Candidate L. pneumophila host factors

Hits in the host factor screen include two members of the syntaxin protein family with roles in the early endocytic system. It is possible that these proteins play a role in phagosome modification by *L. pneumophila*. One of these candidates (SNX18), for instance, is exploited by the intracellular bacterium *S. typhimurium* for the same purpose [13]. The actin regulator WASF2, the early endosomal protein subunit RAB5B, and seven other candidates were confirmed as hits in the secondary screen as well.

Significant negative results in the IFNγ mediator screen

Work by our group and collaborators using knockout cells appeared to rule out a requirement for SNAP29, VTI1B, ARL8B, and AP3B1 in the IFNγ-mediated restriction of *L. pneumophila*. Results in knockout models are considered definitive, but with a caveat: parallel pathways in cells constitutively deficient in a target pathway could be stronger than they would be in cells in which the target pathway were suddenly ablated. However, our work with VTI1B$^{-/-}$ BMMs allowed us to prove that the phenotype observed in the screen was the result of an off-target effect of shVti1b rather than a result of VTI1B depletion. This is a significant negative result. VTI1B is a core member of the fusion machinery required for homotypic fusion of late endosomes [14] or heterotypic fusion of late endosomes with lysosomes [15], or autophagosomes with lysosomes [16]. Therefore, in IFNγ-activated cells, this core fusion machinery is either dispensable for bacterial restriction, or utilizes other SNARE proteins in place of VTI1B.

Candidate IFNγ mediators

Preliminary evidence has suggested that TSPAN6 may be an IFNγ-inducible member of the bacterial restriction machinery that seems to localize to the bacterial phagosome in macrophages. TM4SF4, another high-ranked hit, was not characterized further since an antibody was not available.

If further work validated a potential role for either in the restriction of *L. pneumophila*, it would join the ranks of several other tetraspanins with known roles in immunity. In humans, loss of function of the tetraspanin CD53 has been linked to susceptibility to bacterial, fungal, and viral infections, including the vacuolar pathogens *M. tuberculosis* and *Salmonella* [17]. This tetraspanin is induced in LPS-treated macrophages, and facilitates the activation of iNOS [18] and the oxidative burst [19,20]. Some members of the transmembrane 4 L six family (TM4SF) of tetraspanin proteins, including CD9, CD63, CD81, CD151, and A15, play significant roles in host defense, such as phagocytosis, signal transduction, and the recruitment of phosphoinositol kinases [21]. Multiple tetraspanins, including CD37, CD53, CD63, CD81, and CD82, are found on the membranes of multivesicular body vesicles and on exosomes released by phagocytic cells [22]. IFNγ induces the expression of the tetraspanin CD82, which a mediates signaling from the phagocytic receptor FcR [23], and suppresses the expression of CD9, a negative regulator of macrophage activation [24,25]. Our data suggest that the tetraspanins TSPAN6 and TM4SF4 may function in IFNγ-mediated defense as well, but more work is needed to substantiate these possibilities.

The AP3 complex plays a role in protein sorting and membrane targeting in the biogenesis of lysosomes and lysosome-related organelles [26,27]. The conflicting data we obtained in our work with BMMs deficient in AP3 complex member AP3B1 is still unexplained. shRNA-mediated depletion of AP3 complex subunits AP3S1, AP3S2, and AP3M2 in both WT and AP3B1$^{-/-}$ BMMs, using the same shRNA constructs classified as hits in the primary screen, did not reveal the influence of shRNA off-target effects, as they had for shVti1b. The AP3 subunit β3, known as AP3B1, has been described as an essential member of AP3. It is possible that the requirement for AP3B1 is dependent on some other variable which we did not account for in our experiments, such as the precise length of time that cells were stimulated with IFNγ. The experiments that failed to show a restriction defect relative to WT BMMs may have involved, for example, parallel pathways of

pathogen restriction that obscured the role of AP3. Alternatively, they may have involved an alternative, functional AP3 complex formed without an β3 subunit in AP3B1$^{-/-}$ BMMs.

Effect of innate immune sensing on IFNγ-activated restriction of intracellular pathogens

IRF3

The existence of interactions between innate immune sensing pathways and the IFNγ signaling pathway is well-known, mediated in part by the synergy of TLR-activated NFκB with IFNGR-activated STAT1 homodimers at IFNγ-activated sequences (GAS) within the promoters of IFNγ target genes [28]. Our work has, in contrast, demonstrated a significant effect of the innate immune sensing pathway member IRF3 on the maintenance of IFNγ effector mechanisms in BMMs, independently of IFNγ signaling. We were able to separate the effects of innate sensing on signaling from its effects on IFNγ effector maintenance by prestimulating BMMs with IFNγ, then removing this stimulus prior to infection and therefore prior to innate immune pathogen sensing.

MYD88/TRIF

Notably, our initial work with MYD88$^{-/-}$TRIF$^{-/-}$ BMMs revealed a significant, though relatively small contribution of these adaptor proteins to the maintenance of the IFNγ-activated state. Our work also recapitulated the known requirement for TLR adaptor proteins MYD88 and TRIF in full macrophage activation by IFNγ signaling, which resulted in a far more significant positive effect. While these two effects could be independent, it is also possible that the observed effect of MYD88/TRIF on pre-stimulated BMMs was due to their effect on signaling through IFNGR engaged with residual IFNγ that remained bound during infection and media changes.

STING

We showed that the cytosolic nucleic acid sensing pathway adaptor protein STING, but not MAVS, plays a role in supporting the maintenance of the IFNγ-activated state, although the effect was slight. Our ensuing work, however, showed that the transcription factor IRF3 that acts downstream of STING in macrophages suppressed, rather than supported the maintenance of the IFNγ-activated state. These data are consistent with STING-mediated maintenance of the IFNγ-activated state through a signaling pathway that does not use IRF3. Two such pathways have recently been described, both of which can be activated by either cytosolic dsDNA or cGAMP and which lead to the nuclear translocation of the transcription factor NFκB. In these pathways, STING signals through either TRAF6, or through TBK1 via TRAF3, to activate the canonical IKK kinases (IKKα and/or IKKβ) which phosphorylate the inhibitor of NFκB [29]. It is possible that NFκB activation, in turn, directly or indirectly facilitates the continued expression of IFNγ effectors and therefore enhances the maintenance of the IFNγ-activated state.

STING activation has been observed as a result of sensing of excess cellular or pathogen-derived DNA in BMMs deficient in either the cytosolic nuclease TREX1 [30,31] or the phagolysosomal nuclease DNASE2 [32,33]. Based on our preliminary results, TREX1 deficiency enhanced the maintenance of the IFNγ-activated state, consistent with increased activation of STING. Surprisingly, however, DNASE2 deficiency had the opposite result. A possible unifying model for these data is that excess phagolysosomal DNA in *L. pneumophila*-infected DNASE2$^{-/-}$ BMMs predominantly triggers the IRF3-activating modality of STING and leads to subsequent suppression of the IFNγ-activated state. Meanwhile, excess cytosolic DNA in *L. pneumophila*-infected TREX1$^{-/-}$ BMMs predominantly triggers the NFκB-activating modality of STING and leads to subsequent enhancement of the IFNγ-activated state.

IRF3 activation and localization

IRF3 activated by Ser388 phosphorylation was present in the nuclei of resting, but not IFNγ-activated BMMs after infection with *L. pneumophila,* despite robust phosphorylation of the IRF3 kinases IKKε and TBK1 under both conditions. Furthermore, immunofluorescence microscopy revealed decreased staining density of IRF3 in the nucleus as well as cytosolic speckling in IFNγ-activated BMMs following *L. pneumophila* infection or LPS stimulation. These findings may be unrelated, or they may represent a causal or associative relationship between the speckled distribution and the nuclear exclusion of IRF3. For instance, the recruitment of IRF3 to cytosolic foci could prevent its phosphorylation by active IKKε/TBK1 kinases, or prevent the translocation of phosphorylated IRF3 to the nucleus.

A recent study in mouse embryonic fibroblasts (MEFs) expressing the pestivirus protease N^{pro} revealed formation of cytosolic and peroxisomal puncta containing N^{pro} and IRF3 following cell stress response induction by sodium arsenate [34], though it is unknown whether the localization was driven by IRF3 or by the viral protein; here, N^{pro} led to the degradation of IRF3 to inactivate antiviral responses. Other studied have found that the IRF3 kinase TBK1 localizes to cytosolic speckles together with RIP1, RIP3, and adaptor proteins following signaling from TLR3, TLR4, or DAI [35,36], but IRF3 was thought to be recruited to these granules transiently, followed by TBK1-mediated activation and translocation to the nucleus. Our results so far do not distinguish whether IRF3 recruitment to speckles is related to its activation, degradation, or neither. We found that total IRF3 levels remain constant during IFNγ stimulation and *L. pneumophila* infection, but cannot rule out degradation since IRF3 synthesis could be concomitantly increased to offset a degradative response.

The differential nuclear recruitment or retention of IRF3pSer388 in resting, infected BMMs but not IFNγ-stimulated BMMs suggests that the transcriptional activity of IRF3 is responsible for the phenotype observed, with the caveat that multiple other post-translational modifications could affect IRF3 activity regardless of Ser388 phosphorylation [37]. Furthermore, cytoplasmic IRF3 plays

a variety of other effector roles. At levels of IRF3 activation above a threshold level, for example, IRF3pSer388 directly activates mitochondrial Bax to induce the intrinsic pathway of apoptosis [38,39]. However, we did not detect a difference in levels of cytoplasmic IRF3pSer388 in resting or IFNγ-stimulated BMMs, nor did we observe a decrease in cell counts in IFNγ-activated BMMs relative to WT BMMs following *L. pneumophila* infection. In addition, cytosolic IRF3 can act as a transcriptional repressor, as demonstrated in T cells in which the transcription factor RORγT is sequestered by IRF3 to prevent nuclear translocation [40]. Therefore, the differential nuclear recruitment or retention of IRF3 in resting or IFNγ-stimulated BMMs may or may not be a causative factor for IRF3-mediated suppression of the IFNγ-activated state.

Type I IFNs

Both resting and IFNγ$^{-/-}$ BMMs produced minimal amounts of Type I IFNs upon infection with *L. pneumophila*. Accordingly, the blocking of IFNAR using neutralizing antibody did not affect bacterial growth or restriction in WT or IRF3$^{-/-}$ BMMs, leading us to conclude that IRF3-dependent suppression of IFNγ-mediated bacterial restriction is independent of Type I IFNs. Notably, IRF3 also exerts a Type I IFN-independent effect on *in vivo* infection with the intracellular pathogens *Yersinia pestis*[41] and *Chlamydia muridarum* [42], though in the case of these pathogens, IRF3 is protective.

Interestingly, however, IFNAR$^{-/-}$ BMMs had a slight defect in both the induction and the maintenance of the IFNγ-activated state. This suggests that basal signaling though IFNAR plays a role in enabling BMMs for full IFNγ-mediated defenses. Tonic IFNAR signaling has been predicted to play an immunoregulatory role [43], and examples have been described in cells exposed to commensal microbiota [44]. It is possible that exposure to basal IFNAR signaling in BMMs grown under sterile conditions, perhaps in response to endogenous ligands, maintains these cells in a state of preparedness for future activation, and that addition of anti-IFNAR antibody does not displace existing receptor-ligand pairs that maintain the basal state.

When high levels of IFNβ, which are not endogenous to infected BMMs in culture, are administered to BMMs immediately after infection with *L. pneumophila*, we observed a significant difference in response depending on whether BMMs had been pre-stimulated with IFNγ or whether IFNγ.stimulation was done concurrently with infection and IFNβ administration. While these findings are not central to our results so far, they may be relevant *in vivo*, where macrophages may be exposed to Type I interferons produced by epithelial, dendritic, and other cells. Exogenous IFNβ had a slight restrictive effect on the growth of bacteria in resting BMMs, but a substantially greater restrictive effect in BMMs that had been prestimulated with IFNγ. However, IFNβ administered simultaneously with IFNγ following infection significantly increased bacterial growth, antagonizing IFNγ-mediated restriction. One model consistent with these results is that IFNβ-induced transcription factors differentially modulate the expression of IFNγ effectors depending on the presence of IFNγ-induced transcription factors at their promoters.

Transcriptional effects of IRF3 deficiency

Since IRF3 is involved in signaling pathways downstream of innate immune sensing, it was not surprising that IRF3 deficiency was responsible for significant transcriptional changes in *L. pneumophila*-infected BMMs. Differentially expressed genes included the IFNγ effector NOS2, as well as several other candidates that could potentially be involved in enhanced IFNγ-mediated bacterial restriction in BMMs.

Iron restriction is an important aspect of intracellular pathogen control. In our data, $IRF3^{-/-}$ BMMs exhibited differential expression of lipocalin 2 (LCN2), an iron regulator with roles in restriction of several vacuolar pathogens [45–47], and the iron storage protein ferritin light chain (FTL2) in response to IFNγ stimulation and bacterial infection, suggesting that limiting access to iron be partially responsible for enhanced bacterial restriction in these cells. Several other categories of differentially expressed genes present other opportunities for further exploration, including

transcription factors (LYL1, EGR3, EPAS1, BATF3, KRC), regulators of cell death (CHEK2, NPTX1, SERPINB2, FAH, CD00IF), and protease inhibitors (SERPINB2, subunits of SERPINA3, STFA3, CST7, GM5483).

Unexpectedly, IRF3 deficiency also led to significant gene expression changes in uninfected BMMs. This result suggests a basal role for IRF3, potentially due to endogenous stimuli, such as DNA from dying macrophages. Several of these genes were uniformly induced or repressed by IRF3 across all conditions, like the fatty acid binding protein 7 (FABP7) expressed only in WT BMMs, or several non-coding transcripts that were only significantly expressed in IRF3$^{-/-}$ BMMs. Interestingly, a subset of genes were strongly induced in response to IFNγ stimulation only in IRF3$^{-/-}$ BMMs, though their expression was inhibited by bacterial infection. These include a GBP protein (GBP11) and the protease inhibitor cystatin F (CST7), mentioned above; the role of genes in this cluster in bacterial infection is unknown.

T. cruzi

Our work with *T. cruzi*-infected BMMs confirmed that IRF3 can play a role in suppressing IFNγ-mediated responses to intracellular parasitic as well as bacterial pathogens through a mechanism independent of Type I IFNs. However, several key differences in this experimental system need to be considered in interpreting these results. First, TNFα was used to co-stimulate BMMs together with IFNγ. Second, BMMs were stimulated with IFNγ both before and after *T. cruzi* infection. Therefore, the phenotype observed could be due to suppression of either the establishment or the maintenance of either the IFNγ- or the TNFα-activated state. Finally, two pathogens are controlled by only partially overlapping sets of innate defense mechanisms due to significant differences between their pathogen-associated molecular patterns, virulence mechanisms, and intracellular life cycles. While *L. pneumophila* thrive in a remodeled phagosome that prevents lysosomal fusion, for instance, the intracellular replication program of *T. cruzi* requires exposure to

lysosomal contents and eventual egress into the cytosol [48]. Inside the macrophage, infectious trypomastigotes convert into non-motile, replicative amastigotes; after several rounds of replication, cytoplasmic amastigotes transform back into motile trypomastigotes that lyse the host cell and go on to infect bystander host cells [49].

Interestingly, it appears that the cell membranes of *T. cruzi*-infected WT BMMs were lysed more readily than the membranes of infected, IRF3$^{-/-}$ BMMs. Since the transformation of amastigotes to trypomastigotes is a prerequisite to host cell lysis, it is possible that IRF3$^{-/-}$ BMMs are able to better prevent or delay this stage transition due to the actions of innate immune effectors.

Alternatively, IRF3 deficiency could affect the process of membrane disruption by trypomastigotes. The mechanism of parasite egress from infected cells is poorly understood. Prior work has suggested that mechanical disruption of the cell membrane by a high burden of motile intracellular trypomastigotes contributes to host cell lysis [50,51], while other studies have implicated the role of parasite-derived lipases or proteases, particularly cruzipain [52]. The *T. cruzi* lifecycle has been largely studied in a variety of cell types, such as epithelial cells, myocytes, and fibroblasts; meanwhile, the contribution of macrophage innate immune sensors and effectors to cell membrane breakdown in the macrophage host remains unknown.

Function of IRF3-mediated suppression of IFNγ suppressors

As demonstrated *in vitro*, IRF3 is a novel player in the immunomodulation of macrophage microbicidal activity. Further studies will shed light on the molecular mechanism of this antagonism and its role in diverse infections *in vivo*. The presence of an intrinsic suppressor mechanism for IFNγ-mediated effectors is in line with other homeostatic processes of the immune system. This suppression may have evolved to dampen a potentially damaging anti-bacterial response, and thus to preserve cellular preparedness for antiviral defenses, or to avoid pathology caused by over-exuberant

IFNγ-mediated activation of macrophages downstream of bacterial sensing. Overproduction of nitric oxide, in particular, has been linked with pathology in the liver and lung due to its damaging effects on host DNA, mitochondria, lipids, and enzymes [53] in the context of chronic inflammation, chemical exposure, or exogenous, therapeutic nitric oxide administration [54,55]; in the context of bacterial infection, it has been observed in patients with pre-existing inflammatory conditions [56].

FUTURE DIRECTIONS

Vesicle trafficking screen

The vesicle trafficking screen revealed several candidate *L. pneumophila* host factors, all of which are candidates for further validation and functional characterization. Among candidate IFNγ mediators, meanwhile, TSPAN6 was neither fully characterized nor eliminated by functional characterization due to doubts about the specificity of the anti-TSPAN6 antibody and the low expression of TSPAN6 mRNA by qPCR. In order to better validate TSPAN6 as a candidate IFNγ mediator, several approaches could be taken. First, alternative methods to deplete gene transcripts could be used, such as short interfering RNA (siRNA). We used three different siRNA constructs (Ambion) targeting murine Tspan6 in RAWγNO cells, and compared target gene expression as well as IFNγ-mediated bacterial restriction in these cells relative to cells treated with negative control siRNA (Ambion, Dharmacon) or the positive control siStat1. Depletion of Stat1 transcript was verified by qPCR, and resulted in a drastic reduction in IFNγ-mediated bacterial restriction. However, siTspan6 did not result in consistent depletion of transcripts as measured by qPCR, or of protein, as measured by Western blot analysis.

Second, the TSPAN6 construct could be overexpressed in an attempt to rescue the shRNA knockdown phenotype. In our experience, however, lentiviral-mediated overexpression of the human Tspan6 ORF (which is resistant to knockdown by shRNA constructs targeting murine Tspan6) and of control ORFs in RAWγNO cells was low and transient. In BMMs, meanwhile, the dual rounds of antibiotic-based selection required for lentiviral-mediated overexpression and knockdown of human and murine TSPAN6, respectively, led to unacceptable levels of cell death. A third, more promising approach is the overexpression of TSPAN6 labeled with an HA or fluorescent protein tag in WT BMMs, in order to track its expression and localization, respectively, after IFNγ stimulation and *L. pneumophila* infection. If future results confirm the recruitment of TSPAN6 to bacterial phagosomes, it would be informative to correlate its presence with markers of phagosome maturation or with known effectors, such as the oxidative burst. Since tetraspanins are small proteins mostly buried within the phospholipid bilayer of membranes, however, a tagging approach could be challenging. Finally, genetic deletion of TSPAN6 using knockout mouse models or CRISPR-CAS9 would enable further investigation of the role of TSPAN6 in a clean genetic model.

Because the machinery involved in bacterial restriction in BMMs is redundant, it is possible that false negatives in the secondary screen could be recovered by repeating the screen in BMMs deficient in some of the known mechanisms. To remove the effects of iNOS, for example, BMMs could be treated with a chemical iNOS inhibitor before and after IFNγ stimulation and infection. Furthermore, multiple mechanisms could be disabled simultaneously in order to reveal subtle effects. For instance, a recent study used BMMs deficient in four different resistance mediators (IRGM1, IRGM3, NOS2, and NOX2) to support the conclusion that GBP-mediated mechanisms play a non-redundant role in restriction of *L. pneumophila*.

Effect of innate immune sensing on IFNγ-activated restriction of intracellular pathogens

The priority in our follow-up work regarding the intersection of innate immune sensing and IFNγ-mediated pathogen restriction is the breeding of an IRF3$^{-/-}$IFNAR$^{-/-}$ mouse strain in order to conclusively rule out the role of Type I IFN in the IRF3-mediated suppression of IFNγ effectors *in vitro*, as well as to examine the role of IRF3 in *L. pneumophila* infection in the absence of Type I IFNs *in vivo*. Here, we discuss these priority experiments, as well as opportunities for further study suggested by other results in this project.

Contribution of MYD88/TRIF to the maintenance of the IFNγ-activated state

To confirm that MYD88/TRIF contributes to the maintenance of the IFNγ-activated state by a mechanism completely independent of IFNGR signaling, pre-stimulated MYD88$^{-/-}$TRIF$^{-/-}$ BMMs could be washed extensively and incubated in media without IFNγ to reduce or eliminate the effect of continued signaling through residual IFNGR-IFNγ receptor-ligand pairs that remain on the cell surface after the removal of IFNγ, However, the length of the incubation period required is not clear, especially since signaling from receptor-ligand pairs can continue even after their internalization by endocytosis. Furthermore, attenuation of the IFNγ-activated state during this time could affect the ability to observe a MYD88/TRIF-dependent phenotype thereafter.

Contribution of STING-mediated cytosolic DNA sensing to the maintenance of the IFNγ-activated state

We have hypothesized that enhancement of IFNγ-mediated bacterial restriction in TREX1$^{-/-}$ BMMs is mediated by STING. If this were true, shRNA or siRNA-mediated depletion of Trex1 transcript in STING$^{-/-}$ BMMs should strengthen the phenotype, though it is possible that introduction of foreign RNA (shRNA or siRNA) could trigger confounding sensing pathways. Another approach is to examine whether treatment of WT BMMs with STING-specific ligands such as 3'3'-cGAMP leads to a similar phenotype as that seen in TREX$^{-/-}$ BMMs. Similarly, purified *L. pneumophila* DNA

transfection into the cytosol after infection can simulate TREX1 deficiency in WT and STING$^{-/-}$ BMMs. Our hypothesis would be supported if bacterial DNA sensing enhances IFNγ-mediated *L. pneumophila* restriction more strongly in WT than in STING$^{-/-}$ BMMs. If it did not, however, the hypothesis could not be ruled out, since these exogenously delivered STING ligands may lead to activation of IRF3. According to our model, the effect of STING activation is dependent on a balance of activation of the two arms of the STING response: the IRF3 arm, which suppresses the IFNγ-activated state, and the IRF3-independent arm, including NFκB, which enhances it. In order to compare the activation of these two arms, the nuclear translocation of IRF3 and NFκB in BMMs infected with *L. pneumophila* or stimulated with ligand could be compared, and the expression of genes specifically activated by either of these transcription factors could be quantified.

Contribution of phagolysosomal DNA sensing to IRF3-mediated suppression of the IFNγ-activated state

DNASE2$^{-/-}$ BMMs exhibit lower levels of IFNγ-mediated bacterial restriction than WT BMMs, and these cells are also characterized by activation of IRF3 [32]. To test the hypothesis that these two phenotypes are related, DNASE2 could be depleted in in IRF3$^{-/-}$ BMMs by siRNA or shRNA. If the hypothesis were true, DNASE2 knockdown would suppress IFNγ effectors in WT BMMs significantly more than in IRF3$^{-/-}$ BMMs, though noting the caveats regarding RNAi mentioned above. Furthermore, delivery of mouse or bacterial DNA ligands to phagolysosomes by suspending the ligands in cell media during *L. pneumophila* infection is a way to simulate DNASE2 deficiency, as well as to test whether the source of immunostimulatory DNA (host or pathogen) is relevant to the outcome observed.

IRF3-mediated, Type I IFN-independent suppression of IFNγ effectors

To definitively confirm that the IRF3-mediated suppression of IFNγ effectors is independent of Type I IFNs, we are breeding mice doubly deficient in IRF3 and IFNAR. *In vivo*, we will assess IFNγ-mediated bacterial restriction and NOS2 induction in IRF3$^{-/-}$IFNAR$^{-/-}$ and IRF3$^{-/-}$ BMMs relative to WT and IFNAR$^{-/-}$ controls. Furthermore, RNAseq analysis of gene expression in IRF3$^{-/-}$ IFNAR$^{-/-}$ and IRF3$^{-/-}$ BMMs relative to WT BMMs will refine the list of candidate effectors, eliminating genes whose transcription is modulated by low levels of Type I IFN or those modulated by IRF7 in the existing data set, in which WT and IRF3$^{-/-}$IRF7$^{-/-}$ BMMs were used

We have already begun investigating alternative, known mechanisms without the guidance of candidate genes, including the role of IFNγ-mediated necrosis which, according to our preliminary data, does not seem to play a role in enhanced bacterial restriction in IRF3$^{-/-}$ BMMs. Instead, assays specific to the candidates identified by RNAseq in IRF3$^{-/-}$IFNAR$^{-/-}$ BMMs will help in the identification of IFNγ effectors relevant to the restriction of *L. pneumophila* and specifically repressed by IRF3.

IRF3 localization in IFNγ-activated BMMs

We have observed that IFNγ-activated BMMs form cytosolic speckles that stain positive for IRF3. In order to confirm that these speckles actually represent IRF3, rather than another IFNγ-inducible protein that cross-reacts with anti-IRF3 antibody, we have used two different antibodies targeting IRF3 at different sites of the protein, but neither resulted in satisfactory IRF3-specific staining patterns. Another approach is to overexpress fluorescently-labeled IRF3 in order to eliminate staining pattern ambiguity. A different possibility is that IFNγ induces the expression of alternative isoforms of IRF3, which then forms the speckles observed. In fact, an alternative isoform called IRF3-CL is known to inhibit the activity of full-length IRF3 in human cells [57], but its regulation by IFNγ has not been studied; furthermore, it is unknown whether a corresponding, IRF3-inhibitory variant exists in mouse cells. Detailed analysis of mRNA mapping to IRF3 from our RNAseq data in

resting and IFNγ-stimulated BMMs infected with *L. pneumophila* or stimulated with LPS will allow us to determine whether IRF3 is differentially spliced under these conditions.

Effect of IRF3 on bacterial infection in vivo

Finally, we plan to perform intranasal *L. pneumophila* infection of WT, IRF3$^{-/-}$, IFNAR$^{-/-}$, and IRF3$^{-/-}$IFNAR$^{-/-}$ mice. We will collect data on lung bacterial burden as well as analyze the pathology of lung slices for evidence of tissue damage. WT mice clear *L. pneumophila* infection within about a week. Despite the described role of Type I IFNs in *L. pneumophila* infection *in vitro*, we expect that bacterial clearance in IFNAR$^{-/-}$ mice will be similar to that in WT mice, as shown previously [58,59]. Meanwhile, we expect that IRF3 deficiency on an IFNAR$^{-/-}$ background should enhance the capacity of alveolar macrophages to restrict bacteria, analogous to what we observed *in vitro*. However, as with deficiency in IFNAR, it is not possible to predict whether phenotype *in vitro* will have an effect *in vivo*. Furthermore, the increased activity of IFNγ effectors such as NOS2 may lead to host tissue damage, which could even lead to a paradoxical increase in bacterial burden. In the latter case, the result would support a beneficial role for the immunomodulatory action of IRF3.

REFERENCES

1. Stone DJ, Marine S, Majercak J, Ray WJ, Espeseth A, et al. (2007) High-throughput screening by RNA interference: control of two distinct types of variance. Cell Cycle Georget Tex 6: 898–901.

2. Gebran S, Yamamoto Y, Newton C, Klein T, Friedman H (1994) Inhibition of Legionella pneumophila growth by gamma interferon in permissive A/J mouse macrophages: role of reactive oxygen species, nitric oxide, tryptophan, and iron(III). Infect Immun 62: 3197–3205.

3. Strunnikova NV, Barb J, Sergeev YV, Thiagarajasubramanian A, Silvin C, et al. (2009) Loss-of-function mutations in Rab escort protein 1 (REP-1) affect intracellular transport in fibroblasts and monocytes of choroideremia patients. PloS One 4: e8402. doi:10.1371/journal.pone.0008402.

4. Gordiyenko NV, Fariss RN, Zhi C, MacDonald IM (2010) Silencing of the CHM gene alters phagocytic and secretory pathways in the retinal pigment epithelium. Invest Ophthalmol Vis Sci 51: 1143–1150. doi:10.1167/iovs.09-4117.

5. Laguna RK, Creasey EA, Li Z, Valtz N, Isberg RR (2006) A Legionella pneumophila-translocated substrate that is required for growth within macrophages and protection from host cell death. Proc Natl Acad Sci U S A 103: 18745–18750. doi:10.1073/pnas.0609012103.

6. Liu Y, Gao P, Banga S, Luo Z-Q (2008) An in vivo gene deletion system for determining temporal requirement of bacterial virulence factors. Proc Natl Acad Sci U S A 105: 9385–9390. doi:10.1073/pnas.0801055105.

7. O'Connor TJ, Boyd D, Dorer MS, Isberg RR (2012) Aggravating genetic interactions allow a solution to redundancy in a bacterial pathogen. Science 338: 1440–1444. doi:10.1126/science.1229556.

8. Dorer MS, Kirton D, Bader JS, Isberg RR (2006) RNA interference analysis of Legionella in Drosophila cells: exploitation of early secretory apparatus dynamics. PLoS Pathog 2. Available: http://dx.doi.org/10.1371/journal.ppat.0020034.

9. Ge J, Shao F (2011) Manipulation of host vesicular trafficking and innate immune defence by Legionella Dot/Icm effectors. Cell Microbiol 13: 1870–1880. doi:10.1111/j.1462-5822.2011.01710.x.

10. Cheng W, Yin K, Lu D, Li B, Zhu D, et al. (2012) Structural insights into a unique Legionella pneumophila effector LidA recognizing both GDP and GTP bound Rab1 in their active state. PLoS Pathog 8: e1002528. doi:10.1371/journal.ppat.1002528.

11. Schoebel S, Blankenfeldt W, Goody RS, Itzen A (2010) High-affinity binding of phosphatidylinositol 4-phosphate by Legionella pneumophila DrrA. EMBO Rep 11: 598–604. doi:10.1038/embor.2010.97.

12. Nish S, Medzhitov R (2011) Host defense pathways: role of redundancy and compensation in infectious disease phenotypes. Immunity 34: 629–636. doi:10.1016/j.immuni.2011.05.009.

13. Håberg K, Lundmark R, Carlsson SR (2008) SNX18 is an SNX9 paralog that acts as a membrane tubulator in AP-1-positive endosomal trafficking. J Cell Sci 121: 1495–1505. doi:10.1242/jcs.028530.

14. Antonin W, Holroyd C, Fasshauer D, Pabst S, Von Mollard G, et al. (2000) A SNARE complex mediating fusion of late endosomes defines conserved properties of SNARE structure and function. EMBO J 19: 6453–6464. doi:10.1093/emboj/19.23.6453.

15. Offenhäuser C, Lei N, Roy S, Collins BM, Stow JL, et al. (2011) Syntaxin 11 binds Vti1b and regulates late endosome to lysosome fusion in macrophages. Traffic Cph Den 12: 762–773. doi:10.1111/j.1600-0854.2011.01189.x.

16. Furuta N, Fujita N, Noda T, Yoshimori T, Amano A (2010) Combinational soluble N-ethylmaleimide-sensitive factor attachment protein receptor proteins VAMP8 and Vti1b mediate fusion of antimicrobial and canonical autophagosomes with lysosomes. Mol Biol Cell 21: 1001–1010. doi:10.1091/mbc.E09-08-0693.

17. Mollinedo F, Fontán G, Barasoain I, Lazo PA (1997) Recurrent infectious diseases in human CD53 deficiency. Clin Diagn Lab Immunol 4: 229–231.

18. Boscá L, Lazo PA (1994) Induction of nitric oxide release by MRC OX-44 (anti-CD53) through a protein kinase C-dependent pathway in rat macrophages. J Exp Med 179: 1119–1126.

19. Kim T-R, Yoon J-H, Kim Y-C, Yook Y-H, Kim IG, et al. (2004) LPS-induced CD53 expression: a protection mechanism against oxidative and radiation stress. Mol Cells 17: 125–131.

20. Olweus J, Lund-Johansen F, Horejsi V (1993) CD53, a protein with four membrane-spanning domains, mediates signal transduction in human monocytes and B cells. J Immunol Baltim Md 1950 151: 707–716.

21. Yauch RL, Hemler ME (2000) Specific interactions among transmembrane 4 superfamily (TM4SF) proteins and phosphoinositide 4-kinase. Biochem J 351 Pt 3: 629–637.

22. Escola JM, Kleijmeer MJ, Stoorvogel W, Griffith JM, Yoshie O, et al. (1998) Selective enrichment of tetraspan proteins on the internal vesicles of multivesicular endosomes and on exosomes secreted by human B-lymphocytes. J Biol Chem 273: 20121–20127.

23. Lebel-Binay S, Lagaudrière C, Fradelizi D, Conjeaud H (1995) CD82, tetra-span-transmembrane protein, is a regulated transducing molecule on U937 monocytic cell line. J Leukoc Biol 57: 956–963.

24. Suzuki M, Tachibana I, Takeda Y, He P, Minami S, et al. (2009) Tetraspanin CD9 negatively regulates lipopolysaccharide-induced macrophage activation and lung inflammation. J Immunol Baltim Md 1950 182: 6485–6493. doi:10.4049/jimmunol.0802797.

25. Wang X-Q, Evans GF, Alfaro ML, Zuckerman SH (2002) Down-regulation of macrophage CD9 expression by interferon-gamma. Biochem Biophys Res Commun 290: 891–897. doi:10.1006/bbrc.2001.6293.

26. Chapuy B, Tikkanen R, Mühlhausen C, Wenzel D, von Figura K, et al. (2008) AP-1 and AP-3 mediate sorting of melanosomal and lysosomal membrane proteins into distinct post-Golgi trafficking pathways. Traffic Cph Den 9: 1157–1172. doi:10.1111/j.1600-0854.2008.00745.x.

27. Wenham M, Grieve S, Cummins M, Jones ML, Booth S, et al. (2010) Two patients with Hermansky Pudlak syndrome type 2 and novel mutations in AP3B1. Haematologica 95: 333–337. doi:10.3324/haematol.2009.012286.

28. Schroder K, Sweet MJ, Hume DA (2005) Signal integration between IFNgamma and TLR signalling pathways in macrophages. Immunobiology 211: 511–524. doi:10.1016/j.imbio.2006.05.007.

29. Abe T, Barber GN (2014) Cytosolic-DNA-mediated, STING-dependent proinflammatory gene induction necessitates canonical NF-κB activation through TBK1. J Virol 88: 5328–5341. doi:10.1128/JVI.00037-14.

30. Yan N, Regalado-Magdos A, Stiggelbout B, Lee-Kirsch M, Lieberman J (2010) The cytosolic exonuclease TREX1 inhibits the innate immune response to human immunodeficiency virus type 1. Nat Immunol 11: 1005–1013. doi:10.1038/ni.1941.

31. Manzanillo P, Shiloh M, Portnoy D, Cox J (2012) Mycobacterium tuberculosis activates the DNA-dependent cytosolic surveillance pathway within macrophages. Cell Host Microbe 11: 469–480. doi:10.1016/j.chom.2012.03.007.

32. Okabe Y, Kawane K, Nagata S (2008) IFN regulatory factor (IRF) 3/7-dependent and -independent gene induction by mammalian DNA that escapes degradation. Eur J Immunol 38: 3150–3158. doi:10.1002/eji.200838559.

33. Ahn J, Gutman D, Saijo S, Barber GN (2012) STING manifests self DNA-dependent inflammatory disease. Proc Natl Acad Sci U S A 109: 19386–19391. doi:10.1073/pnas.1215006109.

34. Jefferson M, Whelband M, Mohorianu I, Powell P (2014) The pestivirus N terminal protease N(pro) redistributes to mitochondria and peroxisomes suggesting new sites for regulation of IRF3 by N(pro.). PloS One 9. Available: http://dx.doi.org/10.1371/journal.pone.0088838.

35. Kaiser WJ, Upton JW, Mocarski ES (2008) Receptor-interacting protein homotypic interaction motif-dependent control of NF-kappa B activation via the DNA-dependent activator of IFN regulatory factors. J Immunol Baltim Md 1950 181: 6427–6434.

36. Funami K, Sasai M, Ohba Y, Oshiumi H, Seya T, et al. (2007) Spatiotemporal mobilization of Toll/IL-1 receptor domain-containing adaptor molecule-1 in response to dsRNA. J Immunol Baltim Md 1950 179: 6867–6872.

37. Noyce R, Collins S, Mossman K (2009) Differential modification of interferon regulatory factor 3 following virus particle entry. J Virol 83: 4013–4022. doi:10.1128/JVI.02069-08.

38. Chattopadhyay S, Marques J, Yamashita M, Peters K, Smith K, et al. (2010) Viral apoptosis is induced by IRF-3-mediated activation of Bax. EMBO J 29: 1762–1773. doi:10.1038/emboj.2010.50.

39. Chattopadhyay S, Fensterl V, Zhang Y, Veleeparambil M, Yamashita M, et al. (2013) Role of interferon regulatory factor 3-mediated apoptosis in the establishment and maintenance of persistent infection by Sendai virus. J Virol 87: 16–24. doi:10.1128/JVI.01853-12.

40. Ysebrant de Lendonck L, Tonon S, Nguyen M, Vandevenne P, Welsby I, et al. (2013) Interferon regulatory factor 3 controls interleukin-17 expression in CD8 T lymphocytes. Proc Natl Acad Sci U S A 110: E3189–E3197. doi:10.1073/pnas.1219221110.

41. Patel A, Lee-Lewis H, Hughes-Hanks J, Lewis C, Anderson D (2012) Opposing roles for interferon regulatory factor-3 (IRF-3) and type I interferon signaling during plague. PLoS Pathog 8. Available: http://dx.doi.org/10.1371/journal.ppat.1002817.

42. Prantner D, Sikes J, Hennings L, Savenka A, Basnakian A, et al. (2011) Interferon regulatory transcription factor 3 protects mice from uterine horn pathology during Chlamydia muridarum genital infection. Infect Immun 79: 3922–3933. doi:10.1128/IAI.00140-11.

43. Gough DJ, Messina NL, Clarke CJ, Johnstone RW, Levy DE (2012) Constitutive type I interferon modulates homeostatic balance through tonic signaling. Immunity 36: 166–174. doi:10.1016/j.immuni.2012.01.011.

44. Ivashkiv LB, Donlin LT (2014) Regulation of type I interferon responses. Nat Rev Immunol 14: 36–49. doi:10.1038/nri3581.

45. Guglani L, Gopal R, Javier R-M, Junecko BF, Lin Y, et al. (2011) Lipocalin 2 regulates inflammation during pulmonary mycobacterial infections. PloS One 7. Available: http://dx.doi.org/10.1371/journal.pone.0050052.

46. Bellmann-Weiler R, Schroll A, Engl S, Nairz M, Talasz H, et al. (2013) Neutrophil gelatinase-associated lipocalin and interleukin-10 regulate intramacrophage Chlamydia pneumoniae replication by modulating intracellular iron homeostasis. Immunobiology 218: 969–978. doi:10.1016/j.imbio.2012.11.004.

47. Fritsche G, Nairz M, Libby SJ, Fang FC, Weiss G (2012) Slc11a1 (Nramp1) impairs growth of Salmonella enterica serovar typhimurium in macrophages via stimulation of lipocalin-2 expression. J Leukoc Biol 92: 353–359. doi:10.1189/jlb.1111554.

48. Andrade L, Andrews N (2004) Lysosomal fusion is essential for the retention of Trypanosoma cruzi inside host cells. J Exp Med 200: 1135–1143. doi:10.1084/jem.20041408.

49. Ribeiro-Gomes FL, Lopes MF, DosReis GA (2007) Negative Signaling and Modulation of Macrophage Function in Trypanosoma cruzi Infection. Protozoans Macrophages: 149.

50. Buckner F, Van Voorhis W (2000) Immune response to Trypanosoma cruzi: control of infection and pathogenesis of Chagas disease. Eff Microbes Immune Syst MW Cunningham RS Fujinami Eds Lippincott Williams Wilkins Phila Pa: 569–592.

51. Wendelken JL, Rowland EC (2009) Agglutination of Trypanosoma cruzi in infected cells treated with serum from chronically infected mice. J Parasitol 95: 337–344. doi:10.1645/GE-1757.1.

52. Costales J, Rowland EC (2007) A role for protease activity and host-cell permeability during the process of Trypanosoma cruzi egress from infected cells. J Parasitol 93: 1350–1359. doi:10.1645/GE-1074.1.

53. Gardner CR, Laskin DL (1999) Protective and pathologic roles of nitric oxide in tissue injury. Cell Mol Biol Nitric Oxide: 225–246.

54. Hollenberg SM, Cinel I (2009) Bench-to-bedside review: nitric oxide in critical illness--update 2008. Crit Care Lond Engl 13: 218. doi:10.1186/cc7706.

55. Weinberger B, Laskin DL, Heck DE, Laskin JD (2001) The toxicology of inhaled nitric oxide. Toxicol Sci Off J Soc Toxicol 59: 5–16.

56. Francés R, Muñoz C, Zapater P, Uceda F, Gascón I, et al. (2004) Bacterial DNA activates cell mediated immune response and nitric oxide overproduction in peritoneal macrophages from patients with cirrhosis and ascites. Gut 53: 860–864. doi:10.1136/gut.2003.027425.

57. Li C, Ma L, Chen X (2011) Interferon regulatory factor 3-CL, an isoform of IRF3, antagonizes activity of IRF3. Cell Mol Immunol 8: 67–74. doi:10.1038/cmi.2010.55.

58. Ang D, Oates C, Schuelein R, Kelly M, Sansom F, et al. (2010) Cutting edge: pulmonary Legionella pneumophila is controlled by plasmacytoid dendritic cells but not type I IFN. J Immunol Baltim Md 1950 184: 5429–5433. doi:10.4049/jimmunol.1000128.

59. Spörri R, Joller N, Albers U, Hilbi H, Oxenius A (2006) MyD88-dependent IFN-gamma production by NK cells is key for control of Legionella pneumophila infection. J Immunol Baltim Md 1950 176: 6162–6171.